

University of Montana

## ScholarWorks at University of Montana

---

Graduate Student Theses, Dissertations, &  
Professional Papers

Graduate School

---

2009

### Glacier Monitoring in Ladakh and Zaskar, northwestern India

Martin Edward Byrne

*The University of Montana*

Follow this and additional works at: <https://scholarworks.umt.edu/etd>

**Let us know how access to this document benefits you.**

---

#### Recommended Citation

Byrne, Martin Edward, "Glacier Monitoring in Ladakh and Zaskar, northwestern India" (2009). *Graduate Student Theses, Dissertations, & Professional Papers*. 493.  
<https://scholarworks.umt.edu/etd/493>

This Thesis is brought to you for free and open access by the Graduate School at ScholarWorks at University of Montana. It has been accepted for inclusion in Graduate Student Theses, Dissertations, & Professional Papers by an authorized administrator of ScholarWorks at University of Montana. For more information, please contact [scholarworks@mso.umt.edu](mailto:scholarworks@mso.umt.edu).

GLACIER MONITORING IN LADAKH AND ZANSKAR, NORTHWESTERN INDIA

By

MARTIN EDWARD BYRNE

Bachelor of Arts, Eastern Washington University, Cheney, Washington, 2006

Thesis

presented in partial fulfillment of the requirements  
for the degree of

Master of Science  
in Geography, GIS and Cartography

The University of Montana  
Missoula, MT

June 2009

Approved by:

Perry Brown, Associate Provost for Graduate Education  
Graduate School

Ulrich Kamp, Chair  
Department of Geography

Anna Klene  
Department of Geography

Joel Harper  
Department of Geosciences

Tobias Bolch  
Institute of Cartography, Dresden University of Technology, Germany

GLACIER MONITORING IN LADAKH AND ZANSKAR, NORTHWESTERN INDIA

Chairman: Ulrich Kamp

Abstract

Glaciers in the Himalaya are often heavily covered with supraglacial debris, making them difficult to study with remotely-sensed imagery alone. Various methods such as band ratios can be used effectively to map clean-ice glaciers; however, a thicker layer of debris often makes it impossible to distinguish between supraglacial debris and the surrounding terrain. Previously, a morphometric approach employing an ASTER-derived digital elevation model (DEM) has been used to map glaciers in the Khumbu Himal and the Tien Shan. This project aims first to test the ability of the morphometric procedure to map small glaciers; second, to use the morphometric approach to map glaciers in Ladakh; and third, to use Landsat and ASTER data and GPS and field measurements to monitor glacier change in Ladakh over the past four decades. Field work was carried out in the summers of 2007 and 2008. For clean ice, a ratio of shortwave infrared (SWIR, 1.6-1.7  $\mu\text{m}$ ) and near infrared (NIR, 0.76-0.86  $\mu\text{m}$ ) bands from the ASTER dataset was used to distinguish snow and ice. For debris-covered glaciers, morphometric features such as slope, derived from a DEM, were combined with thermal imagery and supervised classifiers to map glacial margins. The method is promising for large glaciers, although problems occurred in the distal and lateral parts and in the forefield of the glaciers. The morphometric approach was inadequate for mapping small glaciers, due to a paucity of unique topographic features on the glaciers which can be used to distinguish them from the surrounding terrain. A multi-temporal analysis of three glaciers in Ladakh found that two of them have receded—one since at least the mid-1970s, the other since at least 2000—while a third glacier, Parkachik Glacier, seemed to have retreated in the 1980s, only to advance in the 1990s and early 2000s. However, from 2004-2008 it showed only negligible change making its current status difficult to determine without further monitoring. The glacier outlines derived during this project will be added to the Global Land Ice Measurements from Space (GLIMS) database. In testing the limits of the morphometric approach, the thesis has provided a valuable contribution to the present literature and knowledge-base regarding the mapping of debris-covered glaciers.

## Acknowledgements

First and foremost, I wish to thank my advisor, Dr. Ulrich Kamp, who was the catalyst for this project. Indeed, without his guidance and assistance, the idea of glacier monitoring in India would have never come to my mind, and I certainly would not have finished this thesis without him. Thus, I owe him the greatest debt of gratitude, for he pushed me and accorded me an opportunity very few others have experienced. For that I will be forever grateful.

A special recognition is owed to Dr. Tobias Bolch. Through innumerable back-and-forth emails, he patiently explained to me the process of glacier mapping. Without Tobias' generous assistance, assuredly this thesis would have been impossible. There is not a doubt in my mind that his brilliance will one day see him to the upper echelons of the scientific community. It has been an honor to work with him.

My committee members, Dr. Anna Klene and Dr. Joel Harper, have been exceedingly helpful. Not once in the course of this project did I ever feel these two professors would not drop whatever they were doing to help me. Even at the busiest of times, I felt welcomed in their respective offices, and confident they would have the answer to my question. These two are unparalleled as professors and as scholars alike, and it is my great fortune to have had them on my committee.

Skarma Ishey, though he will never read this, was an integral part of field work in Ladakh. He selflessly gave us his time in Ladakh, hiking to the glaciers with us, camping in the rain, and teaching us to make a fire without wood when my stove broke. I have no doubt he had more important things to do—I saw the crops in the field—and a more comfortable place to sleep than in my tent in the mountains, but he unflinchingly joined us. His constant smile, kindness, and curiosity helped us make it through the rain, ice, *dzo* attacks, and everything else that came our way, expectedly or unexpectedly, in the field. He will not be forgotten.

I also wish to extend my gratitude to Jeffrey Olsenholler of University of Nebraska-Omaha, for his help with data processing and DEM creation; and to the GLIMS project, for providing ASTER imagery free of charge for this project.

Finally, field work for this project was made possible through the generosity of the College of Arts and Sciences and the Office of International Programs of the University of Montana. Without the funding provided by these two offices, my trip to India would have remained a pipe dream, and I would have been confined to studying Ladakh's glaciers solely through books and the virtual world. Instead, I was offered an opportunity unlike any I am likely to ever have again. Thank you.

# Table of Contents

|  |           |
|--|-----------|
| Abstract .....                               | ii        |
| Acknowledgements .....                       | iii       |
| Table of Contents .....                      | iv        |
| Table of Figures and Tables.....             | vi        |
| <i>Figures</i> .....                         | vi        |
| <i>Tables</i> .....                          | viii      |
| <b>1. Introduction.....</b>                  | <b>1</b>  |
| <b>2. Background .....</b>                   | <b>6</b>  |
| 2.2 Glacier Studies in Ladakh .....          | 11        |
| 2.3 Glacier Mapping .....                    | 16        |
| 2.4 The GLIMS Project.....                   | 26        |
| <b>3. Study Area .....</b>                   | <b>28</b> |
| 3.1 Ladakh.....                              | 28        |
| 3.2 Himalaya .....                           | 29        |
| 3.3 Tectonic Evolution of the Himalaya ..... | 31        |
| 3.4 Geology .....                            | 34        |
| 3.5 Geomorphology .....                      | 40        |
| 3.6 Rivers .....                             | 40        |
| 3.7 Climate.....                             | 43        |
| 3.8 Glaciers and glaciation.....             | 45        |
| 3.9 Vegetation .....                         | 49        |
| 3.11 Ladakhi People.....                     | 50        |
| <b>4. Methods.....</b>                       | <b>54</b> |
| 4.1 Study Areas .....                        | 54        |
| 4.2 Ground-truth Accuracy Assessment .....   | 61        |
| 4.3 Datasets .....                           | 61        |
| 4.3.1 Landsat Dataset .....                  | 63        |
| 4.3.2 ASTER Dataset.....                     | 66        |
| 4.4 DEM Generation .....                     | 67        |
| 4.5 Mapping Clean Ice.....                   | 69        |
| 4.5.1 Band Ratios.....                       | 69        |
| 4.6 Mapping Debris-covered ice .....         | 70        |
| 4.6.1 Thermal Bands .....                    | 70        |
| 4.6.2 Supervised Classification.....         | 72        |
| 4.6.3 Topographic Analysis .....             | 73        |
| 4.6.4 Cluster Analysis .....                 | 74        |
| 4.6.5 Morphometric Glacier Mapping.....      | 74        |
| 4.7 Multi-temporal Analysis .....            | 77        |

|   |            |
|---|------------|
| <b>5. Results .....</b>   | <b>79</b>  |
| 5.1 Mapping Small Glaciers .....  | 79         |
| 5.2 Mapping Debris-covered Glaciers .....                                     | 81         |
| 5.3 Glacier monitoring.....   | 85         |
| 5.3.1 Himis-Shukpachan .....  | 85         |
| 5.3.2 Drang Drung.....  | 88         |
| <i>Data from a variety of sources were used to monitor Study Area 4</i> ..... | 88         |
| 5.3.3 Parkachik .....   | 90         |
| <b>6. Discussion.....</b>   | <b>93</b>  |
| 6.1 Mapping Small Glaciers .....  | 93         |
| 6.2 Mapping Debris-covered Glaciers .....                                     | 94         |
| 6.3 Glacier Monitoring.....   | 96         |
| 6.3.1 Himis-Shukpachan and Drang Drung .....                                  | 96         |
| 6.3.2 Parkachik Glacier.....  | 97         |
| <b>7. Conclusion .....</b>  | <b>100</b> |
| <b>8. References .....</b>  | <b>105</b> |

## Table of Figures and Tables

### Figures

|  |    |
|--|----|
| Figure 1. Areas where the morphometric approach has been used previously.....    | 4  |
| Figure 2. Giant paleomoraine in the Leh Valley.....                              | 12 |
| Figure 3. Glacially-formed valley in the Zaskar Range.....                       | 15 |
| Figure 4. Organizational block diagram for the GLIMS program.....                | 26 |
| Figure 5. India.....   | 28 |
| Figure 6. Ladakh, a part of Kashmir. ....  | 29 |
| Figure 7. The Trans-Himalaya in Ladakh.....                                      | 31 |
| Figure 8. Norian evolution of the Indian Sub-continent.....                      | 32 |
| Figure 9. Northward drift of India across the Tethys.....                        | 33 |
| Figure 10. Strata of limestone, dolomite and tuffites in the Zaskar Range. ....  | 37 |
| Figure 11. Geological map of Ladakh .....  | 38 |
| Figure 12. Alluvial fan in the Indus Valley .....                                | 41 |
| Figure 13. Irrigation agriculture in the Indus Valley. ....                      | 42 |
| Figure 14. Confluence of the Indus and Zaskar rivers.....                        | 42 |
| Figure 15. Weather patterns in the Himalaya .....                                | 44 |
| Figure 16. Summer storm over the Zaskar Mountains .....                          | 45 |
| Figure 17. The accumulation zone of a glacier in Ladakh.....                     | 46 |
| Figure 18. Vegetation in Ladakh .....  | 49 |
| Figure 19. Irrigated fields in Ladakh. ....                                      | 51 |
| Figure 20. <i>Dzo</i> .....  | 52 |
| Figure 21. Young monks.....  | 53 |
| Figure 22. Map of Study Areas 1-5 in Ladakh. ....                                | 55 |
| Figure 23. The glacier above Igu in Study Area 1 .....                           | 56 |
| Figure 24. One of the three glaciers in Study Area 2.....                        | 57 |
| Figure 25. Another glacier in Study Area 2.....                                  | 57 |
| Figure 26. Study Area 3: Parkachik Glacier .....                                 | 58 |
| Figure 27. Study Area 4: Drang Drung Glacier.....                                | 59 |
| Figure 28. Study Area 5, including Parkachik and Drang Drung glaciers .....      | 60 |
| Figure 29. Landsat image of a debris-covered glacier tongue in Pakistan .....    | 62 |
| Figure 30. Landsat image of Study Area 3. ....                                   | 63 |
| Figure 31. ASTER image of Study Area 3. ....                                     | 67 |
| Figure 32. Elevation map study area 3.....                                       | 69 |
| Figure 33. Flow-diagram of the morphometric glacier mapping (MGM) approach ..... | 75 |
| Figure 34. Ratio of ASTER bands 3 and 4 for Study Area 1.....                    | 79 |
| Figure 35. Topographic analyses for Study Area 1 .....                           | 81 |
| Figure 36. Thermal image for Study Area 3. ....                                  | 82 |
| Figure 37. Cluster Analysis for Study Area 3.....                                | 83 |
| Figure 38. Maximum Likelihood classification for Study Area 3. ....              | 84 |
| Figure 39. Morphometric glacier mapping (MGM) results for Study Area 3. ....     | 86 |
| Figure 40. MGM results for Study Area 3 .....                                    | 86 |
| Figure 41. MGM results for Study Area 4.....                                     | 87 |
| Figure 42. MGM results for Study Area 5.....                                     | 87 |
| Figure 43. Change in the glacier terminus in Study Area 2.....                   | 88 |

|  |    |
|--|----|
| Figure 44. Change in the glacier terminus in Study Area 4..... | 89 |
| Figure 45. Change in the glacier terminus in Study Area 3..... | 91 |



## Tables

|  |    |
|--|----|
| Table 1. Landsat Scenes.....   | 65 |
| Table 2. ASTER Scenes.....   | 68 |
| Table 3. Terminal change of Drang Drung Glacier between 1975 and 2008..... | 89 |
| Table 4. Debris-cover on Drang Drung Glacier between 1990 and 2006. ....   | 90 |
| Table 5: Terminal change of Parkachik Glacier between 1979 and 2008. ....  | 90 |
| Table 6: Debris-cover on Parkachik Glacier between 1990 and 2004.....      | 92 |

# 1. Introduction

Humankind is at a juncture unique in all of history: we have the ability to change the earth's processes, and also now, for the first time ever, the ability to see the effects we have on a worldwide scale. The Earth's climate is changing, likely due to human activities, and its effects on communities and ecosystems are becoming increasingly substantial. Remote sensing gives us the ability to monitor these changes on a scale previously unimagined; thanks to satellite technology, we can now view any given location on earth, without ever setting foot anywhere near that spot (Quattrochi *et al.* 2003; Lillesand *et al.* 2004; Rees 2006). The changes in climate have sometimes been positive for the communities affected by them—often times not. It is imperative for humankind to understand the processes of climate change, and, more importantly, earth's reactions to it (IPCC 2007; Marston 2008).

Worldwide, the majority of mountain glaciers are currently experiencing a period of recession, a trend that began in the mid-Nineteenth Century with the end of the Little Ice Age, continued through the Twentieth Century, and has accelerated over the past three decades (WWF 2005; Ren *et al.* 2006; Barry 2006; Zemp *et al.* 2006; UNEP 2008). Thus, glaciers have come to the forefront of the scientific community's attention in recent decades. Glaciers provide a standard by which the effects of global climate change can be measured, and they also act as harbingers of possible future scenarios (Oerlemans 1994; Hinkel *et al.* 2003). Glaciers are extremely sensitive to even minor changes in climate, so they act as warning signs, telling us what is happening and enabling us to prepare for changes as they become stronger (Maisch 2000; Hinkel *et al.* 2003; Hewitt

2005; Quincy *et al.* 2005; Barry 2006; Kolbert 2006; Zemp *et al.* 2006; Racoviteanu *et al.* 2008; UNEP 2008).

Glaciers' significance to the global community becomes even more apparent when one considers their importance as water resources to literally billions of people around the world. Indeed, glaciers act as earth's "water towers" (Krishna 1996; Mountain Agenda 2002; Viviroli *et al.* 2003, 2007; Messerli *et al.* 2002; WWF 2005; Malanson and Honey 2009), providing water for drinking and food production throughout the year. As such, they also act to buffer short-term changes by providing a steady, reliable source of sustenance, even in periods of reduced precipitation (Krishna 1996; Su and Shi 2002; WWF 2005; Ren *et al.* 2006). This significance is particularly crucial in Asia, where more than fifty percent of the population gets its water from the glaciers and snowfields of the Himalaya (Mountain Agenda 2002; WWF 2005), rendering the people of that continent acutely susceptible to even minor changes in glaciers' size.

It is thus extremely important to be able to map and monitor the world's glaciers, in order to prepare for and mitigate water resource issues before they occur (WWF 2005; IPCC 2007). Technological advances in the past few decades have allowed humans to view glaciers as never before. Remote sensing gives us the ability to monitor glaciers without going anywhere near them. This has rendered it viable for the first time to map and monitor glaciers in remote regions such as Ladakh, India, which had previously been far too difficult to monitor on a large scale over an extended time period (Bishop *et al.* 1998; Kulkarni *et al.* 2007; Racoviteanu *et al.* 2008). Programs such as Global Land Ice Measurements from Space (GLIMS) have begun large-scale efforts to map and monitor

all of Earth's mountain glaciers, but large regions still remain un-monitored (Global Land Ice Measurements from Space 2009).

There are some complications to monitoring glaciers in Ladakh, as well as elsewhere in the Himalaya. Particularly, heavy layers of debris in the glaciers' ablation zones make detection and mapping of glacier margins difficult or even impossible (Bishop *et al.* 2001; Paul *et al.* 2004a; Bolch *et al.* 2008; Racoviteanu 2008). Bolch *et al.* (2007) describes how it is often impossible to detect a glacier's margins even when one is standing atop the glacier.

Yet, if glaciers are to be monitored, they must first be mapped. Thus, while it is possible to effectively map clean-ice glaciers using multispectral imagery, it is important to develop mapping methods that rely on other methods than just multispectral imagery alone to map the glaciers in Ladakh (e.g., Bishop *et al.* 2001; Gao and Liu 2001; Bonk 2002; Bolch and Kamp 2006; Bolch *et al.* 2007; Racoviteanu 2008). A morphometric approach, applying topographic parameters, thermal data, and supervised classifiers, has been used to map debris-covered glaciers on Nanga Parbat (Bishop *et al.* 2001; Bonk 2002) the Khumbu Himal (Bolch *et al.* 2007), the Tien Shan (Bolch and Kamp 2006; Figure 1), and the Alps (Paul *et al.* 2004a). The morphometric approach was proven to be capable of effectively mapping large debris-covered glaciers in the Himalaya. However, it was never attempted on small glaciers, nor has the morphometric approach ever been used to map glaciers in Ladakh. Additionally, glaciers in Ladakh have to date not been monitored, and as such, there is currently a paucity of knowledge and literature regarding their responses to global climate change. Thus, this thesis attempts to answer the following questions:

1. Can the morphometric approach (Bolch *et al.* 2007) be used to delineate small, lightly debris-covered glaciers?
2. Is the morphometric approach (*ibid.*) effective for mapping large, debris-covered glaciers in Ladakh?
3. Have glaciers in Ladakh changed over the past four decades?

In addition to answering these research questions, a set of glacier outlines will be contributed to the GLIMS database at the National Snow and Ice Data Center (NSIDC) in Boulder, Colorado.

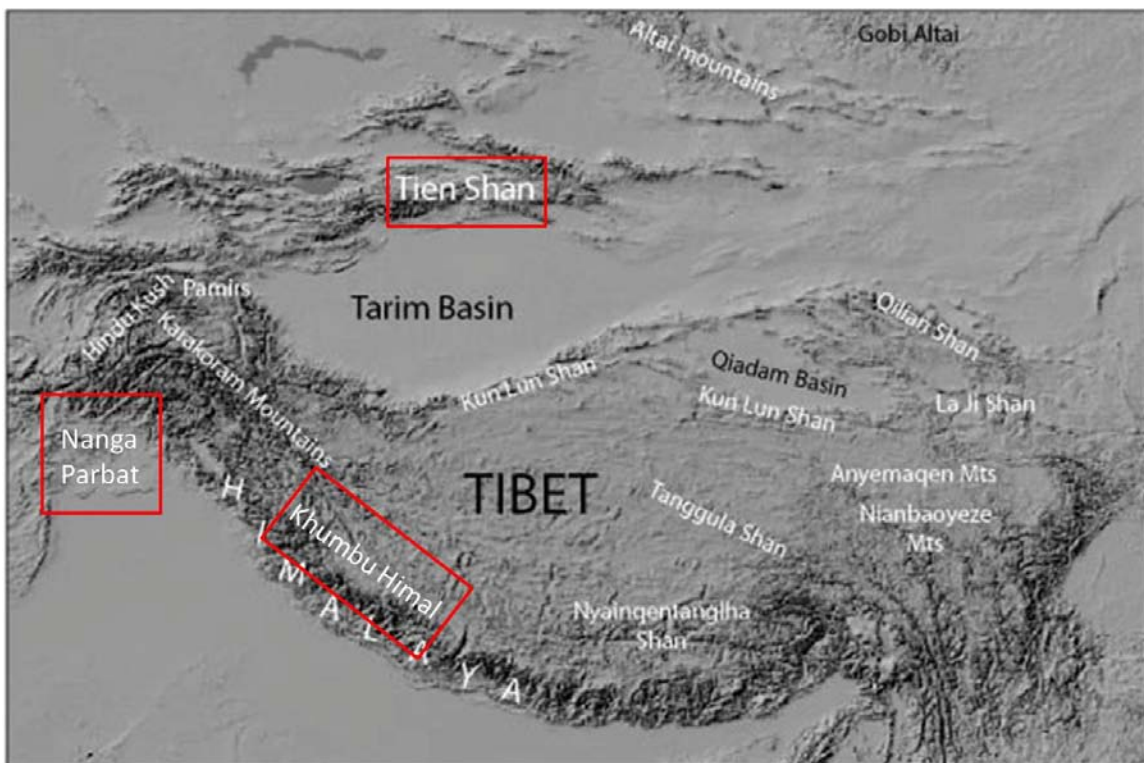


**Figure 1.** Areas where the morphometric approach has been used previously (After Lehmkuhl and Owen 2005).

By answering the aforementioned questions, it is hoped that this thesis will contribute to the current literature regarding the abilities—as well as the limits—of remotely sensed imagery to map and monitor debris-covered glaciers in the Himalaya. Additionally, by determining whether glaciers in Ladakh have changed since the 1970s, it

will be possible to predict how they will act in the coming decades, and thus mitigate possible water-related issues that may occur as a result of glacial change.

## 2. Background

### 2.1 Global Climate and Glacier Change

The Earth's climate is constantly changing (Ruddiman 2001; IPCC 2007), and glaciers act as archives of those changes that have occurred in the past, while recording what is going on in the present, and providing a glimpse of issues that may occur in the future (Krajik 2002; Hinkel *et al.* 2003; WWF 2005; IPCC 2007; UNEP 2008). Now, as global climate change increasingly comes to the attention of the scientific community and the general public alike, the study and monitoring of glacier change is more important than ever (Maisch 2000; Hinkel *et al.* 2003; Benn 2006; Kulkarni 2007; Marston 2008; Racoviteanu 2008).

While the connection between carbon dioxide levels and the global temperature has been recognized for nearly a century and a half (e.g., Tyndall 1861; Langley 1884, 1886; Arrhenius 1896; Chamberlin 1897, 1898, 1899; Wood 1909; Simpson 1928; Jones and Henderson-Sellers 1990; Weart 2008), it was not until the mid-1970s that scientists began to realize that the earth was, indeed, going through a period of rapidly increasing temperatures (Broecker 1975; Weart 2008). Even though all the factors by which climate change is being driven are not yet fully understood, the ability of glaciers to show its effects are well recognized (Maisch 2000; Hinkel *et al.* 2003; Hewitt 2005; Quincy *et al.* 2005; Barry 2006; Kolbert 2006; Zemp *et al.* 2006; Racoviteanu *et al.* 2008). Thus, the study of glaciers and particularly glacial change continues to be an important area of study.

Throughout the world, the majority of mountain glaciers are receding (Paul *et al.* 2004b; WWF 2005; Ren *et al.* 2006; Barry 2006; Kolbert 2006; Zemp *et al.* 2006; UNEP 2008). This trend began as early as the middle of the nineteenth century, with the end of the Little Ice Age (Fagan 2000; Su and Shi 2002; UNEP 2008), and continued through the twentieth century. Within this general trend, glaciers showed marked retreat in the 1920s and 1940s, but experienced a period of relative stability and advances around the 1970s (Khromova *et al.* 2003; Chinn *et al.* 2005; UNEP 2008). This was followed by even more extreme loss in the 1980s and subsequent decades, so that the greatest rates of loss for most mountain glaciers have occurred in the last three decades (Rignot *et al.* 2003; UNEP 2008). This is a trend that can be seen on mountain glaciers throughout the world (Dyurgerov and Meier 2000; Meier *et al.* 2003; Kaser *et al.* 2006), with only a few exceptions (e.g., Chinn 1999; Casassa *et al.* 2002; Chinn *et al.* 2005; Hewitt 2005).

The worldwide trend of glacier retreat is also generally true in the Himalaya and its surrounding mountain ranges (e.g., Kadota *et al.* 2000; Ageta *et al.* 2001; Khromova *et al.* 2003; Kulkarni *et al.* 2005, 2007; WWF 2005; Ren *et al.* 2006; Bolch 2007; IPCC 2007; UNEP 2008). Indeed, the glaciers of the Himalaya are receding faster than in any other area in the world (IPCC 2007). WWF (2005) stated that 67% of glaciers in the Himalaya are retreating—many at an alarming rate. Unfortunately, very little research has been done on Ladakh's glaciers, and no glacier monitoring has been done. However, there is ample evidence of glacier change in Ladakh's neighboring regions. Berthier *et al.* (2007), using remote sensing to calculate glacier change in Himachal Pradesh, found an annual loss of ice thickness of ~ 8 m water equivalent (w.e.) per year during the period



from 1999 to 2004—a rate of loss roughly double the long-term rate experienced between 1977 and 1999.

Narama *et al.* (2007) used CORONA imagery from 1971 and Landsat data from 2002 to perform a multi-temporal assessment of glacier change in the western Terskey-Alatau Range of the northern Tien Shan. They found that, during that time, glaciers in the study region experienced an areal loss of 18.4 km<sup>2</sup>, a decrease of ~ 8%. Khromova *et al.* (2003) found an even higher rate of decrease in the Ak-Shirak Range of the central Tien Shan. They found that the glaciers there had retreated 23% from 1973 to 2001. Bolch (2007) found that glaciers in Zailiyskiy and Kungey Alatau, in the northern Tien Shan, experienced an average areal loss of glacier ice coverage of more than 32% from 1955 to 1999. In the nearby Pamirs, Yablokov (2006) found that glaciers have retreated by 30-35% during the course of the twentieth century. He also found that glaciers in northern Afghanistan have lost more than 50% of their areal coverage.

In Bhutan, glaciers experienced a loss of 8% between 1963 and 1993 (Karma *et al.* 2003). In the Khumbu Himal of Nepal, Bolch *et al.* (2008) used Corona, Landsat and ASTER data to estimate planimetric and volumetric change during the period from 1962 to 2005. They found that the areal ice coverage had decreased by ~ 5%, with the highest rate coming between 1992 and 2005. The most significant change on these glaciers, however, was recognizable through downwasting. Stokes *et al.* (2007) and Bolch *et al.* (2008) noted that recession of debris-covered glaciers leads to an increased areal percent of debris-cover. Ren *et al.* (2006) calculated the decrease in glacier coverage since the 1960s on the north side of Mt. Everest to be 5.5-9.5 m per year, and on the north side of Xixiabangma to be 4.0-5.2 m per year. By looking at climatological records and ice

cores, they determined that the glacier retreat was caused by the combined effect of reduced precipitation and warmer temperatures; they predicted that, as long as the present conditions prevail, the glaciers will continue to retreat.

Kulkarni *et al.* (2005), using satellite data from between 1990 and 2001, found that Parbati Glacier, in the Kullu District of the Himachal Pradesh, retreated 578 m during the span from 1990 to 2001—a rate of recession of ~ 52 m per year. Field observations in 2003 at the glacier terminus confirmed these findings. Kulkarni *et al.* (2007) estimated glacier retreat for 466 glaciers in the Chenab, Parbati, and Baspa basins from 1962 to 2001. They found an overall reduction in glacier area from 2077 km<sup>2</sup> in 1962, to 1628 km<sup>2</sup> in 2001, an overall deglaciation of 21%.

Despite the worldwide trend of glacier recession (WWF 2005; Ren *et al.* 2006; Barry 2006; Kolbert 2006; Zemp *et al.* 2006; UNEP 2008), it is important to note that global warming does not affect all glaciers the same (Dowdeswell *et al.* 2005); that is, while it has led to a recession in the majority of the world's mountain glaciers, there are also instances in which glaciers have advanced as a result of global warming (e.g., Winkler *et al.* 1997; Chinn 1999; Casassa *et al.* 2002; Chinn *et al.* 2005; Hewitt 2005; Andeassen *et al.* 2008). Chinn (1999) described how a number of glaciers in New Zealand—particularly mountain glaciers and valley glaciers—had experienced a reversal in the theretofore long-standing trend of glacial retreat. This period of advance, which seemed to last from approximately 1980 to 2000 (Chinn *et al.* 2005), was uniform on mountain and valley glaciers throughout New Zealand's Southern Alps (Chinn 1999). Chinn *et al.* (2005) explained that the positive balances could be attributed to a change in the Interdecadal Pacific Oscillation (IPO) and an associated increase in El Niño/Southern

Oscillation (ENSO) events over New Zealand, thus increasing precipitation and causing glaciers to advance.

Winkler *et al.* (1997) presented a similar situation—later summarized by Chinn *et al.* (2005)—in Norway. According to Chinn *et al.* (2005), the glaciers of Norway experienced a period of positive glacier mass balances and advance during approximately the same time span as Chinn’s (1999) findings in New Zealand. Also similar to New Zealand, which was influenced by ENSO events, the Norwegian glaciers’ growth was partially attributable to strongly positive North Atlantic Oscillation (NAO) events, which led to increased precipitation during the winter precipitation months, and a general shift of maximum precipitation from autumn toward winter (Chinn *et al.* 2005). Additionally, generally lower temperatures during the ablation season helped contribute to the glaciers’ advance (*ibid.*)

Molnia (2007) found that, while more than 98% of Alaska’s glaciers have been retreating since the end of the Little Ice Age, more than a dozen are advancing. Some of these glaciers have been advancing for more than two centuries. Many of the advancing glaciers are, or were formerly, tidewater glaciers. While these outliers represent less than 2% of Alaska’s glaciers, making them decidedly the exception to the rule, they demonstrate, along with advancing glaciers in New Zealand (Chinn 1999; Chinn *et al.* 2005) and Norway (Winkler *et al.* 1997; Chinn *et al.* 2005), the complexities and the multiple factors involved in a glacier’s recession or advance.

In the Karakoram, Hewitt (2005) found that a number of glaciers have been advancing since the 1990s, and many more have shown surge activity as well. These advances are confined to the glaciers with the highest level of relief, and occur suddenly

and sporadically. Hewitt was quick to note that these anomalous glaciers do not refute the case for global climate change; on the contrary, he felt that climate change is the only viable explanation for these glaciers' advances. That is, warmer air is able to hold more moisture, and thus transport it to higher elevations. Additionally, a greater number of summer storms resulted in an increase in summer-time accumulation, and a general decrease in summer-time mean and minimum temperatures, both of which seemed to contribute to the glaciers' anomalous activity, as well.

Hewitt's (2005) findings were paralleled by Bishop and Shroder (2009), who found an even greater number of glaciers in the Karakoram to be advancing. They found there to be an inverse correlation between precipitation in the Karakoram Range and strength and number of ENSO events in the South Pacific—suggesting that lower pressures over the Indian Ocean produce weak monsoons, which subsequently allows the mid-latitude Westerlies to exert a greater-than-normal influence over the Karakoram.

## **2.2 Glacier Studies in Ladakh**

Some of the earliest maps of Ladakh were produced by the Geological Survey of India in the mid- to late-nineteenth century (Stoliczka 1865, 1866; Lydekker 1876, 1880, 1883). However, these studies focused primarily on the geology of the region, giving little mention to glaciers or glacial features. A number of publications were also produced by various expeditions in those early years (Cunningham 1854; Drew 1875; Lambert 1877; Tanner 1891). These early works tended to focus on the Ladakhi people and their culture, farming methods in Ladakh's harsh environment, and the impressive geomorphology of the region. Lambert (1877:95) mentioned a geomorphologic

formation seen throughout the region which had “every appearance of a huge unfinished railway embankment”. These formations, it was noted, seemed to occur at or near the ends of valleys. Lambert had no hypothesis as to the source of these giant mounds of debris, but now it seems quite obvious: these were ancient moraines from large—in Lambert’s time unthinkable so—former glacial advances (Figure 2). Tanner (1891:409-410) devoted a substantial portion of his paper to a discussion of snowlines and the “great frozen rivers” that flowed from the peaks of the great mountains, describing how the glaciers flowed into the valleys and “dispute[d] with the hardy mountaineers for the possession of the scanty area of the soil”. Tanner also described scenes in which glaciers had flown into villages, overtaking forests, fields, orchards, and people’s houses. However, as Tanner’s paper was presented as an address to the Royal Geographical Society, it did not include any maps of the glaciers he was discussing.



**Figure 2. Giant paleomoraine in the Leh Valley, similar to the “huge unfinished railway embankment” described by Lambert (1877). (Photo by M.E. Byrne, 2007).**

Several decades later, Dainelli (1922) and Klute (1930) produced papers which discussed Ladakh's glaciers. They assumed former glaciations in the region had been primarily restricted to the main ridges of the Himalaya and Karakoram, and only to a few insular higher mountain groups in Ladakh. With a series of publications by de Terra and Paterson (1932), de Terra (1934, 1935), Auden (1935, 1937), Wadia (1937), Norin (1946), and Heim and Gansser's (1939) publication of the findings of a 1936 expedition by the Swiss, the scientific community's understanding of Ladakh's former and recent glacial histories began to form. However, with a few exceptions (e.g., Berthelsen 1953; Wadia 1957; Frenzel 1960; Gansser 1964; Tewari 1964), very few studies were done in Ladakh over the following decades, due to political tensions that began to arise in 1947 between India and its neighbors, Pakistan and China, following India's independence from British colonization, and the concurrent partition which freed the region of Kashmir from the Dogras, under whose rule the state of Jammu and Kashmir had been struggling since 1834 (Lamb 1966; Varma 1971; Lall 1989; Kaul and Kaul 1992; Rahman 1996; Schofield 2003; Bray 2005; Paul 2005; Khan 2007). Such tensions underscored the strategic importance of Ladakh and the areas around it. The Indian Government called for a military buildup in the area; travel in and through Ladakh was highly restricted, and, for most people—particularly foreign scholars and tourists—completely banned. This ban on tourism and foreign travel was not lifted until 1974 (Norberg-Hodge 1991; Loram 1996; Rizvi 1998), rendering field work in Ladakh virtually impossible during the period from 1947 to 1974.

After the Indian Government re-opened Ladakh to foreign travel, it experienced a groundswell of scientific research, particularly on its geology and geomorphology (e.g.,

Shah *et al.* 1976; Frank *et al.* 1977; Bassoulet *et al.* 1978, 1980; Fort 1978, 1983; Pal *et al.* 1978; Sharma and Kumar 1978; Sharma *et al.* 1978; Viridi *et al.* 1978; Andrews-Speed and Brookfield 1980; Brookfield 1981; Thakur 1981; Fort 1983; Burbank and Fort 1985). Fort (1983) used Landsat data to observe glaciers in northern Ladakh. While there is evidence of former glacial advances, the arid environment has led to a current paucity of glaciers. She noted that the upper parts of cirques in this area are primarily occupied by typical rock glaciers, which are strong indicators of an arid climate. In the nearby Zaskar Range, which has a climate regime similar to that of its northern counterpart, the Ladakh Range (Burbank and Fort 1985), Fort (1983) noted that glaciers can often be found flowing from summits of greater than 5500 m above sea level (asl), such as Spongtang (5293 m asl), Stok Kangri (6128 m asl), and Chiberang Ri (5945 m asl). These glaciers tended to be cirque glaciers or small ice-caps, which in some places extend down-valley to become valley glaciers.

The timing of glaciations in Ladakh is not well understood. A few relative chronologies exist for mountain glacier oscillations, but a paucity of numeric ages for most of the glacial stages leaves the current level of knowledge severely lacking (Burbank and Fort 1985; Lehmkuhl and Owen 2005; Phartiyal *et al.* 2005; Damm 2006). There is ample evidence, however, that Ladakh was extensively glaciated during the Quaternary. This can be seen by the presence of wide, U-shaped glacial valleys (Figure 3), well-developed lateral moraines, and large amounts of glaciogenic sediments along the upper course of major rivers (Pant *et al.* 2005).



**Figure 3. Glacially-formed valley in the Zaskar Range. (Photo by M.E. Byrne, 2007).**

There is little consensus regarding the number of Quaternary glacial advances in Ladakh. Using terrestrial cosmogenic nuclide surface exposure dating of moraine boulders and alluvial fan sediments, Owen *et al.* (2006) identified and dated five advances, possibly dating back as far as ~ 430 ka. Owen *et al.*'s (2006) findings are in contrast with the findings of others, such as Taylor and Mitchell (2000), who found there to have been three major glacial advances and one minor one; Osmaston (1994), who found evidence of four periods of glacial advance; and Fort (1983) and Burbank and Fort (1985), who found three former glacial periods. Damm (2006), meanwhile, found evidence of eight prominent former glacial advances in the Zaskar Range.

While there is some literature regarding the Quaternary glacial history of Ladakh (e.g., Fort 1983; Burbank and Fort 1985; Osmaston 1994; Owen *et al.* 1998; Taylor and



Mitchell 2000; Damm 2006), very little exists about current glaciers there and those glaciers' changes since the end of the LIA. An exhaustive glacier inventory, such as those that exist for the European Alps (e.g., Paul 2000, 2002; Kääb *et al.* 2002; Paul *et al.* 2002, 2004b, 2007), Patagonia (Aniya 1988; Casassa 1995; Aniya *et al.* 1996; Casassa *et al.* 2002), southern Baffin Island (Paul and Kääb 2005; Svoboda and Paul 2009), western Canada (Bolch *et al.* 2008b), and various other glaciated regions has not been created for Ladakh, but several less extensive glacier inventories exist for nearby areas of the Himalaya. Additionally, the number of glaciers contained within the GLIMS database continues to increase, and there are currently efforts being made to include glaciers from various parts of the Himalaya in it. Cotton and Brown (1907) were the first to complete a survey of glaciers in the Himalaya, focusing on the Garhwal-Kumaon Himalaya. Mason (1930) studied and mapped 34 glaciers in the Karakoram Range and its neighboring regions. Vohra (1978, 1980) created an inventory of Himalayan glaciers; however, it gave little attention to Ladakh. Dhanju (1990), Kulkarni (1991), Dobhal and Kumar (1996), and Berthier *et al.* (2007) all created inventories of glaciers in the Himachal Himalaya. The International Centre for Integrated Mountain Development (ICIMOD) created an inventory of glaciers and glacial lakes in the Hindu Kush Himalaya in Nepal (Mool *et al.* 2001a) and Bhutan (Mool *et al.* 2001b). However, still no extensive glacier inventory exists for Ladakh.

### **2.3 Glacier Mapping**

One of the most effective methods of measuring glacier change is through the use of remotely sensed images (Gao and Liu 2001; Barry 2006; Bolch *et al.* 2006; Rees 2006;

Buchroithner and Bolch 2007; Racoviteanu *et al.* 2008). Often, in remote areas, remote sensing is the *only* way to map glaciers, and it provides the ability to map and monitor many glaciers over a large area simultaneously—a task that would otherwise be impossible (Bolch *et al.* 2006; Racoviteanu *et al.* 2008). Additionally, semi-automated processes now make glacier monitoring viable on a larger scale than ever before (Racoviteanu *et al.* 2008). The plethora of available sensors provides the opportunity for a multitude of methods to be used to map the various glacier types (Gao and Liu 2001; Hubbard and Glasser 2005; Rees 2006).

The use of remotely sensed images to map glaciers is hardly a new concept. It was less than two months after the launch of the first ERTS (later renamed the Landsat 1) satellite in 1972 that the first glacier, Iceland's Myrdasjokull Glacier, was imaged by satellite (Williams *et al.* 1997). Since then, the number of multi-spectral sensors has proliferated, vastly increasing the ability to view glaciated regions from space. In addition to the Multispectral Scanners (MSS) aboard Landsat 1-3, other medium-resolution (10-90 m) imagery is available from the following sensors: Landsat Thematic Mapper (TM), aboard Landsats 4 and 5; Landsat Enhanced Thematic Mapper Plus (ETM+), aboard Landsat 7; Satellite Pour l'Observation de la Terre (SPOT); Advanced Spaceborne Thermal Emission and Reflection Radiometer (ASTER), aboard the Terra Satellite; the Indian Remote Sensing Satellite (IRS); and more recently the Advanced Land Observing Satellite (ALOS), which was launched in 2006. Additionally, sensors with meter and sub-meter spatial resolution, such as IKONOS, Quickbird, and GeoEye-1, provide imagery comparable to aerial photography; however, these sensors have a narrow swath size and long revisit intervals, which, along with the high cost of their imagery,

limits their use for glacier mapping in most instances. Additionally, high resolution imagery from CORONA, the American intelligence spy satellite series, was declassified in 1995, providing imagery and stereo imagery of glaciated areas for the period from 1960 to 1972 (Altmaier and Kany 2002; Lillesand *et al.* 2004; Bolch *et al.* 2008; Racoviteanu *et al.* 2008).

The Global Climate Observing System (GCOS) defines the basic measurements of glacier characteristics as length and mass balance (GCOS 2003). However, Barry (2006) explained that glacier area, as well as glacier volume and ice velocities are also subjects of interest when studying glacier change. When using remotely sensed imagery, one's options differ from those available with field data. Gao and Liu (2001) explained that remote sensing can be used for mapping glaciers, monitoring their spatial variations, determining flow velocities, estimating mass balance, and modeling snowmelt runoff. These options are limited, however, by the type of remotely sensed data available (Hubbard and Glasser 2005; Rees 2006). Additionally, supraglacial debris often complicates the process of mapping glaciers due to its spectral similarity to the surrounding topography (Bishop *et al.* 1995; Ranzi *et al.* 2004; Kääb 2005; Bolch *et al.* 2006; Racoviteanu *et al.* 2008).

One of the most effective methods of mapping clean ice is with the use of band ratios and the normalized difference snow index (NDSI) (e.g., Klein and Isacks 1998; Sidjak and Wheate 1999; Paul 2000a, 2000b; Gao and Liu 2001; Paul *et al.* 2002; Kääb *et al.* 2003; Ranzi *et al.* 2004; Bolch and Kamp 2006; Narama *et al.* 2006; Rees 2006; Racoviteanu *et al.* 2008). Sidjak and Wheate (1999) examined the effectiveness of band

ratios and the NDSI for creation of a glacier inventory in the Illecillewaet Icefield in British Columbia, Canada.

Single band ratios involve taking the ratio of a visible band (VIS) and a short-wave infrared, such as Landsat 4/Landsat 5, or ASTER 3/ASTER 4. Band ratios were used effectively by Paul *et al.* (2002) and Kääb *et al.* (2002) to map clean glaciers for the Swiss Glacier Inventory (SGI). They were also used by Narama *et al.* (2006) and by Bolch (2007) to map glaciers and glacier change in the northern and inner Tien Shan. Bolch and Kamp (2006) used band ratios to map the clean ice as part of a morphometric analysis of glaciers in the Bernina Group of the Swiss Alps, and the northern Tien Shan.

NDSI is similar to the Normalized Difference Vegetation Index (NDVI), which is used for mapping vegetation, but the NDSI uses ASTER bands 1 and 4 ( $\text{VIS} - \text{SWIR} / \text{VIS} + \text{SWIR}$ ). Racoviteanu *et al.* (2008) explained that band ratios and the NDSI take advantage of the high reflectivity values of snow and ice in the visible wavelengths, allowing the user to distinguish them from darker values associated with rocks and debris, soil, and vegetation.

Another method of mapping glaciers that has been used with some success is the application of thermal bands from Landsat TM and ETM+ (Band 6), and, particularly, the ASTER dataset (Bands 10-14) (e.g., Rana *et al.* 1997; Nakawo and Rana 1999; Taschner and Ranzi 2002; Ranzi *et al.* 2004; Bolch and Kamp 2006; Suzuki *et al.* 2007; Racoviteanu *et al.* 2008). This method takes advantage of the fact that glaciers, being composed of ice, release very little heat, and thus have a thermal signature that is different from that of their surroundings (Racoviteanu *et al.* 2008). However, the ability to distinguish glaciers with thermal imagery is hindered when the thickness of the debris

atop the glacier passes a certain threshold (Nakawo and Rana 1999; Taschner and Ranzi 2002; Ranzi *et al.* 2004; Bolch and Kamp 2006; Bolch *et al.* 2007; Racoviteanu *et al.* 2008). Nakawo and Rana (1999) demonstrated the threshold at which glacier debris begins to confound thermal sensors to be  $\sim < 2$  cm. They used thermal imagery to estimate debris-cover thickness and ablation rate on glaciers in Nepal. Ranzi *et al.* (2004), however, disagreed with this estimate, claiming that thermal imagery can be used effectively to determine glaciated areas as long as the debris cover is less than 40-50 cm. They used thermal data and band ratios to map Miage and Belvedere Glaciers, a pair of debris-covered glaciers in the Italian Alps.

Bolch and Kamp (2006) used thermal bands as part of a multidimensional approach to map glaciers in the Bernina Group and the northern Tien Shan. Buchroithner and Bolch (2007) and Bolch *et al.* (2007) used thermal data as part of a similar method to map glaciers in the Khumbu Himal, around Mt. Everest in Nepal. All three of these papers echoed Ranzi *et al.*'s (2004) finding that thermal bands are effective for mapping debris-covered glaciers, as long as the debris cover is less than  $\sim 40$ -50 cm thickness.

Supervised and unsupervised classifiers can be helpful for distinguishing glaciers from surrounding terrain (e.g., Gratton *et al.* 1990; Aniya *et al.* 1996; Brown *et al.* 1998; Bishop *et al.* 1999, 2001; Sidjak and Wheate 1999; Paul 2000a, 2000b; Gao and Liu 2001; Herzfeld and Zahner 2001; Paul *et al.* 2002, 2004; Zollinger 2003; Rees 2006; Bolch *et al.* 2007); however, their effectiveness as an individual mapping method—that is, when it is not used in conjunction with another approach—is limited on debris-covered glaciers (Paul 2000a, 2000b; Gao and Liu 2001; Paul *et al.* 2002, 2004; Bolch *et al.* 2007). Aniya *et al.* (1996) used the ISODATA cluster analysis, followed by Parallel

Piped and Maximum Likelihood classifiers to map glaciers in the Southern Patagonia Icefield (SPI) from Landsat TM imagery. The Parallel Piped classifier was used first because of its simplicity, but when areas were found misclassified the researchers reclassified those areas with the Maximum Likelihood classifier. Sidjak and Wheate (1999), similar to Aniya *et al.* (1999), used a Maximum Likelihood classifier with Landsat TM images to map glaciers for a glacier inventory of Illecillewaet Icefield, British Columbia.

Bishop *et al.* (1999) compared the abilities of two different classifiers to determine supraglacial characteristics around Nanga Parbat, Pakistan. The first method they tested was an artificial neural network (ANN), which was given a minimal amount of training input. The ANN output was compared with the output of a stratified unsupervised classification approach using the ISODATA clustering algorithm. Accuracy assessment and comparative visual analysis suggested that the ANN was more effective for mapping the glacier characteristics than the unsupervised approach. Bishop *et al.* (2001) also used an unsupervised classification approach with the ISODATA clustering algorithm as part of a two-tiered hierarchical approach for mapping glaciers around Nanga Parbat.

The use of a digital elevation model (DEM) or a digital terrain model (DTM) greatly enhances the ability to characterize features in a mountainous environment. They are increasingly being used for glacier mapping and terrain analyses (e.g., Duncan *et al.* 1998; Sidjak and Wheate 1999; Paul 2000a, 2000b; Bishop *et al.* 2001, 2003; Gao and Liu 2001; Paul *et al.* 2002, 2004, 2007; Kääb *et al.* 2003; Kamp *et al.* 2003, 2005; Bolch *et al.* 2005, 2006, 2007; Eckert *et al.* 2005; Kääb 2005; Quincey *et al.* 2005; Narama *et*

*al.* 2006; Buchroithner and Bolch 2007; Berthier and Toutin 2008; Bolch *et al.* 2008a; Racoviteanu 2008). Racoviteanu (2008) explained that DEMs can be used in a GIS to extract a number of various parameters from a glacier. Sidjak and Wheate (1999) similarly detailed the ability of DEMs, when combined with thematic maps, to derive various glacier attributes. Gao and Liu (2001) described the significance of the ability of DEMs to eliminate the effects of topographically-created shadows, as well as their ability to distinguish topographic features, thus nullifying some of the deficiencies of multi-spectral data.

Digital Elevation Models were essential in the calculation of glacier parameters in the creation of the Swiss Glacier Inventory (SGI) (Paul 2000a, 2000b; Paul *et al.* 2002, 2004, 2007). Kamp *et al.* (2003, 2005), meanwhile, generated DEMs of Cerro Sillajhuay, a volcano in the Andes of Chile/Bolivia. The DEMs were then used to calculate geomorphic parameters, which can be used to identify and describe geomorphologic forms and processes. The morphometric parameters extracted were elevation, aspect, slope angle, vertical curvature, and tangential curvature. They explained that the DEMs were helpful in examining macro- and meso-relief and that they provide the ability to map at medium to large scales (1:100,000 and 1:50,000). Bolch *et al.* (2008a) created DTMs for the Khumbu Himal from ASTER data and compared CORONA and ASTER imagery, allowing them to calculate the amount of planimetric and volumetric change there since 1962.

Kääb (2005) used DEMs from two different data sources—SRTM3 and ASTER—to create a single master-DEM. He then used the ASTER imagery to derive glacier surface velocities in the Bhutan Himalaya through image matching. He explained

that the DEMs from the two data sources were generally of equal accuracy, but the SRTM3 data contained fewer gross errors. However, the SRTM3 data had a number of “holes” in the DEM, hence the need for two data sources. Similarly, Bolch *et al.* (2005) used ASTER-derived DEMs to map mountain areas in four distinct locations: Cerro Sillajhuay, of the Andes of Chile/Bolivia; the Central Cordillera de Merida of the Venezuelan Andes; Tirich Mir, of the Eastern Hindu Kush of Pakistan; and the Northern Tien Shan of Kazakhstan/Kyrgyzstan. SRTM data was used to correct artifacts in the ASTER data. Bolch and Kamp (2006) compared ASTER-derived DEMs with SRTM3 DEMs. They found that, in areas of high elevation and relief, ASTER data tends to have values that are a bit too high; and SRTM3, conversely, gives values that are slightly too low. Still, they found the DEMs from both datasets to be of good use for glacier delineation.

Increasingly, morphometric parameters and multi-dimensional approaches are being used to map glaciers and glacial characteristics (Dikau 1989; Schmidt and Dikau 1999; Sidjak and Wheate 1999; Bishop 2001; Bonk 2002; Paul *et al.* 2002, 2004a; Zollinger 2003; Solomina 2004; Bolch *et al.* 2005, 2006, 2007; Bolch and Kamp 2006; Bolch 2007; Buchroithner and Bolch 2007; Bolch *et al.* 2008a; Racoviteanu 2008). Sidjak and Wheate (1999) applied a number of different inputs for their glacier inventory of the Illecillewaet Icefield employing band ratios and NDSI, image differencing, and a principal components analysis (PCA), all of which were then used as input bands for a supervised Maximum Likelihood classification. Paul *et al.* (2002) paralleled this approach when creating the SGI, combining band ratios with an unsupervised classifier and then with a supervised classifier. They also attempted the process with NDSI, PCA,



and with atmospheric corrected TM bands, but concluded that those methods were less accurate than the ones they ultimately used.

Bishop *et al.* (2001) used a two-tiered hierarchical model to map Raikot Glacier, on the north side of Nanga Parbat in northern Pakistan. The first tier of their approach included the calculation of glacier parameters, including slope angle, slope aspect, profile curvature, and tangential curvature. These parameters were then used to calculate terrain form objects (TFOs), from which the glacier's features could be characterized. They concluded that the two-tiered hierarchical model was able to reasonably distinguish and map Raikot Glacier, but that a three-level hierarchical model shows much greater promise in the future. Bonk (2002) used the same method on Sachen Glacier, also on Nanga Parbat, but concluded that the two-level hierarchical model is inadequate for mapping complex glacial and mountain environments. He also felt that a morphometric approach could be effective.

Paul *et al.* (2004a) used a multi-dimensional approach for mapping glaciers in the Swiss Alps. They combined supervised classifiers with slope information derived from a DEM and then applied neighborhood analysis and change detection to the resulting image. The biggest advantage of this approach was that the majority of the processes were done automatically. Even when some manual editing was required, it was still much faster than manually delineating hundreds of glaciers separately. The results were compared with the results of an ANN, and the ANN by itself was found to be ineffective for mapping debris-covered glaciers. However, Paul *et al.* (2004a) suggested that, if combined with slope data, an ANN could also be effective.

Bolch and Kamp (2006) used a method similar to the one used by Paul *et al.* (2004a). However, they used several other morphometric parameters in addition to slope. These morphometric parameters were combined with a cluster analysis to map glaciers in the Bernina Group and in the northern Tien Shan. One large difference between the two approaches was that the slope threshold used by Paul *et al.* (2004a) in the Alps was too high when applied to the Tien Shan. When it was lowered from ~ 24 degrees in the Alps to < 12 degrees for the Tien Shan, it produced a much more favorable result. Bolch and Kamp (2006) found that the method has difficulty mapping glaciers that have a smooth transition from ice to valley—that is, glaciers with little or no lateral or terminal moraines. However, they concluded that this method produced satisfying results on debris-free and large debris-covered glaciers.

Bolch *et al.* (2007) used an even more robust approach, combining morphometric parameters and thermal data with a supervised classifier to map debris-covered glaciers on the Nepalese side of Mt. Everest. The results were promising; however, the method was inadequate in the distal areas of glaciers, where stagnant ice confounds delineation, and where it is often even difficult to distinguish between active and dead ice when one is in the field. As DEMs with greater spatial resolution become available, this method will become more effective. Buchroithner and Bolch (2007) used thermal data and morphometric parameters for glaciers in the same study area and came to the same conclusion: the method was a success, but it still has difficulty in the distal areas of glaciers. They also state that this method will be improved by the availability of better resolution DEMs.

## 2.4 The GLIMS Project

The Global Land Ice Measurements from Space (GLIMS) project is an international cooperative effort, with the goal of inventorying and monitoring as many of the Earth's glaciers as possible (Schicker 2006; Raup *et al.* 2007a, 2007b; Global Land Ice Measurements from Space 2009). Started in 1995 as an Advanced Spaceborne Thermal Emission and Reflection Radiometer (ASTER) Science Team effort, GLIMS uses a system of Regional Centers to acquire satellite images of glaciers from around the world, analyze them for glacier extent and changes, and to assess the changes in terms of forcings (Figure 4). As of March 2006, the GLIMS project involved seventy-one Regional Centers, Stewards, and core institutions, located in twenty-seven different countries (Raup *et al.* 2007a).

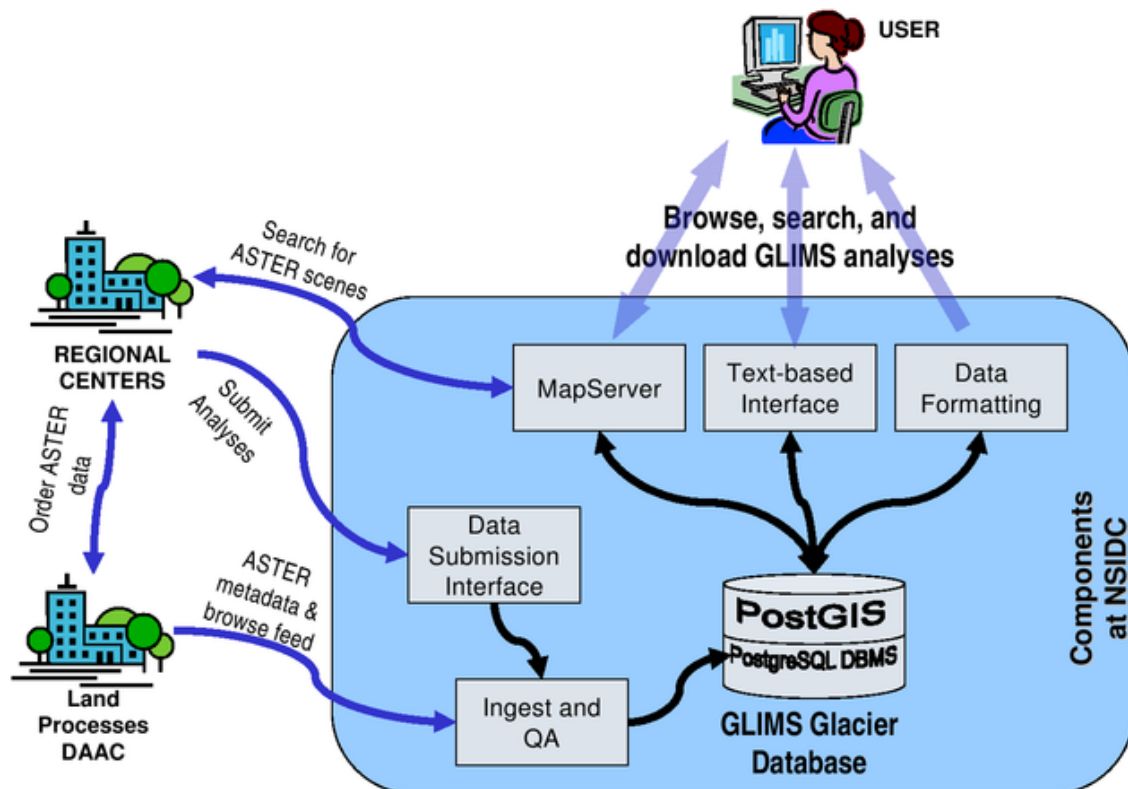


Figure 4. Organizational block diagram for the Global Land Ice Measurements from Space (GLIMS) program. DAAC: Distributed Active Archive Center; QA: Quality Assessment. (Global Land Ice Measurements from Space 2009).

As a Steward office for the South Asia Region, the University of Montana serves as a direct correspondent to the International Centre for Integrated Mountain Development (ICIMOD), the Regional Center for the Indian, Nepal, and Bhutan Himalaya. Thus, when the University of Montana wishes to submit glacier outlines to the National Snow and Ice Data Center (NSIDC), where all GLIMS's glacier database is stored, it does so by sending the data to ICIMOD, rather than directly to NSIDC (Global Land Ice Measurements from Space 2009).

### 3. Study Area

#### 3.1 Ladakh

Ladakh, in the northwestern part of India (Figure 5), makes up more than half of the Indian State of Jammu and Kashmir, in the region of Kashmir (Figure 6). Norberg-Hodge (1995:142) aptly described it as “a harsh and mountainous desert of wild beauty, set among the jagged peaks of the western Himalaya.” In its center, it is crossed from

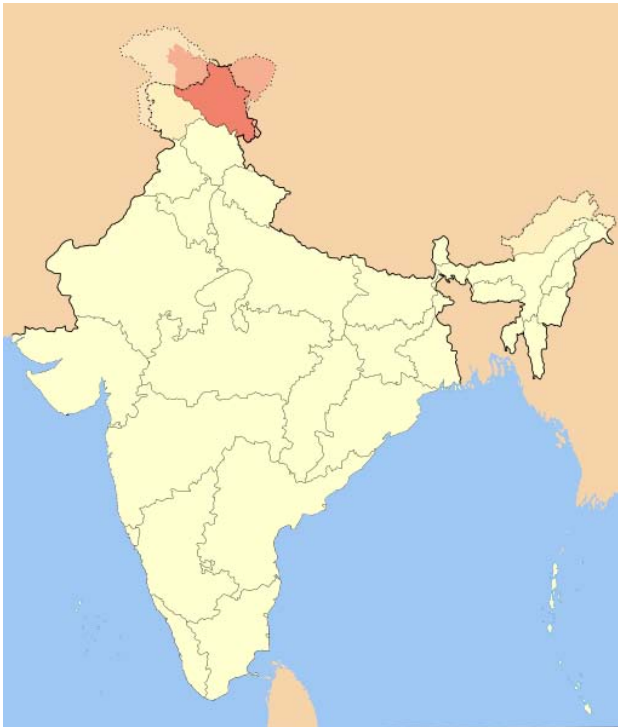


**Figure 5. India** ([www.permaculture.org.au/category/permaculture-projects/demonstration-sites/](http://www.permaculture.org.au/category/permaculture-projects/demonstration-sites/)).

Northwest to Southeast by the Ladakh and Zaskar Mountain Ranges, at the Western end of the Himalayas. To the north and south of Ladakh lie the Karakoram and Greater Himalaya ranges, respectively (Loram 1996). Bisecting the region is the Indus River and the Indus River Valley, separating the Ladakh Mountains, in the north, from the Zaskar Mountains in the south.



of between 2700 and 4200 m (Negi 2002), with its highest points at Nun (7135 m asl) and Kun (7077 m asl) (Weare 2002).

The Himalaya mountain system can be divided into any number of smaller, less extensive ranges. Zgorzelski (2006) first divides the Himalayas into two parts: the external arc, or the Great Himalayas, to the south, and the internal arc, or Trans-Himalayas, in the north. The external arc can be further divided into—from east to west—the Eastern Himalayas, Bhutan Himalayas, Sikkim Himalayas, Central Himalayas (also known as the High, Great, or Nepal Himalayas), Garhwal Himalayas, and Western Himalayas.

The Trans-Himalaya, meanwhile, includes the Zaskar and Ladakh mountain ranges, which together cover the majority of Ladakh (Figure 7), as well as the East Karakoram, Kanjiroba Himal, and the Kailash mountain ranges. The Trans-Himalaya can be differentiated orographically between the east and west. The ridges in the eastern part generally do not follow a distinct orientation, but rather it is a system of basins bounded by these ridges and connected by river gorges. The western and central parts of the Trans-Himalayas follow a more distinct east-west orientation. On the western end of the Trans-Himalayas, the Zaskar range, combined with the Ladakh Batholith, make up the transitional zone between the Trans-Himalayas, on the Indian continent, and the Eastern Karakoram, on the Eurasian continent (Zgorzelski 2006).

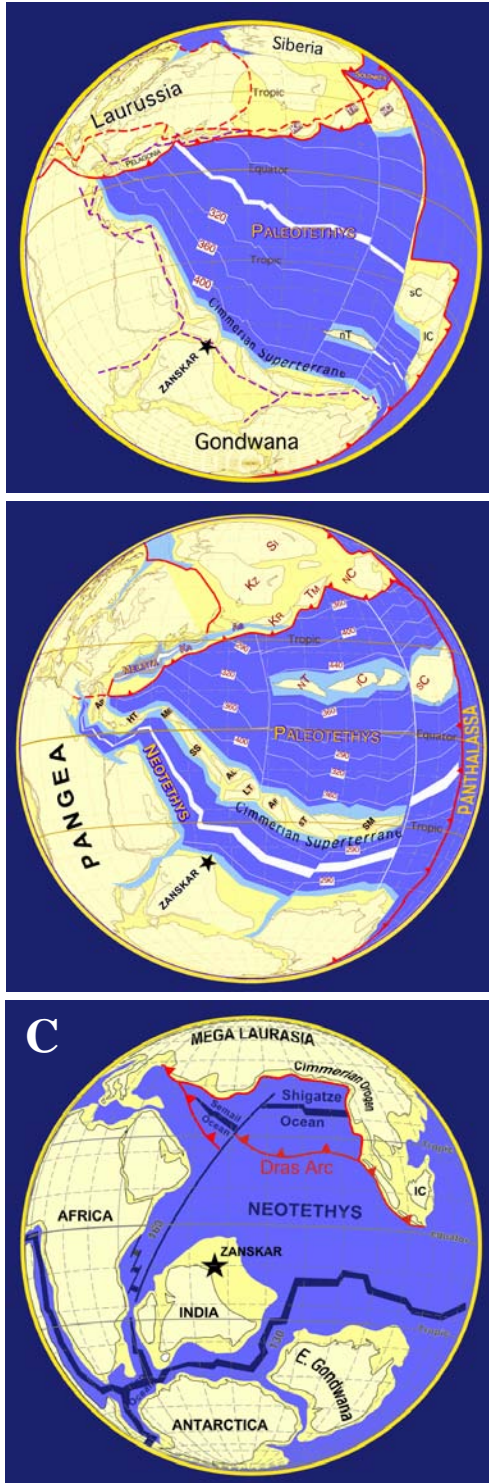


Figure 7. The Trans-Himalaya in Ladakh (<http://www.global-lab.org/mt/BBFall07/>).

### 3.3 Tectonic Evolution of the Himalaya

A number of terranes—the Cimmerian Superterrane—broke away from the Indian continent, then a part of Gondwana, during the Early Carboniferous (Figure 8A). The rift between Gondwana and these superterrane developed into the Neotethys Ocean during the early Permian, as the superterrane continued to drift northward, away from Gondwana (Figure 8B). The Indian continent, along with Australia and Antarctica, was split from the rest of Gondwana by a major rifting event in the Norian, 210 Ma, to form





**Figure 8. The Indian sub-continent broke away from Gondwana in the Norian, eventually crossing the Neotethys and colliding with Eurasia. (Patriat and Achache 1984; Stampfli and Mosar 1998; Dèzes 1999).**

East Gondwana (Figure 8C). East and West Gondwana separated from one another, with oceanic crust being created between them, in the Callovian (160-155 Ma), and India struck off on its own during the Early Cretaceous (130-125 Ma), and opened the “South Indian Ocean” (Shroder 1993; Dèzes 1999). The Indian continent moved northward at an average speed of 16 cm/year, covering a distance of 6000 km (Figure 9; Dèzes 1999).

Meanwhile, a series of volcanic arcs, including the Ladakh-Kohistan arc terrane, had formed in the northern part of the Neo-Tethys Ocean straits between Eurasia and the northward moving Indian continent. The arc collided into the Karakoram plate along the Shyok Suture Zone (SSZ) and was deformed by the intense heat and pressure of the collision, forming the southern edge of the Eurasian continent between 102 and 80 Ma (Shroder 1993; Hodges 2000; Weinberg and Dunlap 2000; Owen 2003). As the Indian plate continued to move northward, the Neo-Tethys crust was subducted beneath Ladakh-Kohistan and

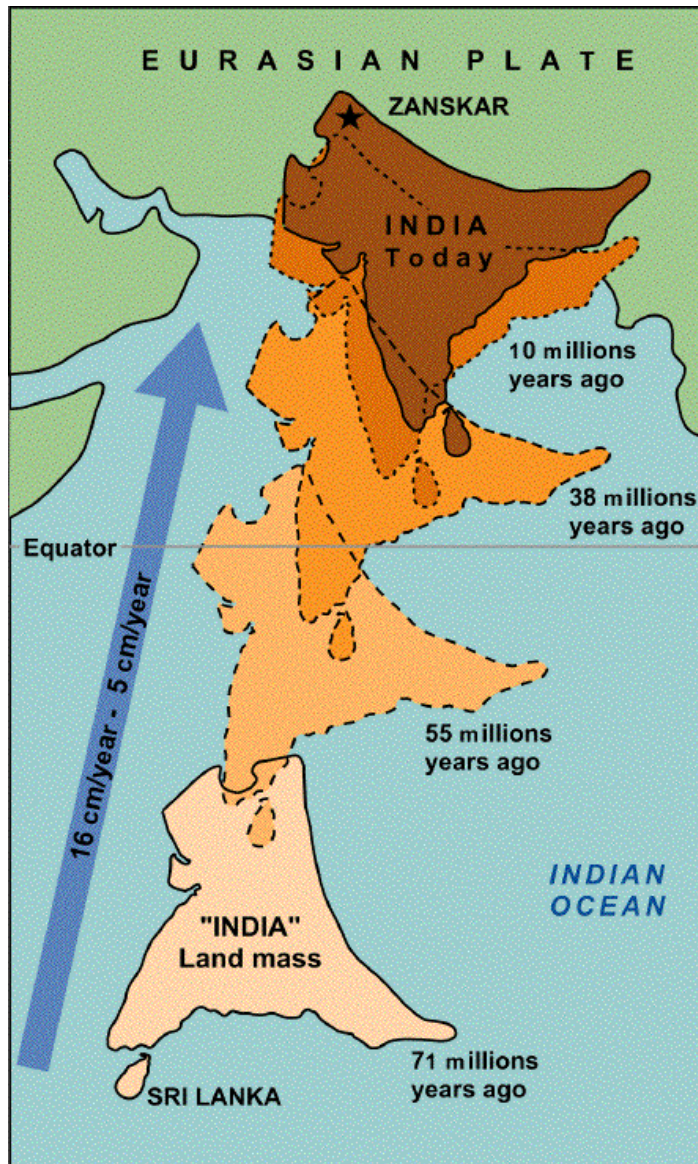


**Figure 9.** India drifted northward at a rate of ~ 16 cm per year. (Patriat and Achache 1984; Stampfli and Mosar 1998; Dèzes 1999). Dèzes (1999) noted that the dates on this figure are incorrect; India collided with Eurasia ~ 55 Ma.

the Eurasian plate.

The Indian continental lithospheric plate crashed into the Eurasian continental lithospheric plate between 70 and 50 Ma (Weinberg and Dunlap 2000; Yin and Harrison 2000; Owen 2004), creating the Himalayas, as well as the Karakoram, the Pamirs, the Hindu Kush, the Tien Shan, and the Kun Lun mountain ranges (Coxall and Greenway 1996).

There is, however, little consensus as to when exactly the collision of the two plates took place. Singh *et al.* (2007) and

Leech *et al.* (2005) claim the

collision took place no later than  $57 \pm 1$  Ma; Shroder (1993) says the collision began perhaps 60-50 Ma; and Weinberg and Dunlap (2000) cite strong evidence that the collision took place 52-50 Ma. Regardless of the exact date, the highly deformed Ladakh island arc terrane was sandwiched between the two continental plates and thrust violently upward (Shroder 1993; Loram 1996; Rizvi 1998; Owen 2003; Zgorzelski 2006; Singh *et*

*al* 2007). It is possible that parts of the batholith experienced additional melting between 50 and 46 Ma (Weinberg and Dunlap 2000; Bhutani 2004). The oceanic crust, too, was thrust upward to form the Zaskar mountain range.

The collision that created the Ladakh and Zaskar ranges took place along the Indus-Tsangpo Suture Zone (ITSZ) and Shyok Suture Zone (SSZ) (Gansser 1964; Dewey and Bird 1970; Dewey and Burke 1973; Le Fort 1975, 1986; Thakur 1993; Searle *et al.* 1988; Jain *et al.* 2002, 2003; Bhutani *et al.* 2004; Singh *et al.* 2007). Following the subduction and closure of the Neo-Tethys, the continental crust continued to subduct beneath the Eurasian Plate, reaching a minimum depth of 90 km at  $53.3 \pm 0.7$  Ma (de Sigoyer *et al.* 2000; Guillot *et al.* 2003; Singh *et al.* 2003, 2007; Sachan *et al.* 2004; Leech *et al.* 2005). Over the past 50-40 Ma, the Indian plate has continued to move northward, forcing itself into the Eurasian plate at a nearly constant rate of  $\sim 5$  cm per year (Owen 2003), with pressure being most intense  $\sim 30$  Ma (Shroder 1993).

This continued northward pressure has led to a crustal shortening of between 1400 and 2000 km (Molnar and Tapponier 1975; Patriat and Achache 1984; DeMets *et al.* 1994; Dèzes 1999; Yin and Harrison 2000; Owen 2003; Harris 2007). Much of this crustal shortening was distributed across the Himalayas, leading to the uplift of the Great Himalayas and later, to the rapid uplift of Tibet, which began around 20 to 13 Ma, with a possible earlier uplifting event  $\sim 40$  Ma (Chung *et al.* 1998).

### **3.4 Geology**

The southernmost part of Ladakh lies in the aptly titled Higher Himalaya, the zone of the Himalaya with the highest elevation. The Higher Himalaya is a 10-15 km thick crystalline sequence comprised of metamorphics and granitoids, which represents a

Proterozoic basement—a part of the upper crust which became active once again with the beginning of the Himalayan orogeny when the Indian Sub-continent collided with Eurasia. In southern Ladakh, the Higher Himalaya are overlain by the Zaskar Crystallines, or Central Crystallines, a Tethyan Himalaya sequence of late Precambrian to Cretaceous-Eocene age, which stretch from the Zaskar Valley to the Chenab Valley in a NW-SE trending belt (Thakur 1992).

In the Suru Valley, the Zaskar Crystallines are overlain by the Sankoo Formation, of which the Nun Kun Massif (Nun: 7135 m asl; Kun: 7087 m asl) is a part. Stretching from Pensi La to the village of Sankoo, the Sankoo Formation represents the base of the Palaeozoic-Mesozoic sequence of the Zaskar Tethys Himalaya. It is made of low grade metasedimentaries and granites (*ibid.*).

Within the Zaskar Crystallines, infolded synclines of metamorphosed volcanics and carbonate beds occur. The metamorphosed volcanics are of Permian origin, while the carbonates are Lower Triassic in age. Later generation folds caused an already infolded Permian-Triassic sequence to be refolded along with the underlying Precambrian Zaskar Crystallines. This second-generation folding created the Suru dome, or Nun-Kun Dome, a massive NW-SE trending, doubly-plunging antiformal structure. Overprinting of amphibolite facies metamorphism at several locations near Nun-Kun Dome suggests a post-Mesozoic (Himalayan) age of metamorphism (Thakur *et al.* 1990; Thakur 1992).

The Zaskar Crystallines are overlain by the Tethys Himalaya along a tectonic contact called the Tethyan Thrust. The Tethyan sequence is separated from the Indus Suture Zone to its north by a south hading thrust, designated the Counter Thrust or the

Zaskar Thrust. On its eastern reaches the Tethyan zone extends along the southern margins of the Tibetan Plateau. Thus, this portion is sometimes called the Tibetan Zone. Approximately 40 km wide, the Tethys Himalaya consists of a 10 km thick sedimentary sequence, with ages ranging from the Late Precambrian to the Lower Eocene. The rocks of this sequence are predominantly fossiliferous, representing marine facies from the ancient Tethys Sea regime. The Tethyan sequences are exposed in the Zaskar Mountains, as well as in northern Kumaun, the Spiti Basin, and the Kashmir-Chamba Basin sequence, which is located to the south of the Higher Himalaya, but still part of the Tethyan Zone (Thakur 1992).

In the Zaskar Mountain Range, the Tethys Himalaya Zone is 70 km wide and ~ 15 km thick. Here the Tethys Sequence forms the Zaskar Synclinorium, with a northwest closure and a large klippe—the Spongtang Klippe, with its roots in the Indus Suture Zone—of the ophiolitic rocks occurring in the core of the synclinorium. Two distinct facies of Mesozoic origin can be found: the shallow shelf and deeper basin to slope facies of the Tethys Sea. Included within the Zaskar Synclinorium are the Zaskar Carbonates, which form the mountains of northern Zaskar. The carbonates are 1 km thick, and composed of thick-bedded grey, blue, and black limestones and dolomites together with intercalations of argillites, as well as thick green colored horizons of tuffites near the basal portion (Figure 10; *ibid.*).





**Figure 10. Strata of limestone, dolomite and tuffites in the Zaskar Range. (Photo by M.E. Byrne, 2007).**

To the north of the Tethys Himalaya lies the Trans-Himalaya which is separated from the former by the sharply defined Indus-Tsangpo Thrust. This area is home to the Indus Suture Zone, which includes the Ladakh Plutonic Complex, or the Ladakh Mountains (Figure 11). Also included in the Trans-Himalaya are the Shyok Suture Zone and the Karakoram Mountains, as well as the Kohistan Sequence, the Kailash Range, the Yarlungo-Tsangpo belt, and the Lahasa block of southern Tibet (Thakur 1992).

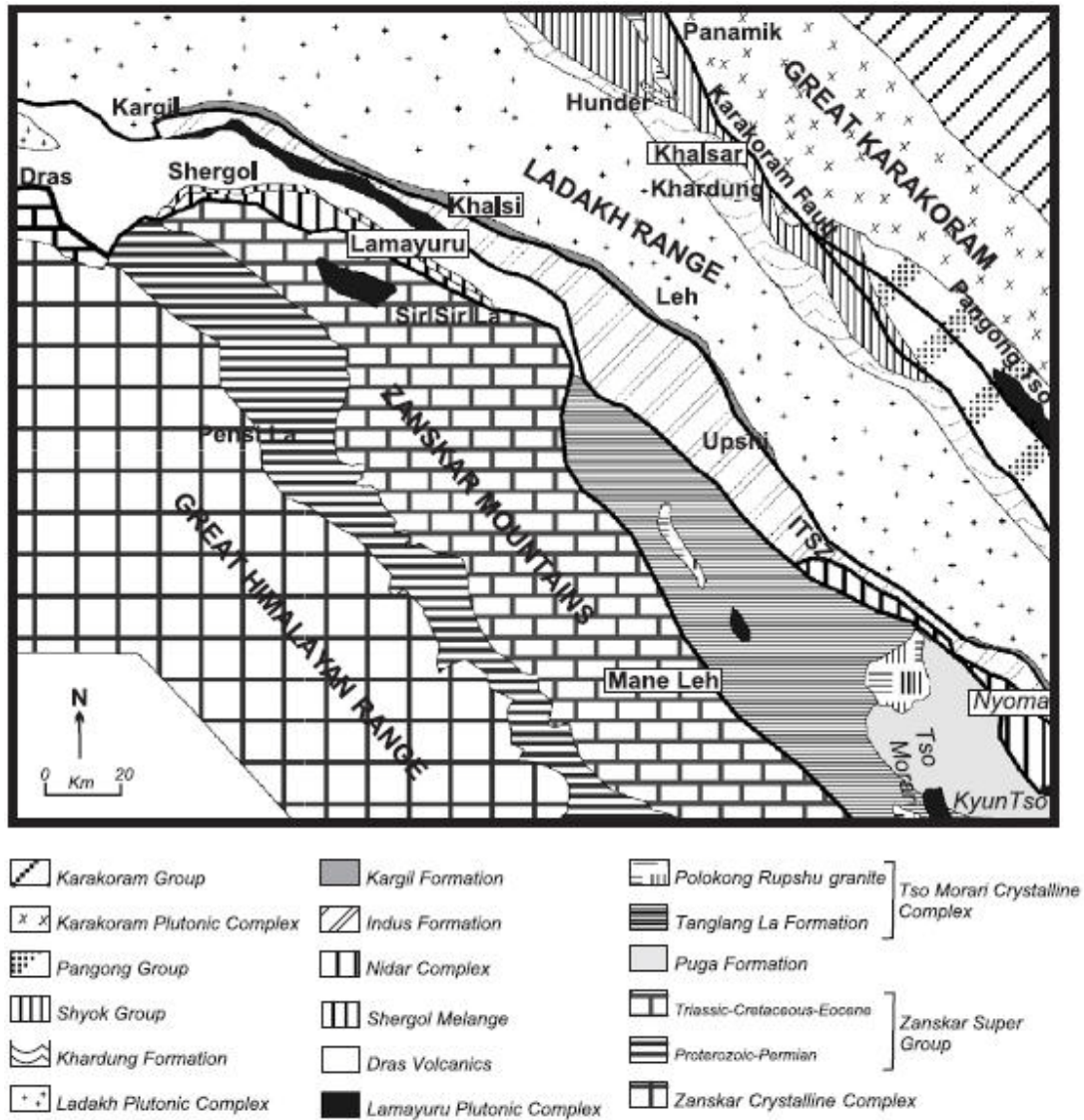


**Figure 11. Geological map of Ladakh (Phartiyal *et al.* 2005).**

On the southern edge of the Trans-Himalaya lies a 5 km thick sedimentary belt, which extends from northwest to southeast for more than 500 km strike-wise. This structure has been called the Indus Flysch (Dainelli 1934), the Indus Molasse (Tewari 1964; Frank *et al.* 1977), and the Indus Formation (Pal *et al.* 1978; Sharma and Kumar 1978; Thakur 1992). This sedimentary belt can be divided into two distinct tectonostratigraphic units: the autochthonous Kargil Formation, which overlies the granitoids of the Ladakh Plutonic Complex with a transgressive contact; and the para-

autochthonous Indus Formation, which at some points overthrusts the Kargil Formation, and at other points the Ladakh Plutonic Complex (Thakur 1981).

The Ladakh Plutonic Complex, also called the Ladakh Intrusives (Frank *et al.* 1977), Ladakh Granites (Sharma *et al.* 1978; Negi 2002), Ladakh Batholith (Honegg *et al.* 1982; Rai 1983; Scharer *et al.* 1984), and Ladakh-Deosai Batholith (Brookfield and Reynolds 1981), forms the Ladakh Range. It extends more than 600 km in a northwest to southeast direction, is 20-50 km wide, and has about 5 km of exposed thickness. The complex is composed primarily of quartz diorite, granodiorite, and monzodiorite to granite, with occasional plutons of gabbro, norite, anorthosite, and pyroxenite. Additionally, xenoliths of basic and metamorphic rocks are enclosed within the marginal parts of the complex. The basic rocks include metavolcanics, diorite, and amphibolites; the metamorphics contain quartzite, mica schist, and marble (Thakur 1992).

Overlying the northern margin of the Ladakh Plutonic Complex in the Shyok Valley and dipping 30° to 50° northeastward is the Khardung Formation. It is ~ 2 km thick, and consists primarily of acid with some intermediate volcanics together with volcanoclastic sedimentaries in the upper section. These rocks are predominantly rhyolitic, with subordinate dacitic and andesitic flows and thin bands of pyroclastic and tuffaceous material (*ibid.*).

To the north of the Khardung Formation lies the Shyok Suture Zone and, to the north of that, the Karakoram Mountains, which belong to a group of mountain belts that includes the Pamirs and the Tien Shan to the north, the Aghil and the Kunlun to the east, the Hindu Kush to the west, and the Kashmir Himalaya to the south (*ibid.*).



### **3.5 Geomorphology**

The geomorphology of Ladakh is heavily influenced by frost cracked rocks, boulders, scree and talus deposits, and by Quaternary glacial deposits, which are subsequently reworked and transported by glacial runoff, snowmelt, and mass movement processes (Jamieson *et al.* 2004). River valleys and gorges are dominated by large amounts of talus, scree cones, huge alluvial fans, and sediments. The cold, arid climate accelerates the disintegration of rocks through frost action, leading to extensive amounts of talus covering the slopes (Phartiyal *et al.* 2005). Another distinct feature of Ladakh's geomorphology is the presence of lacustrine sediments, dated at ~ 35-40 ka, located at the distal ends of alluvial fans that discharge into the Indus Valley. Such deposits can be found at Lamayuru and at Leh, and have been interpreted to have been created when large valley glaciers retreated during the Upper Pleistocene, and their moraine sediments were remobilized by mass movements to create large dams on their rivers (Jamieson *et al.* 2004).

### **3.6 Rivers**

The main river in Ladakh is the Indus. The Indus River begins at the glaciers of Mount Kailas in western Tibet, and flows, ultimately, to the Arabian Sea (Clift 2002; Phartiyal 2005). It enters the Himalaya in southeastern Ladakh, near its confluence with the Gurtang River, at ~ 4200 m asl (Negi 2002). It flows through Ladakh in a generally northwesterly direction along the Indus Suture Zone (Thakur 1992), effectively separating the Ladakh Mountain Range from the Zaskar Mountain Range. The Indus Valley has several terrace levels, which are often covered by large alluvial cones

deposited by incoming tributaries from the Ladakh and Zaskar Mountains (Figure 12). The Indus is also widely used by Ladakhis as a source of irrigation for the cultivation of crops (Figure 13; Zgorzelski 2006).



**Figure 12. Alluvial fan, reaching down from the Zaskar Range into the Indus Valley. (Photo by M.E. Byrne, 2007).**

Two other important rivers in Ladakh are the Zaskar and the Shyok rivers. The Zaskar Valley is deeper than the Indus and Shyok valleys. Its valley walls are steep (Zgorzelski 2006), forming a deep gorge through the Zaskar Mountains before joining the Indus about 40 km downstream of Leh (Figure 14; Negi 2002).



**Figure 13. Irrigation agriculture in the Indus Valley with the Zaskar Range to the left and the Ladakh Range to the right. (Photo by M.E. Byrne, 2007).**



**Figure 14. Confluence of the Indus (left) and Zaskar (center) rivers ~ 40 km downstream of Leh. (Photo by M.E. Byrne, 2007).**

The Shyok River Valley is as deep as the Indus Valley, but the valleys of its tributaries only occasionally form large alluvial cones; more often, they overhang the Shyok Valley (Zgorzelski 2006). After its origin from Rimo Glacier—one of the tongues of Siachen Glacier—the Shyok River flows in a southeastward direction, before turning sharply and running northwest after hitting the Pangong Range. The Nubra River, which also originates from Siachen Glacier, flows in the same direction, then joins the Shyok at the point where they turn to the northwest. This suggests a series of palaeofault lines trending NW-SE along the upper reaches of the rivers (Phartiyal *et al.* 2005).

### **3.7 Climate**

Ladakh is essentially a desert. The weather station at Leh records an average of ~ 80 mm of precipitation a year (Fort 1983), with the majority coming in the winter as snowfall, and the rest falling as rain between the months of July and September (Fort 1983; Negi 2002; Lehmkuhl and Owen 2005). The data recorded at Leh is not a perfect representation of the weather of Ladakh, as the weather station is located in the Leh Valley at ~ 3500 m asl. Higher elevations may receive a higher percentage of precipitation as snow, but a paucity of weather stations in Ladakh makes Leh's the only reliable source of climate data for the region.

The Himalaya-Tibet mountain system is influenced by four major climatic systems: the mid-latitude westerlies, the south Asian monsoon, the Mongolian high-pressure system, and the El Nino Southern Oscillation (ENSO). However, each system's level of influence varies throughout the range (Lehmkuhl and Owen 2005; Figure 15). In Ladakh, the two prevailing weather influences are the mid-latitude westerlies and the

Indian monsoon. The systems are blocked by the Greater Himalaya however, and their moisture contents are thus greatly reduced when they reach Ladakh (Fort 1983).

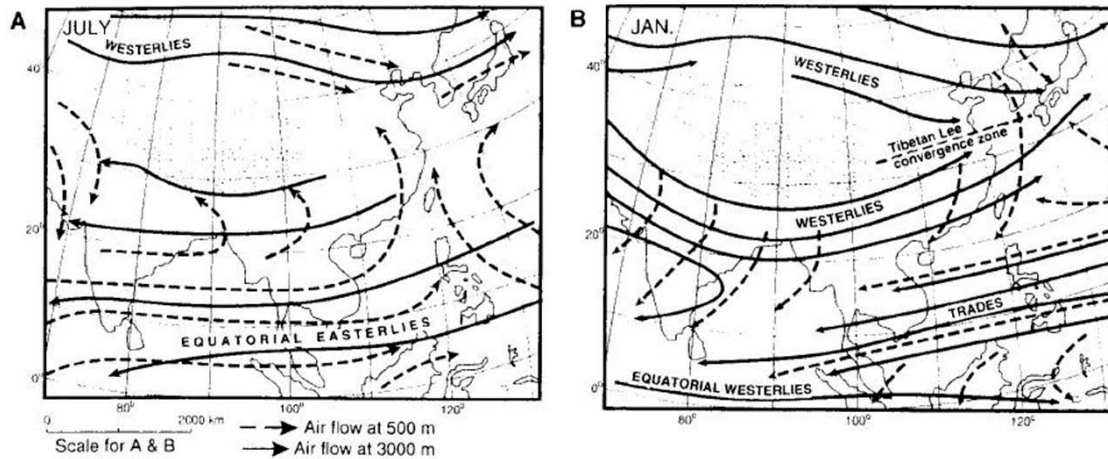


**Figure 15. Summer (A) and winter (B) weather patterns in the Himalaya (After Owen *et al.* 1998).**

In the summer the Indian monsoon advances past the Greater Himalayas, though it is greatly depleted by the time it reaches Ladakh (Figure 16). The summer regime is characterized by rain and snow, depending on elevation, latitude, aspect, etc. (Fort 1983; Zgorzelski 2006). To the north of Ladakh, in the Karakoram, Hewitt (2005) found that one-third of snow accumulation on glaciers occurs during the summer, which suggests that the monsoon passes at least that far north in most years, implying that Ladakh is impacted by it as well.

In winter, due to continentality, Ladakh's average temperature is below freezing, with large amounts of precipitation being brought to the region by the Mediterranean influences of the mid-latitude westerlies. Winter precipitation is mostly snow, with the exception coming at lower elevations, where it occasionally rains (Fort 1983; Negi 2002).



**Figure 16.** A summer storm moving northward over the Zaskar Mountains. (Photo by M.E. Byrne 2007).

### **3.8 Glaciers and glaciation**

In a presentation to the Royal Geographical Society in 1891, H.C.B. Tanner (1891:410) explained that “as the latitude decreases Himalayan glaciers lose much of their picturesque and striking appearance, and...many glaciers are so buried beneath mud and rocks that the ice is seldom visible, and then only by kicking away the stones.” More than one hundred years later, Tanner’s portrayal of glaciers in the Himalaya still holds true.

The Himalayas and the Tibetan Plateau form the greatest glaciated region in the world, excluding the Polar Regions (Benn and Owen 2002; Owen *et al.* 2002; Kulkarni 2005, 2007; Lehmkuhl and Owen 2005; WWF 2005; IPCC 2007; Racoviteanu 2008). Geologists of the Geological Survey of India (GSI) recently counted 5,218 glaciers in the Himalayas (WWF 2005), covering an estimated 33,050 km<sup>2</sup> (UNEP 2008), or about 17



percent of the Himalaya (IPCC 2007). This can be contrasted with the Swiss Alps, of which just 2.2 percent are glaciated (*ibid.*).

Glaciers in the Himalaya accumulate mass in three ways: by direct snowfall, blowing snow, and by avalanching. Due to the tendency of many mountains in the region to be extremely high and steep, they often will intercept snowfall, but cannot retain it (Benn and Owen 1998; Benn and Evans 1998; Figure 17). The Khumbu Glacier of Nepal, for instance, accumulates an estimated 2.8 times more of its mass from avalanching than it does from direct snowfall (Inoue 1977). Additionally, the typically steep valley walls deposit large quantities of debris on the glaciers, which is carried down-valley and accumulates near the terminus, resulting in an extensive debris cover in most Himalayan glaciers' ablation zones (Benn and Owen 1998), giving them the unattractive appearance described by Tanner (1891).



**Figure 17.** The accumulation zone of a glacier in Ladakh. (Photo by M.E. Byrne, 2007).

Due to the increasing aridity as one moves northward through Ladakh, valley glaciers and tongue glaciers generally only form in the southern part of the region, in areas such as southern Zaskar and the Nun Kun Massif. In the northern part of Ladakh, valley glaciers rarely form (Zgorzelski 2006). Instead, cirque glaciers are very common, particularly in the Ladakh Range. These glaciers tend to range in area from 0.5 to 2 km<sup>2</sup>, and are generally located on northwest to northeast facing slopes. The steady state Equilibrium Line Altitude (ELA) for glaciers in Ladakh with a northwest to northeast orientation is between 5200 and 5400 m asl (Burbank and Fort 1985).

Owen *et al.* (2006) identified and dated five glacial advances in Ladakh: the Indus Valley, Leh, Kar, Bazgo, and Khalling glacial stages. The oldest recognizable glacial advance, the Indus Valley glacial stage, was dated from 130 to 385 ka, but may have been as old as 430 ka. The Leh glacial stage has ages from 79 to 369 ka that cluster between 100 and 200 ka, suggesting that it occurred during the penultimate glacial cycle in Marine Isotope Stage (MIS) 6.

The next stage, the Kar glacial stage, has proven difficult to date, but seems to have occurred during the early part of the last glacial, most likely during MIS 5. This was followed by the Bazgo glacial stage, aged at ~ 41-74 ka, suggesting that it took place during the middle part of the last glacial cycle, during MIS 3 and/or MIS 4. The youngest stage, the Khalling stage, appears to have occurred in the early Holocene (Owen *et al.* 2006).

During the five glacial cycles identified by Owen *et al.* (2006), the extent of the glaciations progressively decreased. A decrease in precipitation is suggested, possibly due to tectonic uplift of the Himalayan ranges to the south of Ladakh, which gradually



reduced the ability of the Indian monsoon to penetrate northward and to dump precipitation on the glaciers of Ladakh (Taylor and Mitchell 2000; Owen *et al.* 2006). Another possibility is that the decrease in precipitation was part of a global trend of decreasing precipitation and progressively less extensive glaciation in mountain regions throughout the Pleistocene (Owen *et al.* 2006).

The youngest glacial stage in Ladakh, the Khalling stage, appears to have occurred at a period when the global insolation levels were at a maximum, and the majority of high-latitude Northern Hemisphere glaciers were receding, or already had (Owen *et al.* 2006). This is consistent with studies throughout the Western Himalaya and Tibet (e.g., Benn and Owen 1998; Owen *et al.* 2001, 2002; Finkel *et al.* 2003; Barnard *et al.* 2004a, b) which also identified early Holocene advances, implying that there is a local control—possibly increased monsoonal precipitation during the early Holocene insolation maximum—which has influenced glaciers. Indeed, dating and reconstructions of Quaternary glaciations in Lahul and Garhwal (Owen *et al.* 1997; Barnard 2004), Hindu Kush (Owen *et al.* 2002), Nanga Parbat (Phillips *et al.* 2000), the Khumbu Himal (Finkel 2003), and Tibet (Finkel 2003; Thompson *et al.* 2006) have all suggested Quaternary glacial histories that were asynchronous with high-latitude glacial periods throughout the rest of the Northern Hemisphere. This pattern implies that the strongest influence on glaciers in the region is the south Asian monsoon (Benn and Owen 1998; Owen *et al.* 2002; Finkel *et al.* 2003).

### 3.9 Vegetation

Due to the aridity and harsh conditions of Ladakh, vegetation is sparse. The plants that do survive are well adapted to the extreme climate (Figure 18). Dwarfed and stunted shapes are common, and xerophytic shrubs and bushes, such as *Caragana*, *Artemisia*, and *Juniperus*, can be found the most frequently. The largest exception occurs in flood plains, where shrubby forests are found to survive. Other vegetation types are restricted to specific locations based on suitability of topography, moisture, and the quality of soil, but the vegetation cover, in general, is very sparse (Fort 1983; Phartiyal *et al.* 2005).



**Figure 18.** Vegetation, where it exists, is sparse and well adapted to the harsh climate in Ladakh. (Photo by M.E. Byrne, 2007).

### 3.10 Erosion and Denudation

The rate of denudation in the Himalaya is extremely high. Shroder (1989) explained that the calculation of long-term sediment deposition in the Indian Ocean equates to a

denudation rate of 0.2 mm per year; currently, the rate is between 1 and 1.8 mm per year. Vance *et al.* (2003), meanwhile, calculated an erosion rate in the High Himalaya of  $2.7 \pm 0.3$  mm/yr ( $1\sigma$  errors); a rate of  $1.2 \pm 0.1$  mm per year along the southern edge of the Tibetan Plateau; and  $0.8 \pm 0.3$  to  $< 0.6$  mm per year in the foothills to the south of the High Himalaya.

Erosion in Ladakh occurs by a number of different mechanisms, including conversion of bedrock to regolith, creep, landsliding on soil-mantled slopes, bedrock incision by rivers, bedrock landsliding, glacial erosion (Burbank 2002), and frost shattering of rocks (Benn and Evans 1998; Jamieson *et al.* 2004). Shroder (1998) describes the three main agents of denudation in the Himalaya as slope failure, glaciers, and rivers. More specifically, Shroder and Bishop (1998) explain that the process generally begins with mass movements and slope failures onto glaciers and into river valleys, and then continues by glacial and fluvial transport.

### **3.11 Ladakhi People**

Culturally and genetically similar to the people of Tibet, the majority of Ladakhis live a subsistence farming lifestyle. Most Ladakhis live in small mountain communities, typically working two to four acres of farmland for each family (Norberg-Hodge 1995). Ladakhis are dependent on snow and glacial meltwater to irrigate their fields: villages will often have elaborate systems of channels, bringing the water to their fields in a way in which it can be used most efficiently and shared among all residents of that particular village (Figure 19). The primary crop among Ladakhis is barley and, to a smaller degree, wheat. Additionally, many families have small gardens of peas and turnips, and in

valleys below 3500 m asl, apricot and walnut trees are common. Finally, Ladakhis depend to a large degree on animal husbandry. Common domesticated animals include sheep, goats, donkeys, horses, cows, yaks, and *dzo*, a cross-breed between a yak and a cow (Norberg-Hodge 1991; Figure 20). Relative to other Himalayan peoples, many of whom have more abundant natural resources, Ladakhis enjoy greater level of prosperity and happiness (Norberg-Hodge 1995).



**Figure 19. Irrigated fields in Ladakh. Note the stark contrast between vegetated cultural and non-vegetated natural landscapes. (Photo by M.E. Byrne, 2007).**





**Figure 20. The *dzogru*, a cross-breed between a cow and a yak, plays an important role in the Ladakhi lifestyle. (Photo by M.E. Byrne, 2007).**

The two main religions in Ladakh are Islam and Buddhism, with some Hinduism to be found, particularly in larger cities such as Leh and Kargil. Of the two main religions, Buddhism is the more dominant (Figure 21), with Islam primarily found only in the Kargil district and in scattered pockets in the larger towns such as Leh. Buddhism came to Ladakh as far back as the seventh century (Loram 1996), and it has been the primary religion there since the fourteenth century (Weare 2002).



**Figure 21. Young Ladakhi monks-in-training at Thikse Monastery, Ladakh. (Photo by M.E. Byrne, 2007).**

## 4. Methods

### 4.1 Study Areas

Five study areas were used for this project (Figure 22). The first two, located in the Ladakh Range, held small glaciers, and were visited in August and September of 2007. The last three, located in the Greater Himalaya Range, held large valley glaciers, and were visited in August of 2008. The first study area is located ~ 45 km southeast of Leh, at the head of the Igu Valley. This study area will henceforth be called *Igu* or Study Area 1. The glacier used for this study was a small cirque glacier, with an area of ~ 0.23 km<sup>2</sup>, ~ 2% of which was covered with debris (Figure 23). The terminus was at ~ 5350 m asl. The meltwater from Igu Glacier forms a small river which, after joining several other rivers coming from nearby glaciers, supports the people of the several villages located in Igu Valley, which include Phu, Nichoku, Sachum, Zardong, and Igu, before emptying into the Indus River<sup>1</sup>.

---

<sup>1</sup> The term *igu* means ‘snake’ in Ladakhi, and was given to the river due to its winding, snakelike appearance.



# Locations of Study Areas 1-5 Ladakh, India

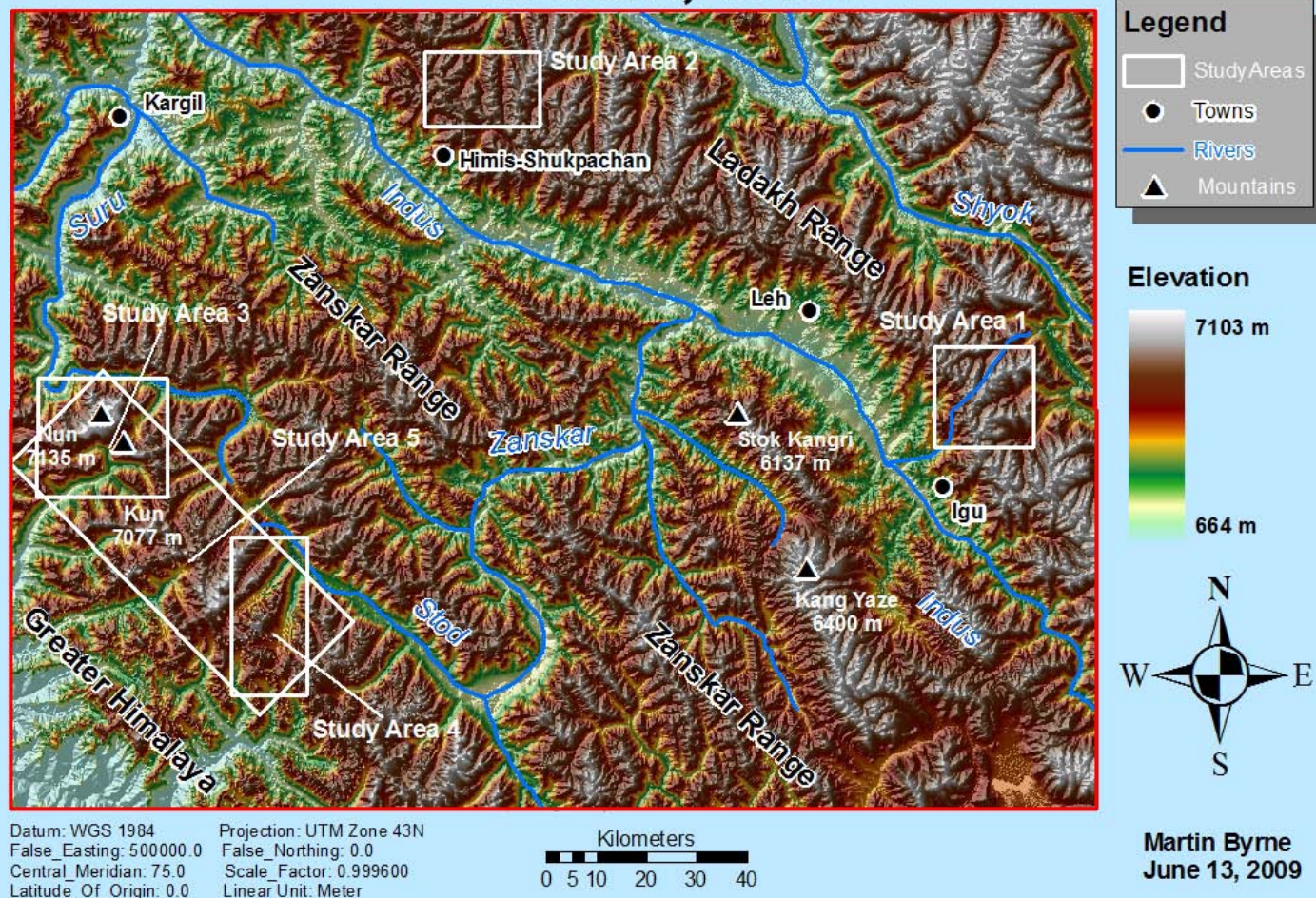


Figure 22. Map of Study Areas 1-5 in Ladakh.





**Figure 23. The glacier above Igu in Study Area 1. (Photo by M.E. Byrne, 2007).**

The second study area included three glaciers at the head of the valley above the village of Himis-Shukpachan, ~ 50 km northwest of Leh. This study area will henceforth be referred to as *Himis-Shukpachan* or Study Area 2. The three glaciers, from east to west, had areas of 0.9 km<sup>2</sup>, 0.34 km<sup>2</sup>, and 0.92 km<sup>2</sup>, respectively. The easternmost glacier's terminus (Figure 24) was located at ~ 5134 m asl, while the middle glacier (Figure 25) ended at about 5068 m asl, and the westernmost glacier's terminus was at ~ 5080 m asl. The smallest of these three glaciers ends in a small (0.02 km<sup>2</sup>) lake. Meltwater from the three glaciers combines near the head of the valley to form a small river, which supports the villages of Himis-Shukpachan, Shushut, Rzingla, and Rong, before joining the Indus River ~ 50 km from Leh.



**Figure 24. One of the three glaciers in Study Area 2. (Photo by M.E. Byrne, 2007).**



**Figure 25. Another glacier in Study Area 2. The glacier ends in a small lake. (Photo by M.E. Byrne, 2007).**



The third study area was the area surrounding Parkachik Glacier (Figure 26), a large glacier fed by the peaks of Nun Kun Massif. Approximately 55 km south-southwest of Kargil, and 145 km west-southwest of Leh, Parkachik Glacier flows northward, ~ 12 km down the slope of Nun Kun, before ending abruptly in the Suru River, at an elevation of ~ 3560 m asl. This study area will henceforth be referred to as *Parkachik Glacier*, or Study Area 3. Another large glacier, apparently unnamed, flows westward down Nun Kun's slopes, and was also included in this study area.



**Figure 26. Study Area 3: the terminus of Parkachik Glacier in the Suru River. (Photo by U. Kamp, 2008).**

The fourth study area was the area around Drang Drung Glacier, the second largest glacier in Ladakh, surpassed only by ~ 70 km long Siachen Glacier (Negi 2002; Figure 27). Drang Drung Glacier, flowing from the peaks of the Zaskar Massif, lies directly southwest of Pensi Pass (Pensi La), sometimes called the “Gateway to Zaskar”,

and forms the headwaters of the Stod River, a tributary of the Zaskar River. It is ~ 43 km from Parkachik Glacier, ~ 83 km from Kargil, and ~ 117 km from Leh. From the top of its catchment area to its terminal margin, the glacier is more than 23 km long, and its terminus is at ~ 4100 m asl. A number of large glaciers in this area have their accumulation zones in the upper reaches of the Zaskar Massif. The largest, however, is Drang Drung Glacier, and so this study area will henceforth be referred to as *Drang Drung* or Study Area 4.



**Figure 27. Study Area 4: Drang Drung Glacier in the Greater Himalaya Range in southern Ladakh. (Photo by U. Kamp, 2008).**

Finally, a fifth study area was developed which included both Parkachik Glacier and Drang Drung Glacier, as well as all the glaciers between the two—essentially the whole of the range between the Nun Kun Massif and the Zaskar Massif (Figure 28). This study area allowed the morphometric approach to be applied over a much larger area than Study Area 3 or Study Area 4 alone. It contained an area of ~ 1770 km<sup>2</sup>, spanning

from just northwest of Parkachik Glacier to just southeast of Drang Drung Glacier (a distance of 43 km, as the crow flies). This area will be referred to as Study Area 5.

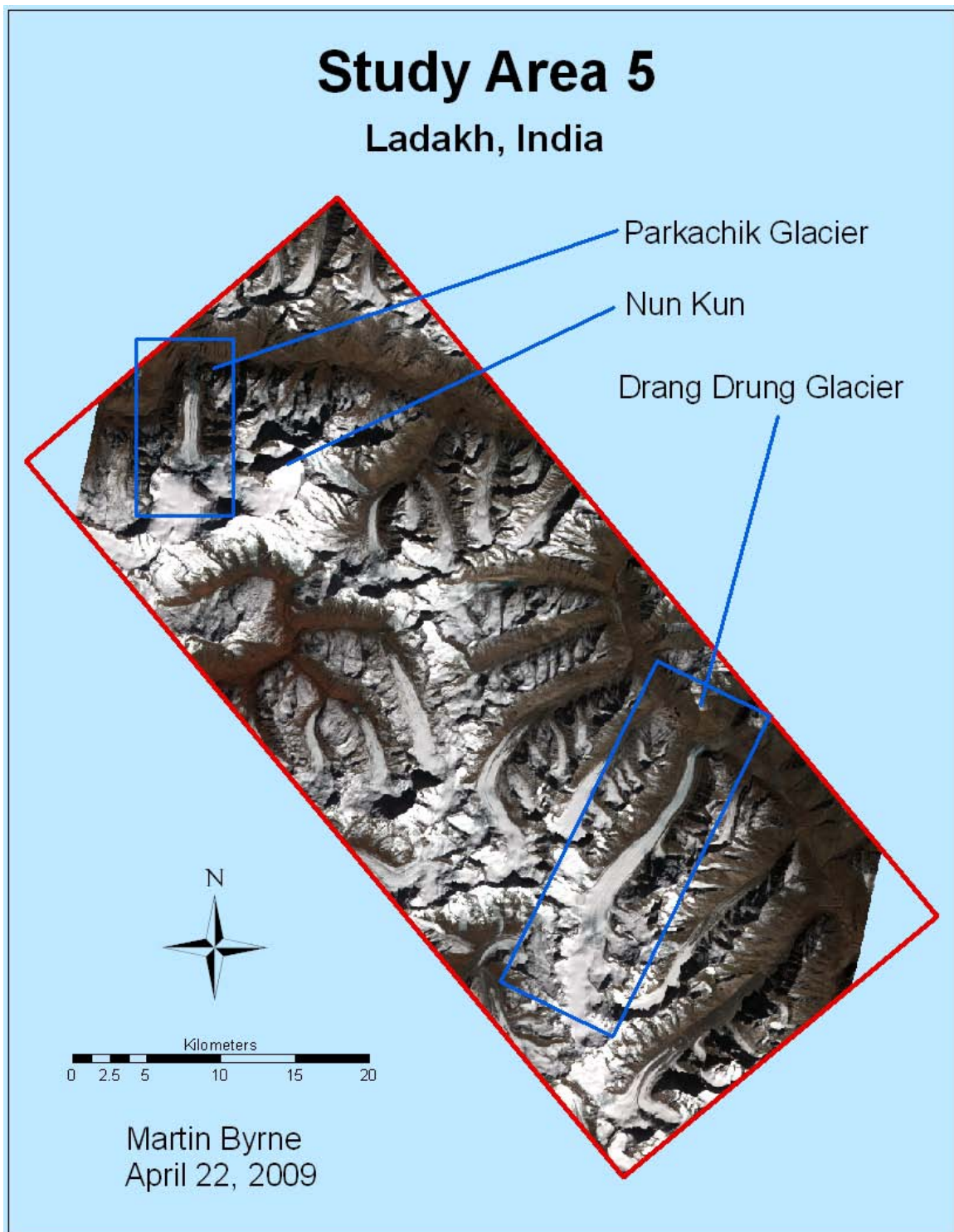


**Figure 28. Study Area 5, including Parkachik and Drang Drung glaciers in the Greater Himalaya Range in southern Ladakh.**



## 4.2 Ground-truth Accuracy Assessment

Due to the inherent uncertainty involved when mapping debris-covered glaciers with satellite imagery, it is necessary to conduct a ground-based accuracy assessment to ensure that the outputs attained through the morphometric procedure are correct (Bishop *et al.* 2001; Pope *et al.* 2007; Pelto 2008). For this reason, field work was undertaken in the summers of 2007 and 2008 on all five study areas. The field work involved taking photographs and GPS points around areas of interest such as glacial margins, and geomorphological mapping. The GPS points and the photographs were particularly important when monitoring recent change in the glaciers; this data made it possible to identify the active ice margins, which often are difficult to identify in satellite images. As was previously mentioned, it is often impossible to distinguish a glacier's margins in the Himalaya due to heavy debris-cover, so it is essential to have ground data for verification of results.

## 4.3 Datasets

Due to numerous factors, including the remoteness of Ladakh, difficult terrain, underdeveloped road systems, and logistical problems involving the Indian Government and military, it is impossible to access every glacier in the field. Additionally, due to military complications in the region, aerial photography is effectively prohibited (Bishop *et al.* 1998; Damm 2006; Kulkarni 2007; Racoviteanu *et al.* 2008). These difficulties mean the only effective means of mapping glaciers in Ladakh is through the utilization of satellite imagery. Unfortunately, as mentioned earlier, the large amounts of debris-cover on most of the glaciers in the region makes it difficult or impossible to map them using

multi-spectral imagery alone (Bishop *et al.* 2001; Paul *et al.* 2004; Bolch *et al.* 2008; Racoviteanu *et al.* 2008; Figure 29). Data from two different multispectral datasets were used for this project: ASTER and Landsat. Because of the large quantities of debris covering glaciers in the study area, it was necessary to use a number of different morphometric parameters, such as slope threshold, thermal bands, and supervised classifications, to first map the glaciers, and secondly to perform a multi-temporal analysis to determine how the glaciers have changed over the past three decades.



**Figure 29. Landsat 7-5-1 image of a debris-covered glacier tongue in northern Pakistan. Note that the margins are indiscernable and do not differ in spectral signature from the glacier forefield.**

#### 4.3.1 Landsat Dataset

The earlier of the two multispectral datasets used in this project was from Landsat. For this project, Multispectral Scanner (MSS), Thematic Mapper (TM), and Enhanced Thematic Mapper Plus (ETM+) and panchromatic images were used (Figure 30).

Landsats 1-3 were launched in 1972, 1975, and 1978, respectively, and provide MSS imagery, which includes four bands of multispectral imagery (0.5-1.1  $\mu\text{m}$ ), with a spatial resolution of  $\sim 80$  m.

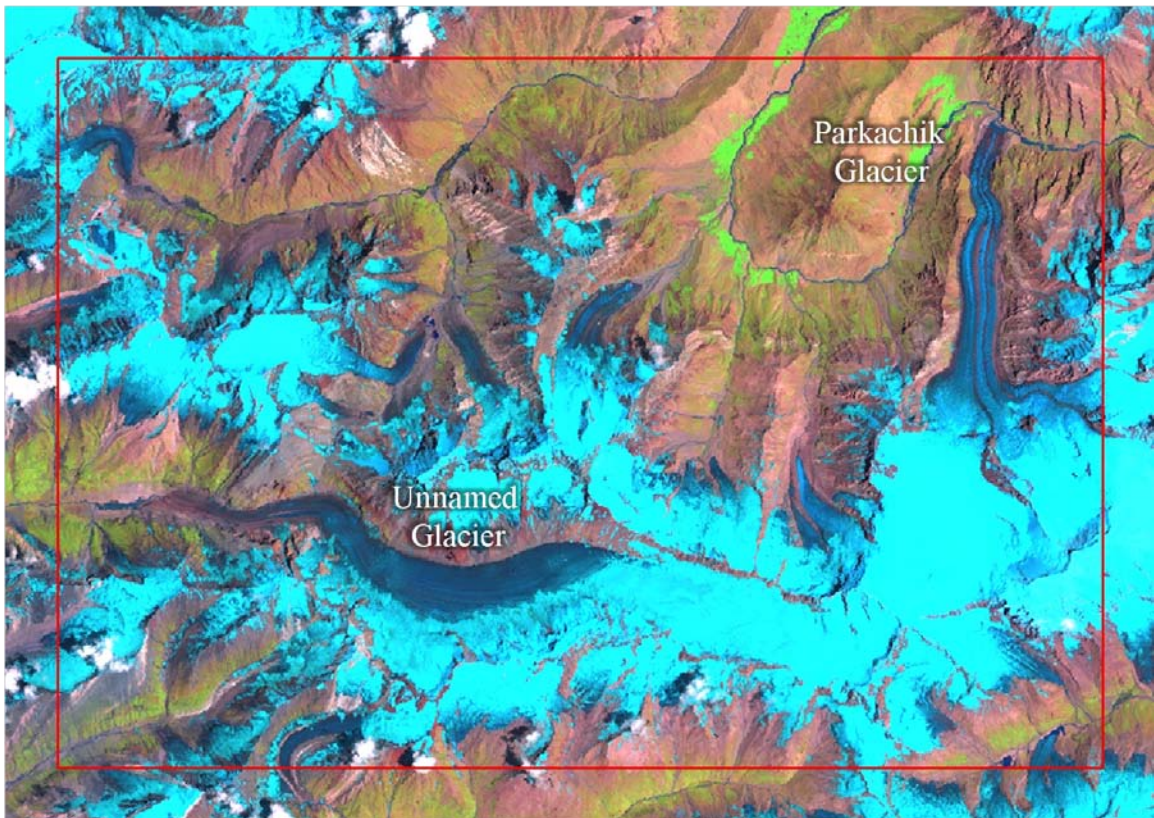


**Figure 30. Landsat ETM+ false color composite (FCC) (5-4-2) image of Study Area 3.**

Launched in 1982, 1984, respectively, Landsats 4 and 5 collect TM data with a spatial resolution of 30-m in bands 1-5 (0.45-1.75  $\mu\text{m}$ ) and band 7 (2.08-2.35  $\mu\text{m}$ ); band 6 (thermal, 10.4-12.5  $\mu\text{m}$ ) has a 120-m resolution. Landsat 7, launched in 1999, employs the ETM+ sensor, providing a spectral range and spatial resolution similar to TM for



bands 1-5 (30-m, 0.45-12.5  $\mu\text{m}$ ) and band 7 (30-m, 2.09-2.35  $\mu\text{m}$ ). However, band 6 (thermal, 2.09-2.35  $\mu\text{m}$ ) provides an improvement over TM, with 60-m resolution. Additionally, ETM+ has a 15-m resolution panchromatic band (band 8, 0.52-0.9  $\mu\text{m}$ ), which allows the creation of pansharpened imagery from 1999 on (Lillesand *et al.* 2004; National Aeronautics and Space Administration 2009), from which a multi-temporal approach can be taken for glacier monitoring.

While Landsat data have proven to be very effective for mapping clean glacier ice (Kääb *et al.* 2002; Paul *et al.* 2002), debris-covered glaciers are much more difficult (Bolch and Kamp 2006; Bolch *et al.* 2006). TM and ETM+ bands alone are unable to detect glacier margins in high-debris areas. Thus, the Landsat images must be viewed in combination with a Digital Elevation Model (DEM) in order to account for slope and curvature as a means of detecting the vertical characteristics of the glaciers' surfaces (Bolch *et al.* 2005; Kamp *et al.* 2005; Paul and Kääb 2005). However, Landsat scenes are effective for viewing scenes in the same area on the same day, due to their wide ( $180 \times 180 \text{ km}^2$ ) area of coverage (Narama *et al.* 2006).

All Landsat scenes for this project were downloaded free of charge from the Global Landcover Facility (GLCF) at the University of Maryland (Table 1). It should also be noted that no suitable images were available for Study Area 1.

**Table 1. Landsat Scenes.**

| <b>GLCF Scene ID</b>       | <b>Acq. Date</b> | <b>Sensor</b> | <b>Path</b> | <b>Row</b> | <b>Bounding Coord. (N)</b> | <b>Bounding Coord. (S)</b> | <b>Bounding Coord. (W)</b> | <b>Bounding Coord. (E)</b> | <b>Study Area</b> |
|----------------------------|------------------|---------------|-------------|------------|----------------------------|----------------------------|----------------------------|----------------------------|-------------------|
| <b>p159r37_2m19751110</b>  | Nov. 10, 1975    | MSS           | 159         | 37         | 34.151515° N               | 32.164607° N               | 75.059002° E               | 77.620256° E               | 4                 |
| <b>p159r36_3m19790607</b>  | June 7, 1979     | MSS           | 159         | 36         | 35.439521° N               | 33.584896° N               | 75.383176° E               | 77.920249° E               | 3                 |
| <b>p147r36_5t19900629</b>  | June 29, 1990    | TM            | 147         | 36         | 35.611280° N               | 33.609778° N               | 76.548655° E               | 79.247184° E               | 3, 5              |
| <b>p148r36_5t19900629</b>  | June 29, 1990    | TM            | 148         | 36         | 35.572587° N               | 33.613096° N               | 75.095773° E               | 77.557135° E               | 3, 4, 5           |
| <b>p148r37_5t19920704</b>  | July 4, 1992     | TM            | 148         | 37         | 34.127754° N               | 32.17162° N                | 74.668867° E               | 77.088964° E               | 4                 |
| <b>p148r036_7k19990716</b> | July 16, 1999    | ETM+          | 148         | 36         | 35.602692° N               | 33.616588° N               | 75.015871° E               | 77.714561° E               | 3, 4              |
| <b>p148r037_7k20001022</b> | October 22, 2000 | ETM+          | 148         | 37         | 34.170422° N               | 32.18288° N                | 74.626955° E               | 77.29422° E                | 4                 |
| <b>p147r036_7t20001031</b> | October 31, 2000 | ETM+          | 147         | 36         | 35.61128° N                | 33.609778° N               | 76.548655° E               | 79.247184° E               | 2                 |
| <b>p148r037_7p20021028</b> | October 28, 2002 | ETM+          | 148         | 37         | 34.183787° N               | 32.16944° N                | 74.622257° E               | 77.299216° E               | 4                 |

#### 4.3.2 ASTER Dataset

The later of the two datasets used in this project comes from the Advanced Spaceborne Thermal Emission and Reflection Radiometer (ASTER) multispectral imaging system, a high-resolution sensor aboard the TERRA satellite (Figure 31). Launched in December, 1999, TERRA is a part of NASA's Earth Observing System (EOS). ASTER data have been collected since February, 2000. An ASTER scene covering  $61.5 \text{ km} \times 63 \text{ km}$  contains 14 spectral bands of information. These bands are divided into three separate subsystems based on their spatial resolution, which is dependent on which wavelength range is being viewed. The first subsystem includes three bands in the visible and near infrared spectral range (VNIR,  $0.5\text{-}1.0 \mu\text{m}$ ), which provide 15-m spatial resolution; the second subsystem includes six bands in the shortwave infrared spectral range (SWIR,  $1.0\text{-}2.5 \mu\text{m}$ ), which provide 30-m resolution; and the third subsystem includes five bands from the thermal infrared spectral range (TIR,  $8\text{-}12 \mu\text{m}$ ), which provide 90-m resolution. In addition, in the VNIR spectral range, ASTER has one nadir-looking (3N,  $0.76\text{-}0.86 \mu\text{m}$ ) and one backward-looking (3B,  $27.7^\circ$  off-nadir) telescope which provide black-and-white stereo images that can be used to generate an along-track stereo image pair with a base-to-height ratio of  $\sim 0.6$  (Kamp *et al.* 2003; Lillesand *et al.* 2004; Bolch *et al.* 2005). ASTER's ability to cross-track point out to 136 km gives it the ability to view almost any point on the planet at least once every sixteen days. Each day, ASTER can produce up to 771 stereo pairs (Kamp *et al.* 2003).

All ASTER scenes were received free of charge as part of the GLIMS program (Table 2).

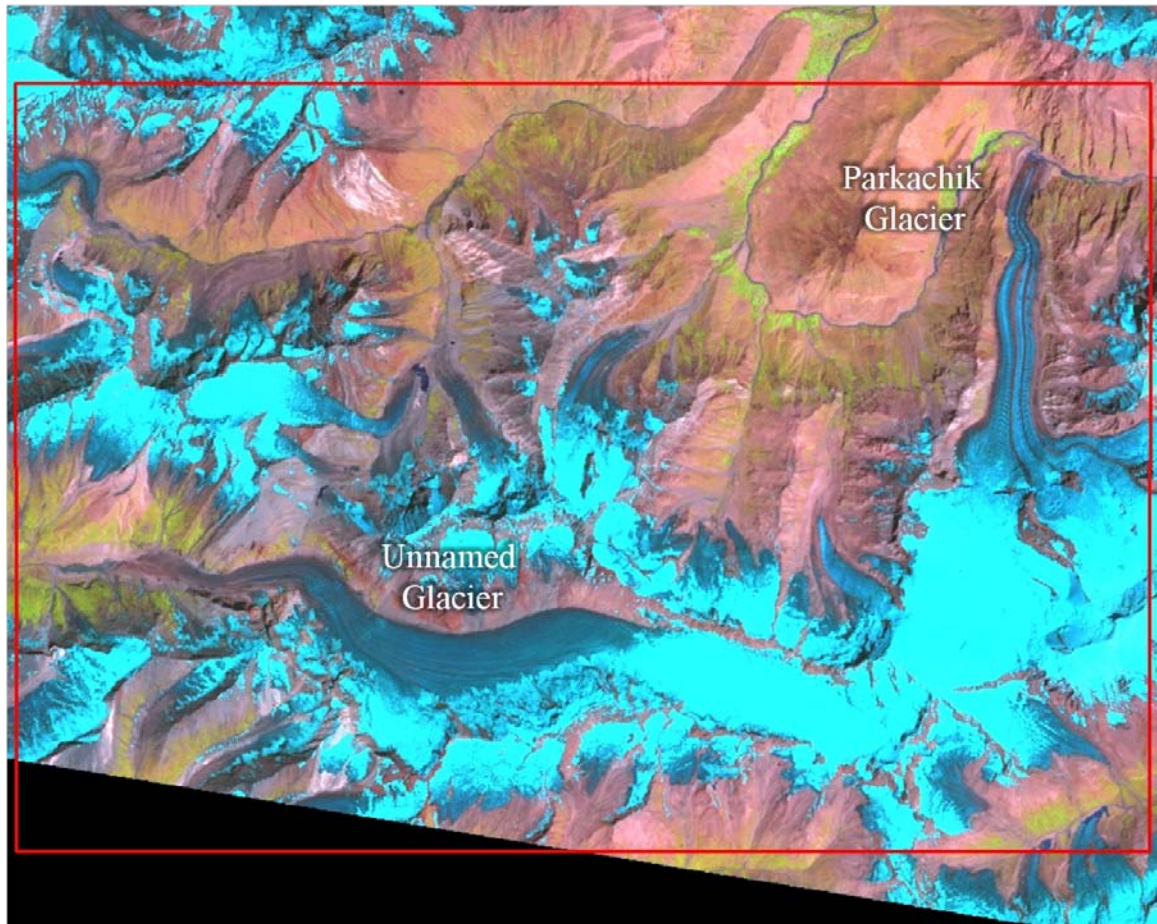


Figure 31. ASTER false color composite (FCC) (4-3-2) image of Study Area 3.

#### 4.4 DEM Generation

When creating a DEM from ASTER data, the VNIR nadir and backward images (3N and 3B) are used. The spatial resolution of the ASTER dataset allows DEMs to be generated with a spatial resolution of 15-30 m, and a potential accuracy of around  $\pm 7$  to  $\pm 50$  m (RMSE<sub>Z</sub>; Kamp *et al.* 2003; Toutin 2008), which is generally sufficient for most applications (Bolch *et al.* 2005). ASTER scenes come in HDF-EOS format, from which they can be imported by Silcast 1.07 (e.g., Kamp *et al.* 2008). The DEM generation was carried out by Jeffrey Olsenholler, University of Nebraska-Omaha, using Silcast 1.07 (Figure 32).

**Table 2. ASTER Scenes.**

| Scene ID                  | Date of Acq.      | Path | Row | Bounding Coord. (N) | Bounding Coord. (S) | Bounding Coord. (W) | Bounding Coord. (E) | Study Area |
|---------------------------|-------------------|------|-----|---------------------|---------------------|---------------------|---------------------|------------|
| SC:AST_L1A.003:2004041808 | August 29, 2001   | 148  | 36  | 34.344661° N        | 33.684214° N        | 75.26051° E         | 76.105941° E        | 3          |
| SC:AST_L1A.003:2008640550 | October 3, 2002   | 148  | 36  | 34.322176° N        | 33.660738° N        | 75.408621° E        | 76.254933° E        | 3          |
| SC:AST_L1A.003:2018322550 | October 31, 2003  | 148  | 36  | 34.481927° N        | 33.827489° N        | 75.882176° E        | 76.702189° E        | 3, 5       |
| SC:AST_L1A.003:2008738811 | October 12, 2002  | 148  | 37  | 33.89045° N         | 33.243309° N        | 76.09378° E         | 76.913466° E        | 4          |
| SC:AST_L1A.003:2018322593 | October 31, 2003  | 148  | 37  | 33.950712° N        | 33.297261° N        | 75.737366° E        | 76.551122° E        | 4, 5       |
| SC:AST_L1A.003:2025327640 | August 14, 2004   | 148  | 36  | 34.545731° N        | 33.894179° N        | 75.425482° E        | 76.24669° E         | 3          |
| SC:AST_L1A.003:2025691837 | September 8, 2004 | 147  | 36  | 34.49683° N         | 33.840061° N        | 77.330461° E        | 78.15291° E         | 1          |
| SC:AST_L1A.003:2031347799 | October 20, 2005  | 148  | 37  | 33.909438° N        | 33.252492° N        | 76.027633° E        | 76.846971° E        | 4          |
| SC:AST_L1A.003:2031347799 | October 20, 2005  | 148  | 37  | 33.909438° N        | 33.252492° N        | 76.027633° E        | 76.846971° E        | 4          |
| SC:AST_L1A.003:2037582690 | October 7, 2006   | 148  | 36  | 34.95236            | 34.294185           | 76.44516            | 77.277971           | 2          |

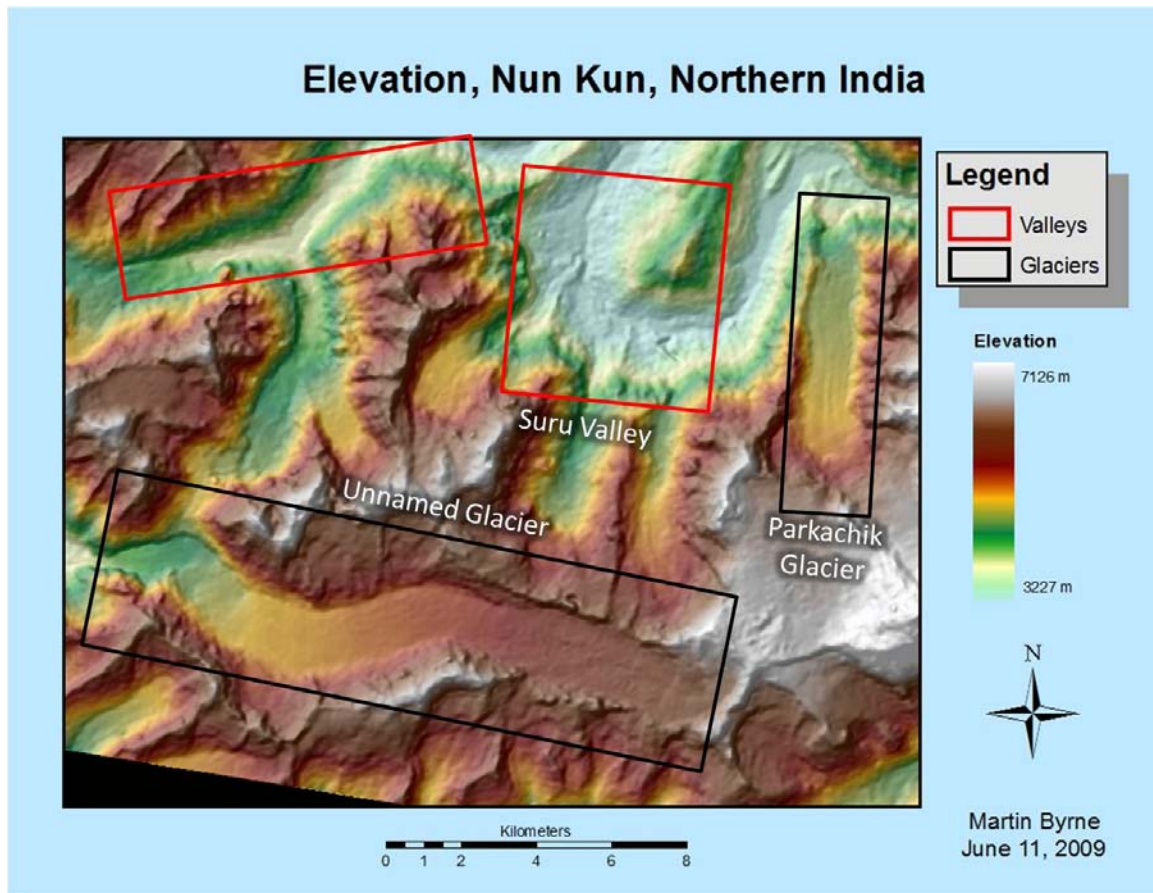


Figure 32. Elevation map derived from ASTER DEM of study area 3.

## 4.5 Mapping Clean Ice

### 4.5.1 Band Ratios

Clean ice glaciers—that is, glaciers which lack a cover of debris—can be mapped effectively with the use of band ratios (e.g., Sidjak and Wheate 1999; Paul *et al.* 2002; Kääb *et al.* 2003; Ranzi *et al.* 2004; Bolch and Kamp 2006; Narama *et al.* 2006; Racoviteanu *et al.* 2008). This process involves taking a ratio of a NIR band (e.g., Landsat TM or ETM+ bands 3 or 4, or ASTER band 3) and a SWIR band (e.g., Landsat TM or ETM+ band 5, or ASTER band 4). Band ratios take advantage of the high reflectivity values of snow and ice in the visible spectrum, effectively contrasting them

with darker surrounding material, such as rocks and debris, snow, and vegetation (Hall and Martinec 1985; Racoviteanu *et al.* 2008).

Band ratios are ineffective, however, when applied to heavily debris-covered glaciers (Bolch and Kamp 2006). While band ratios can effectively differentiate ice from surrounding debris, even a light cover of debris atop the glacier will cause that area to be classified as debris, rather than as glacier. However, mapping the clean ice and snow is essential when mapping glaciers, regardless of whether the glaciers contain a debris-covered portion. Furthermore, correctly classified areas of ice can effectively be used to eliminate falsely classified areas of debris when using the morphometric approach (e.g., those areas which are *not* touching clean ice or snow can be considered to be falsely classified; Tobias Bolch, December 12, 2007, pers. comm.).

Thus, a ratio of ASTER bands 3 and 4 was used to extract clean ice in all five study areas for this project. The band ratios were followed by the use of Feature Analyst<sup>©2</sup>, an extension package for ArcGIS designed for intuitive feature extraction and recognition, to extract and delineate the areas of clean ice and snow.

## **4.6 Mapping Debris-covered ice**

### ***4.6.1 Thermal Bands***

Due to the inability of band ratios to differentiate between supraglacial debris and non-glacial debris, it is helpful to use information from ASTER's thermal sensor (e.g., bands 10-14) as a method of distinguishing glaciers (Ranzi *et al.* 2004; Bolch and Kamp 2006). This method takes into account the fact that supraglacial debris is cooled by the

---

<sup>2</sup> Produced by Visual Learning Systems (VLS), Missoula, MT (<http://www.vls-inc.com/>).

underlying ice, and, in some cases, to some extent, ice is exposed at the surface of the glacier, thus giving it a thermal signature which is cooler than its surrounding, non-glacial, debris (*ibid.*). Ranzi *et al.* (2004) demonstrated that this method is only effective on glaciers on which the cover of debris is less than ~ 40-50 cm thick. When debris becomes thicker than that, it works as an insulator, and the debris is no longer cooled noticeably by the underlying ice of the glacier. An additional problem associated with the use of thermal data to map glaciers is that debris receiving direct radiation in the afternoon becomes much warmer than debris which is in shadow, causing areas in perpetual shade, such as north-facing ridges and slopes, to be misclassified as glaciers (Bolch *et al.* 2007).

Using first a composite of ASTER bands 3-2-1—due to the high spatial resolution of the visible and near infrared datasets—a set of training sites was drawn near the glaciers' termini. The training sites were evenly distributed across a number of glaciers in each study area, and were designed to represent the typical surface characteristics of all glaciers in each individual study area. The thermal bands (10-14) were then examined, and statistical parameters were calculated for the area within the training sites, for each band individually. The calculated parameters were minimum value, maximum value, mean, and standard deviation ( $\sigma$ ). Then, by calculating, for example,  $\text{mean} \pm 1\sigma$ , and extracting the values within those parameters throughout the entire study areas, it was possible to determine which areas had the correct thermal signature to be glaciers. After applying the parameters to all five thermal bands, the output could then be intersected, using Raster Calculator, with Boolean operators such as 'AND' and 'OR' for a complete representation of glaciers based on thermal information.



#### ***4.6.2 Supervised Classification***

Supervised classification schemes can be used to determine land cover classifications (Aniya *et al.* 1996; Brown *et al.* 1998; Sidjak and Wheate 1999); however, they lack the precision necessary to effectively delineate debris-covered glaciers by themselves (Bishop *et al.* 2001; Bolch *et al.* 2007). When used in conjunction with other mapping techniques, such as thermal information or slope thresholds, they can be used effectively (*ibid.*).

Due to the relative strength of its classification programs, IDRISI Andes was used for the supervised classifiers. For Parkachik Glacier, a Maximum Likelihood (MAXLIKE) classifier was used. The scene was divided into ten classes: snow, clean ice, supraglacial debris, vegetation and vegetated landcover, water, dark non-glacial debris, light non-glacial debris, rocks in shadow, ice in shadow, and no-data areas outside the scene. Prior probabilities were also added to the classification; snow and dark non-glacial debris were given the highest probability rankings, because those two landcover types cover the largest areas in the scene; conversely, water, ice in shadow, and no-data areas, each of which covers only a very small fraction of the scene, were given the lowest probability rankings.

The Maximum Likelihood classifier proved to be ineffective for classifying the scene surrounding Drang Drung Glacier; however, Minimum-Distance-to-Means (MINDIST) and K-Nearest-Neighbor (KNN) classifiers were better able to classify the area. For the Drang Drung study area, the number of training sites was condensed to seven: snow, clean ice, supraglacial debris, vegetation and vegetated landcover, non-glacial debris, shadow, and once again, the no-data areas outside the scene.

The supervised classifiers were exported from IDRISI into ArcGIS. Here they could be used in conjunction with other parameters, such as the aforementioned band ratio outputs, thermal information, or morphometric thresholds (e.g., Bishop *et al.* 2001; Bolch *et al.* 2007).

#### ***4.6.3 Topographic Analysis***

While glaciers in Ladakh are difficult to distinguish from multispectral imagery alone, it is possible, just as with other glaciers throughout the Himalaya, to differentiate them from surrounding debris by their surface characteristics (Bishop *et al.* 2001; Bonk 2002; Paul *et al.* 2004; Bolch and Kamp 2006; Bolch *et al.* 2008). The aforementioned DEMs were used to calculate surface features for each study area. The outputs of these surface analyses included slope, aspect, planimetric curvature, profile curvature, and hillshade images. This process was completed in ArcGIS, using the Spatial Analyst toolbox.

Morphometric parameters were determined by the same method that was used for thermal information. Training sites were defined on an ASTER 3-2-1 composite image, distributed so they would represent typical characteristics of the glaciers' ablation zones. Parameters were calculated for the area within the training sites. These parameters were the same ones that were calculated for the previously mentioned analysis of the thermal bands: minimum value, maximum value, mean, and standard deviation ( $\sigma$ ). The calculated parameters were used to calculate a range (e.g.,  $\text{mean} \pm 1\sigma$ ), within which a glacier is likely to exist. This same method was applied to all surface analysis images, thus creating a range for slope, aspect, planimetric curvature, and profile curvature. Aspect was excluded because it has been proven to be ineffective for morphometric

mapping (Bolch *et al.* 2007). Additionally, planimetric curvature and profile curvature did not show a significant correlation to glaciated areas, so those were also excluded.

#### ***4.6.4 Cluster Analysis***

A cluster analysis can be used to combine areas on a glacier with similar surface characteristics, such as slope, planimetric curvature, and profile curvature (Bishop *et al.* 2001; Bolch and Kamp 2006; Bolch *et al.* 2007). In ArcGIS, this method was realized with the IsoCluster tool, followed by the Maximum Likelihood tool. Though the aforementioned surface features were all examined, slope proved to be the only effective topographic input. Varying numbers of output classes were also tried, with eight classes proving to be the most effective.

#### ***4.6.5 Morphometric Glacier Mapping***

Morphometric glacier mapping (MGM) involves a combination of various parameters which, when combined, can sometimes delineate glaciers effectively, despite heavy debris-covers or other potential hindrances (Bolch and Kamp 2006; Bolch *et al.* 2007; Figure 33). For this project, MGM involved a combination of the above-mentioned results, namely, thermal information from all five thermal bands, the supervised classification results, cluster analysis, slope thresholds, and the clean ice, as delineated with band ratios.

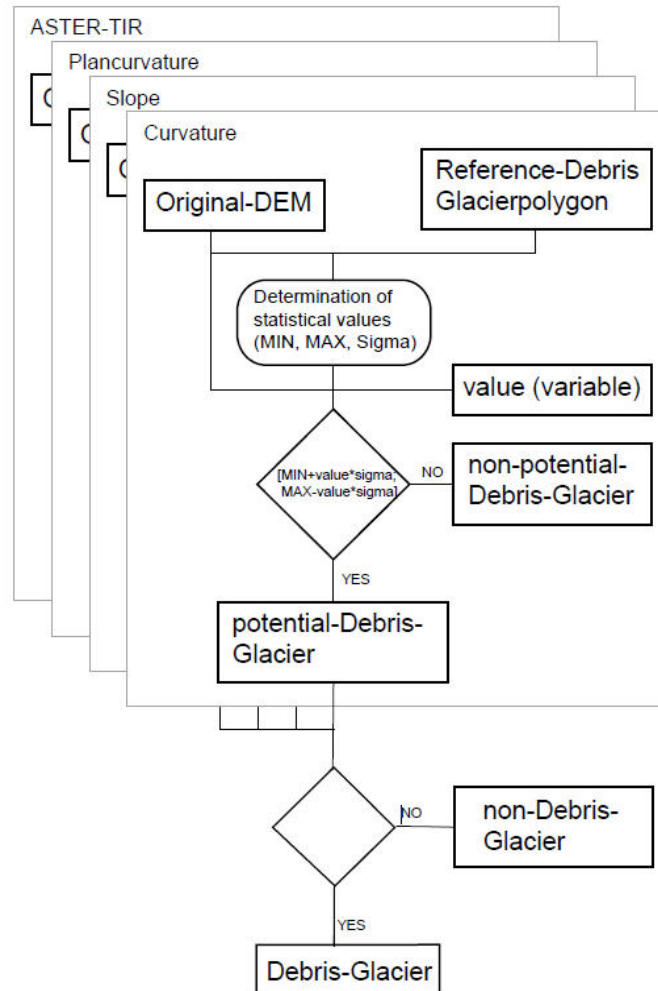


**Figure 33. Flow-diagram of the morphometric glacier mapping (MGM) approach (Buchroithner and Bolch 2007).**

For Parkachik study area, using the Raster Calculator in ArcGIS, thermal and slope were combined, using the Boolean ‘AND’ operator. The most effective thresholds were decided upon before this step, based on which values most effectively represented the glacier areas. Next, areas classified with the Maximum Likelihood classifier and the cluster analysis as either debris-covered ice or clean ice were included—again, using the ‘AND’ operator—and everything else (e.g., vegetation, water, non-glacial debris, etc.) was excluded.

A smoothing filter was used to fill small holes in post-processing. Next, all areas considered too small to be a glacier ( $< 0.1 \text{ km}^2$ ) were eliminated. This threshold was chosen with the assumption that any area smaller than  $0.1 \text{ km}^2$  represents a snow or ice patch, but is too small to be a glacier. This step helped to identify and eliminate features such as seasonal snow patches that were erroneously classified as glaciers due to their similar spectral signatures. To eliminate misclassified areas down-valley from the glaciers, all polygons not touching clean ice were eliminated using select by location in ArcGIS. Finally, in a number of areas, it was necessary to manually edit the polygons, so they would better represent the glaciers and their margins.

The final output of the MGM was a polygon layer of all areas classified as debris-covered glacier or clean ice. As a final step, this layer was merged with the clean ice and snow layer developed with band ratios, creating a third and final polygon layer; this layer contained every area that could be classified as debris-covered glacier, clean ice, or snow—in other words, it delineated the glaciers.

For Drang Drung Glacier Study Area, as well as for Study Area 5, between Drang Drung and Parkachik glaciers, the process was nearly identical to the MGM for Parkachik, with a few exceptions. The thresholds for the thermal bands and slope needed to be adjusted slightly, due to slightly different terrain. Additionally, the two supervised classifiers used for this area—Minimum-distance-to-means and K-nearest neighbor—were combined, using the Boolean ‘OR’ operator, before being used in the MGM. Excepting these small differences, however, the process was the same.

#### 4.7 Multi-temporal Analysis

In order to monitor glaciers, it is important to understand how they are behaving, and how they have changed over time. By viewing a glacier's changes over time, it is possible to see if the glacier has been receding or advancing (or neither), and to estimate whether that trend will continue into the future (Chinn 1999; Gao and Liu 2001; Bishop *et al.* 2004; Khalsa *et al.* 2004; Kulkarni *et al.* 2005, 2007; Raup *et al.* 2007a, 2007b; Bolch *et al.* 2008).

A multi-temporal analysis was executed in Study Areas 2, 3 and 4. All available data were used, including Landsat MSS, TM and ETM+ data, ASTER data, GPS points, and field notes. As the morphometric approach's results were not precise enough to measure glacier change, the analysis was done visually in ArcGIS, by manually delineating the glaciers' terminal margins from each available year. For the most recent years, in which satellite data was not yet available, GPS points and field measurements were used to approximate the margins. Glacier change was determined by averaging the terminus's position relative to a fixed line in front of the glacier. Each year's average distance from that point could then be subtracted from the previous year's average to determine terminal change in that time span.

An additional clue to a glacier's behavior can be found in the relative percentage of debris covering the glacier's tongue. It can generally be expected that a glacier which is losing mass will have an increasingly large percentage of its ablation zone covered with debris (Bolch *et al.* 2008; Tobias Bolch, April 1, 2009, pers. comm.). Thus, the amount of debris on the glaciers' tongues was also measured with the aforementioned satellite images.

Due to a lack of suitable images, Study Area 1 was excluded from the multi-temporal analysis. This was due in part to the glacier's high elevation, as well as the fact that it is situated in a cirque on a north-facing slope. These two factors cause the entire glacier to be covered in snow for large portions of the year, making it difficult to view the margins in most years. All study areas were characterized, to varying degrees, by this problem. Particularly prior to the introduction of Landsat 7 in 1999 and ASTER data in 2000, a paucity of suitable images presents a challenge when monitoring glacier change.

## 5. Results

### 5.1 Mapping Small Glaciers

The morphometric approach's utility for mapping small glaciers was tested in Study Areas 1 and 2. The first step involved the use of band ratios to extract clean ice. This method proved to be very effective for extracting clean ice and snow. The ratio of ASTER bands 3 and 4 allowed small glaciers to be distinguished from surrounding topography, as long as they were debris-free (Figure 34A). Feature Analyst had no problem extracting the ice and snow areas after using band ratios (Figure 34B).

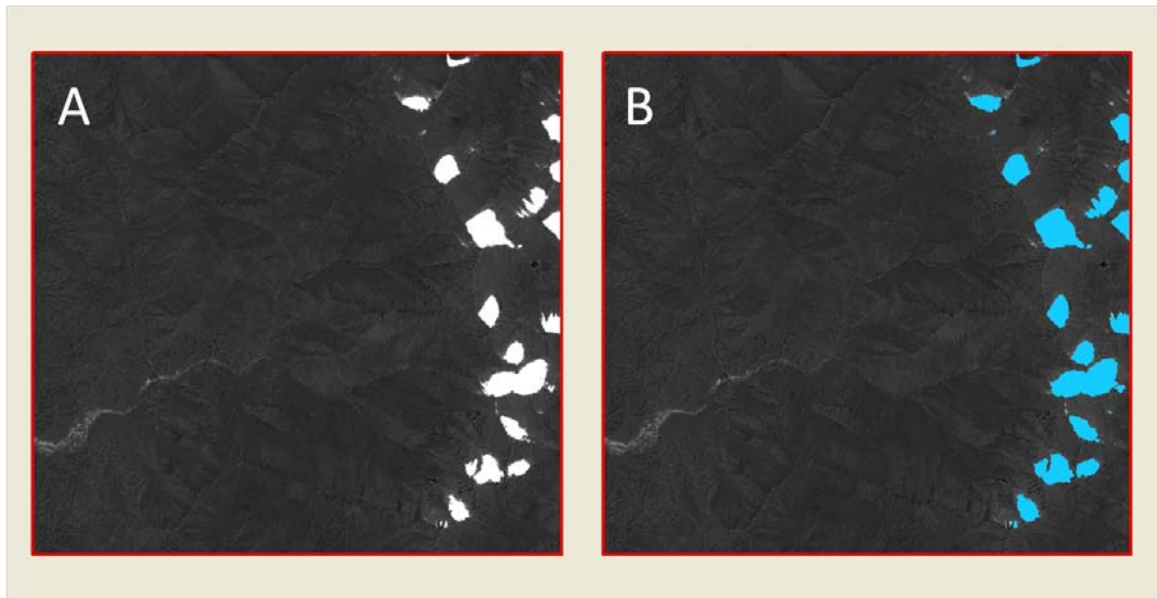


**Figure 34. Ratio of ASTER bands 3 and 4 for Study Area 1: (A) result of the band ratio; (B) glaciers, shown in blue, as delineated by Feature Analyst.**

The largest problem with using band ratios to map glaciers is that even a light cover of debris confounds the process. This hinders their ability to map debris-covered glaciers, and it decreases their precision for mapping the glaciers' edges if any amount of debris has fallen on the ice whatsoever. Still, as long as this deficiency is taken into



account, band ratios are an effective method for mapping clean ice and small clean glaciers.

An additional difficulty is the inability of both band ratios and Feature Analyst to distinguish seasonal snow on a mountainside from snow in a glacier's accumulation zone. Patches of snow which have accumulated on north-facing slopes, for instance, have the same spectral signature as snow in a catchment basin, and thus both will be extracted when Feature Analyst is used. This problem can be partially mitigated by eliminating all polygons considered too small to be a glacier (e.g.  $< 0.1 \text{ km}^2$ ).

A morphometric glacier mapping (MGM) approach (e.g., Bolch *et al.* 2007), on the other hand, was found to not be a viable method for mapping small glaciers. The basis in MGM is the use of topographic thresholds, derived from a DEM. However, in order for these thresholds to be usable, the glacier must be distinguishable, topographically, from its surrounding terrain. Without distinguishable topographic features, the glacier cannot be extracted using surface analyses, and thus statistical parameters cannot be determined.

Such was the case in Study Areas 1 and 2, characterized by small cirque-type glaciers, the largest of which was just  $0.92 \text{ km}^2$ . Being only small masses of ice, the glaciers essentially had conformed to their surrounding topography, and their morphometric parameters were not sufficiently different from the rest of the landscape (Figure 35). Thus, without the ability to use topographic features, the morphometric approach is not possible on small glaciers when using DEMs created from ASTER imagery.

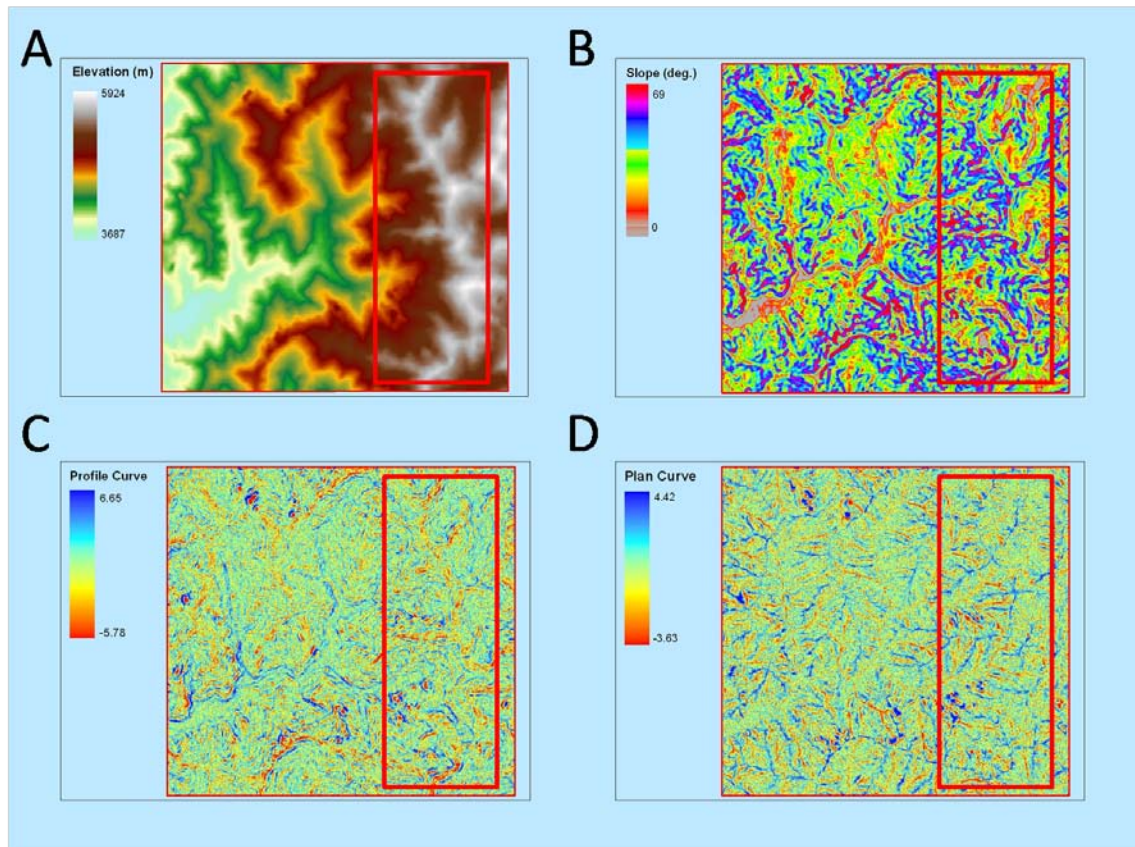


**Figure 35. Topographic analyses for Study Area 1. The red boxes demark the areas where glaciers are located; the glaciers are not readily distinguishable from their surrounding terrain.**

## 5.2 Mapping Debris-covered Glaciers

The morphometric approach (Bolch *et al.* 2007) proved to be useful for mapping debris-covered glaciers in Study Areas 3-5. A combination of thermal data, cluster analysis, supervised classifier, and morphometric thresholding allowed for an adequate delineation of debris-covered glaciers. These outputs could then be merged with clean ice—derived from band ratios—to create a map of glaciers in the areas surrounding Parkachik Glacier, Drang Drung Glacier, and the Nun Kun and Zaskar Massifs.

Thermal bands were an effective input to the MGM. Because ice is generally colder than its surrounding terrain, it is possible to extract glaciers with thermal data

(Figure 36). The biggest drawback of ASTER's thermal bands is their relatively low spatial resolution of  $90 \times 90$  m, which does not allow the level of precision necessary for glacier monitoring. Additionally, when deriving statistical parameters, a number of areas were erroneously classified as glaciers, due to conditions that caused them to be colder than typical non-glacier areas. Particularly, areas in shadow tended to confound the process, as did north-facing slopes, and bodies of water. The time of day also needed to be taken into account. Images taken in the early morning were characterized by very cold thermal output, even for non-glacial debris, and as such led to a number of false positives. Finally, a thick layer of debris inhibits the ability of thermal bands to recognize underlying ice.

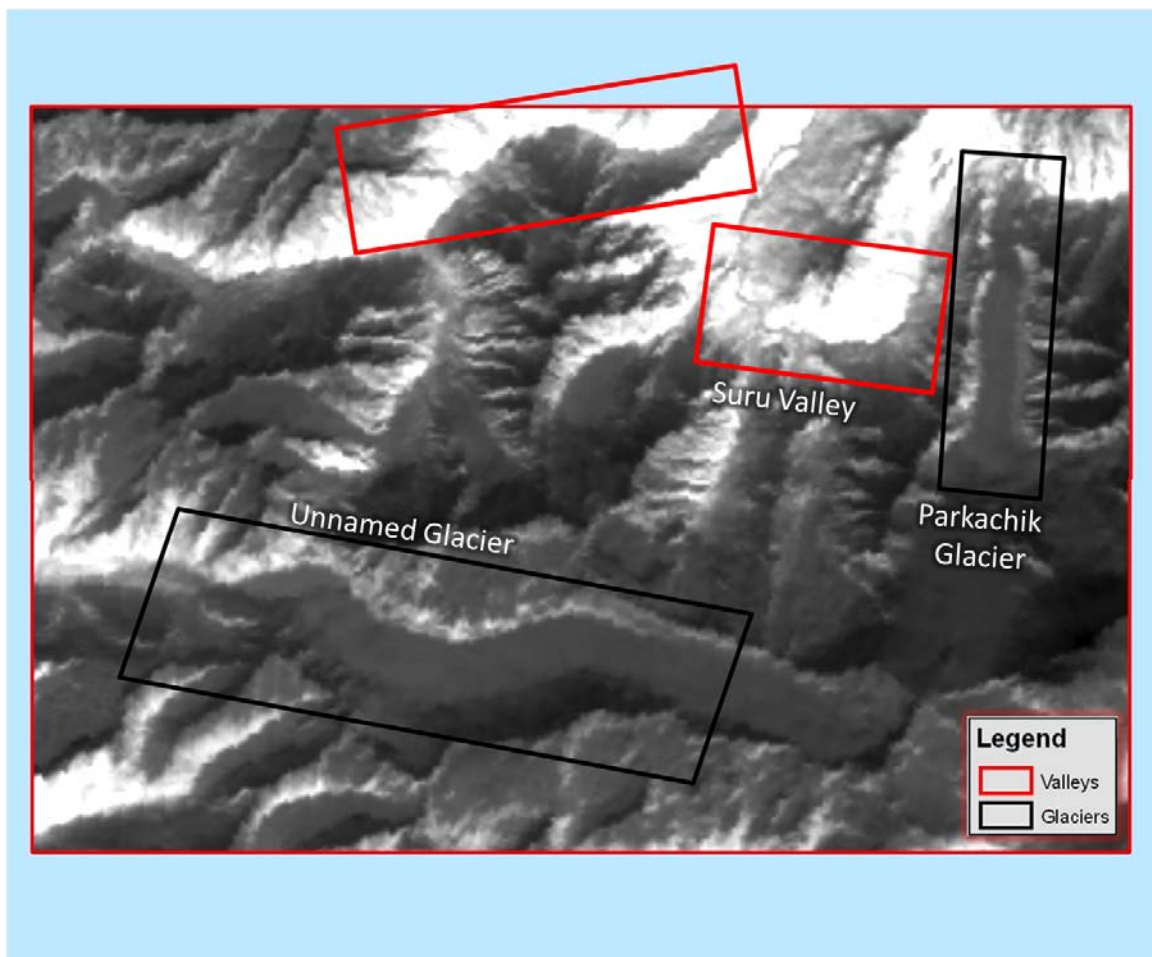


**Figure 36. Thermal image from ASTER band 10 for Study Area 3.**

Supervised classifiers and cluster analyses also provide an effective method of distinguishing glaciers from other land cover features. In ArcGIS, the IsoCluster tool, followed by the Maximum Likelihood classifier produced an effective output image to be used in MGM (Figure 37). Slope was used as the only input band, as it was the only topographic input that proved to be useful. The others—profile curvature, and planimetric curvature—produced inadequate results. Various numbers of output classes were tried, with eight classes proving to be the most effective.

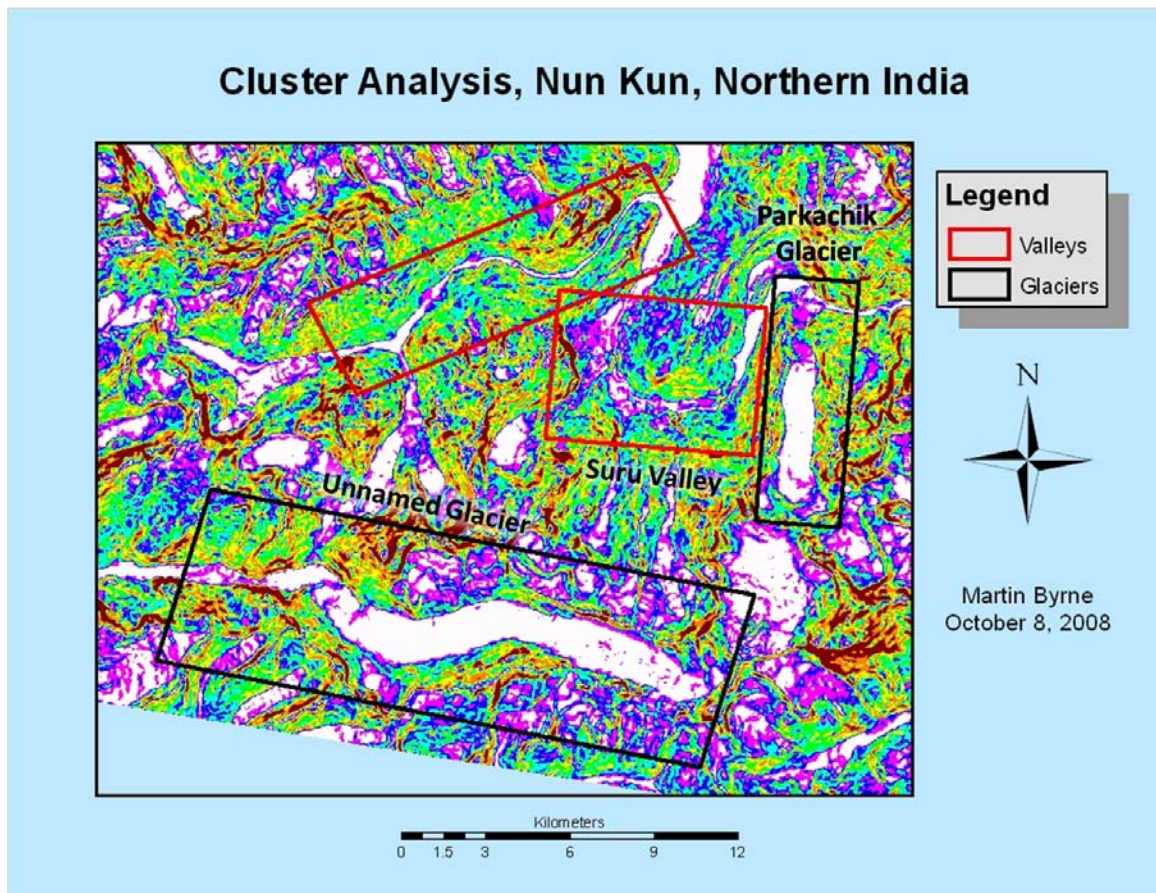
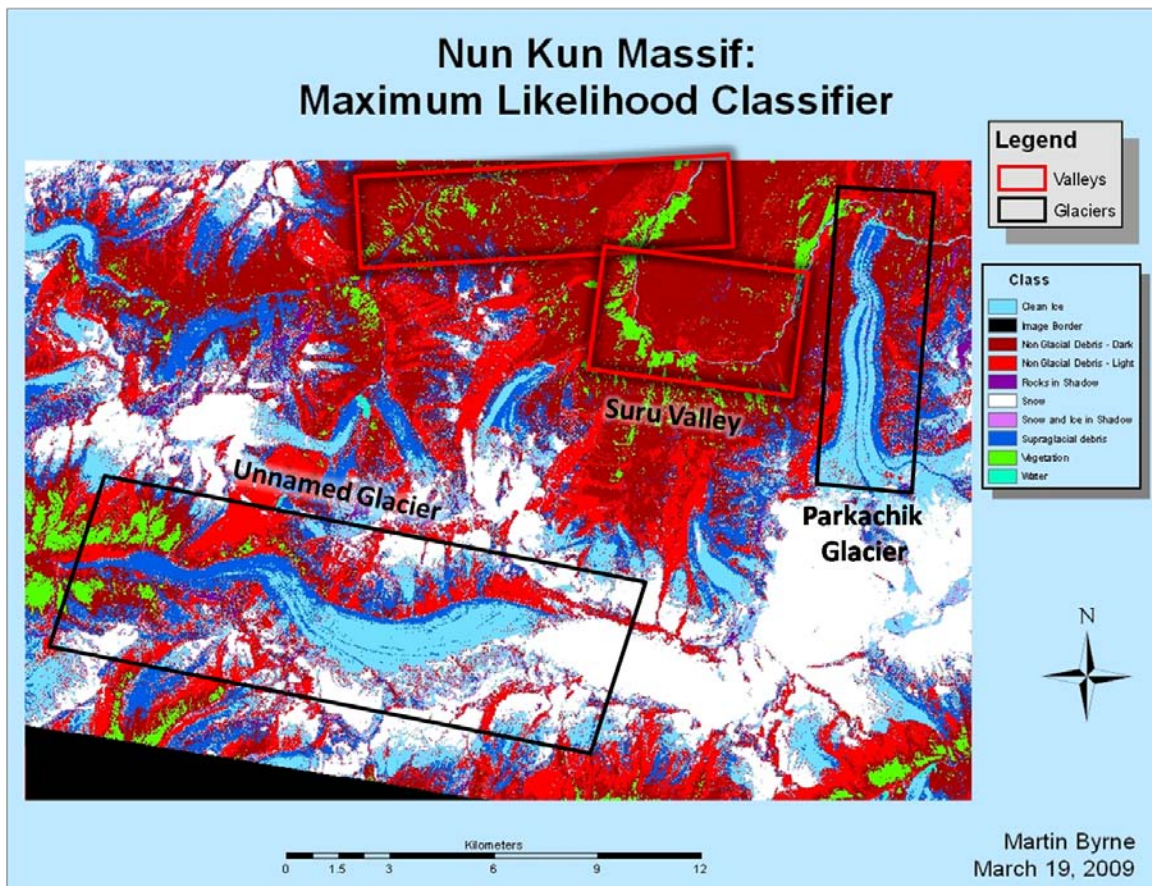


Figure 37. Cluster Analysis for Study Area 3.

IDRISI's Maximum Likelihood classifier was also effective, but only for Study Area 3 (Figure 38). For study areas 4 and 5, its output was inadequate and unacceptable. It proved categorically unable to distinguish between glacial debris and the valley sides,



and its distinction of other land cover classes was similarly questionable. However, Minimum-Distance-to-Means and K-Nearest-Neighbor were able to classify the area effectively. Both of these classifiers produced acceptable outputs, yet they varied slightly from one another, and so both were used as inputs for the MGM of Study Areas 4 and 5.



**Figure 38. Maximum Likelihood classification for Study Area 3.**

Morphometric parameters produced varying results. The most effective topographic input in all three study areas was slope. Profile curvature was the only other topographic feature that gave the slightest suggestion of being useful. When viewed at a small scale, glaciers' features were visible; however, this proved to be misleading, as the values were too varied—even along glaciers' edges—to be used for any kind of analysis.

Planimetric curvature was even less useful than profile curvature, so neither of these topographic variables was used in the final output image.

The final glacier outlines required a good deal of manual editing. The outlines were adequate for large glaciers (Figures 39- 42), but sometimes they extended past the glacier's true terminus by several to several dozen meters. This was especially true in areas where there was a smooth transition from glacier to forefield, and in areas where stagnant and relict ice still remained but was detached from the active ice margin.

Another issue that confounded the MGM process was topographic variability on the glacier surface. Parkachik Glacier, for instance, contains a large icefall ~ 2 km from its terminus. The slope of this icefall did not fit within the slope threshold; however, if the threshold was raised, it would be too steep, and valley sides would be falsely included in the output image. And finally, as mentioned above, the morphometric procedure is incapable of mapping small glaciers. Thus, in the final output image, many of the smaller glaciers had to be delineated manually.

## **5.3 Glacier monitoring**

### ***5.3.1 Himis-Shukpachan***

A Landsat 7 image from 2000 was compared with GPS points and field measurements from the 2007 field campaign for the glacier at Himis-Shukpachan. The 2000 margin was manually delineated based on visual interpretation. In that seven-year span, the glacier terminus receded ~ 63 m—an average of 9 m of recession per year (Figure 43).

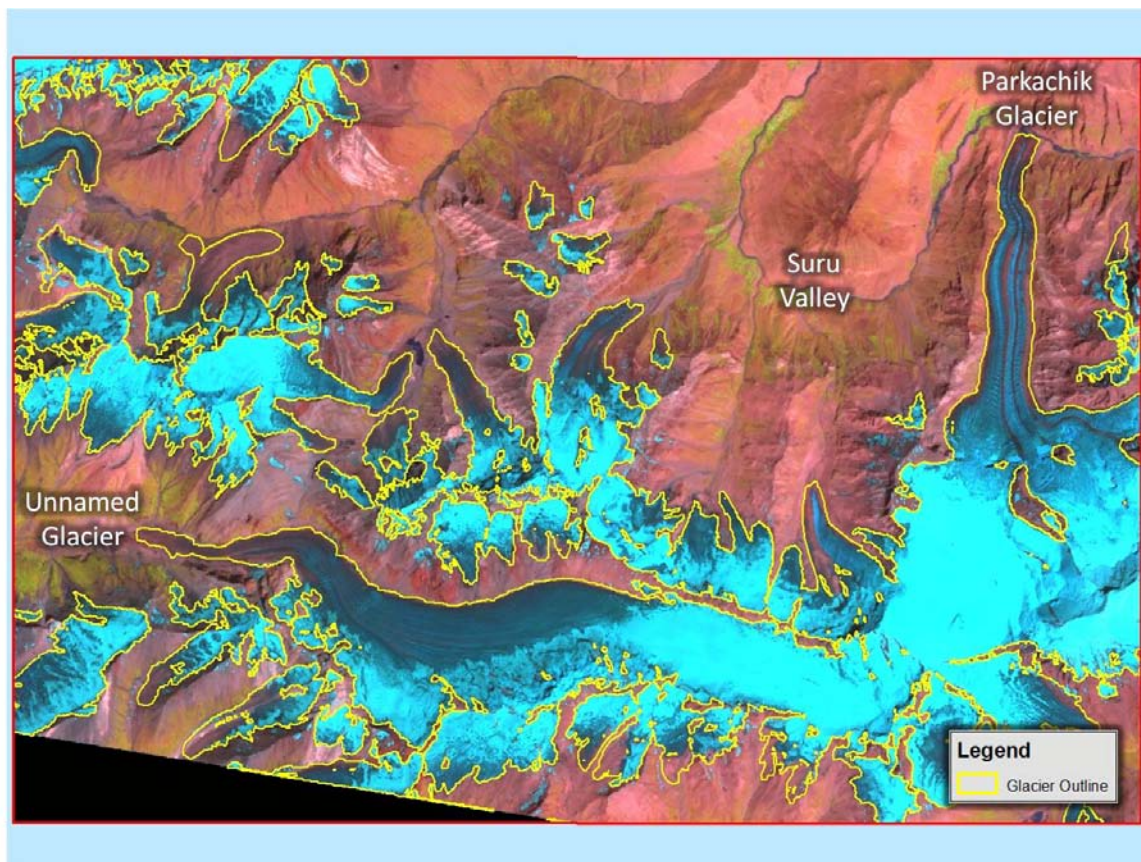


**Figure 39. Morphometric glacier mapping (MGM) results for Study Area 3.**

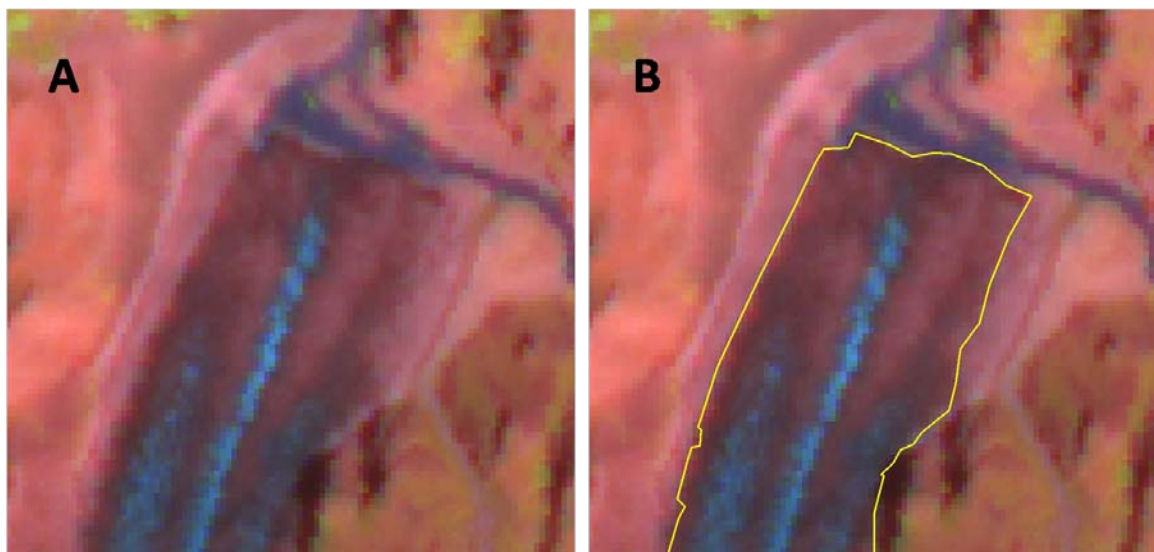


**Figure 40. MGM results for Parkachik Glacier, Study Area 3. (A) Glacier terminus before MGM; (B) MGM results for the glacier terminus.**



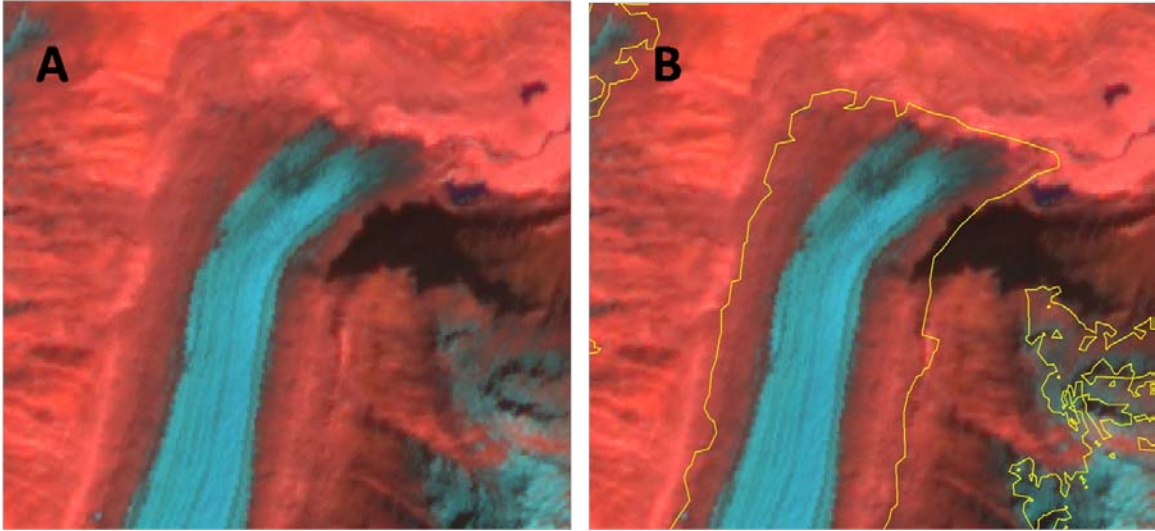


**Figure 41. MGM results for Drang Drung Glacier, Study Area 4. (A) Glacier terminus before MGM; (B) MGM results for the glacier terminus.**

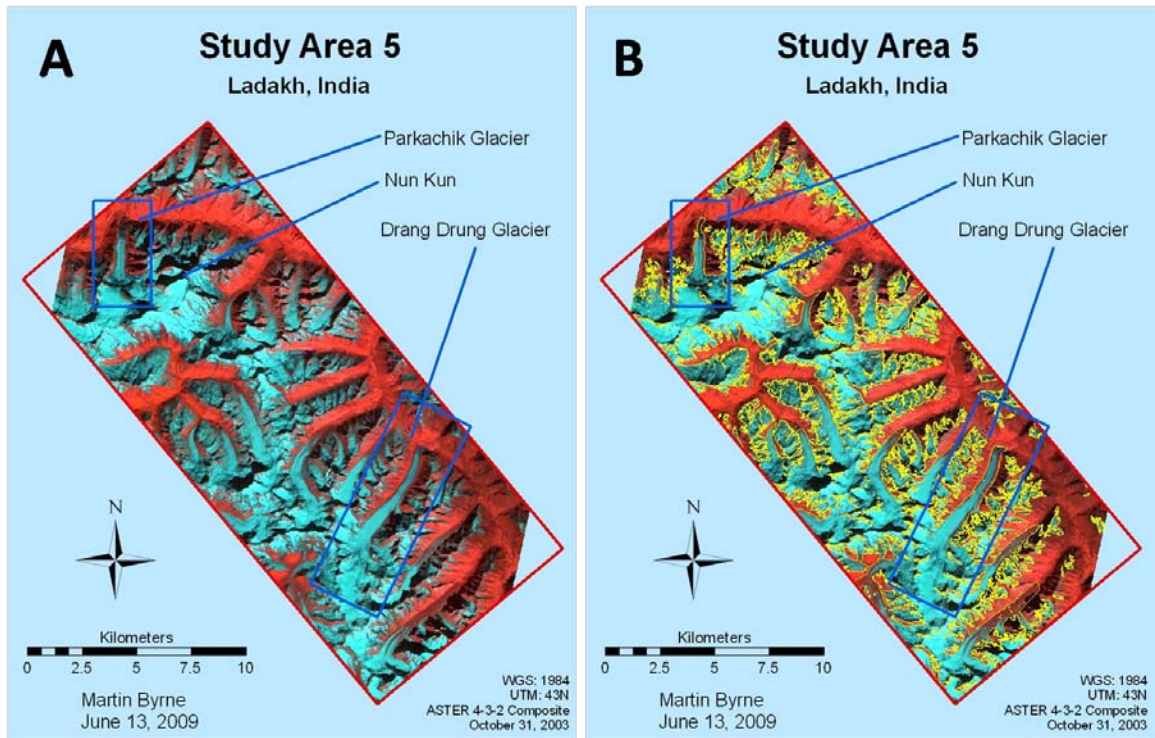


**Figure 42. Morphometric glacier mapping (MGM) results for Study Area 5. (A) Study area before MGM; (B) MGM results.**



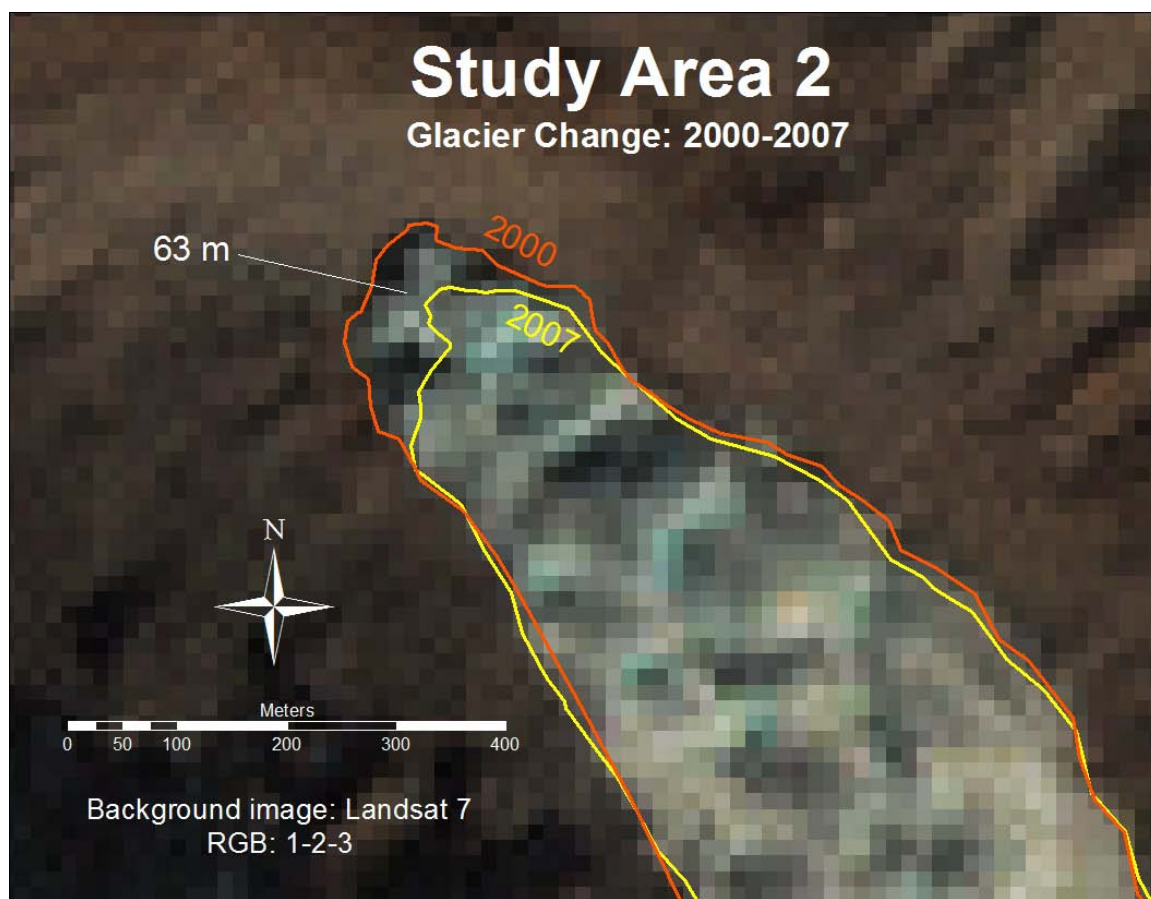


Figure 43. Change in the glacier terminus from 2000 to 2007 in Study Area 2.

### 5.3.2 Drang Drung

Data from a variety of sources were used to monitor Study Area 4. In the 33-year span between 1975 and 2008, Drang Drung Glacier experienced a total recession of 311 m—an overall rate of recession of  $\sim 9$  m per year (Table 3; Figure 44). The recession was constant and steady, with a possible increase in speed after 1999.

**Table 3. Terminal change of Drang Drung Glacier between 1975 and 2008.**

| <i>Time Span</i> | <i>Number of years</i> | <i>Total change<br/>(in meters)</i> | <i>Avg. change per year<br/>(in meters)</i> |
|------------------|------------------------|-------------------------------------|---|
| 1975-1990        | 15                     | -80                                 | -5.33                                       |
| 1990-1992        | 2                      | -35                                 | -17.5                                       |
| 1992-1999        | 7                      | -46                                 | -6.57                                       |
| 1999-2000        | 1                      | -20                                 | -20   |
| 2000-2002        | 2                      | -13                                 | -6.5  |
| 2002-2003        | 1                      | -30                                 | -30   |
| 2003-2005        | 2                      | -15                                 | -7.5  |
| 2005-2006        | 1                      | -25                                 | -25   |
| 2006-2008        | 2                      | -47                                 | -23.5                                       |
| 1975-2008        | 33                     | 311                                 | -9.42                                       |

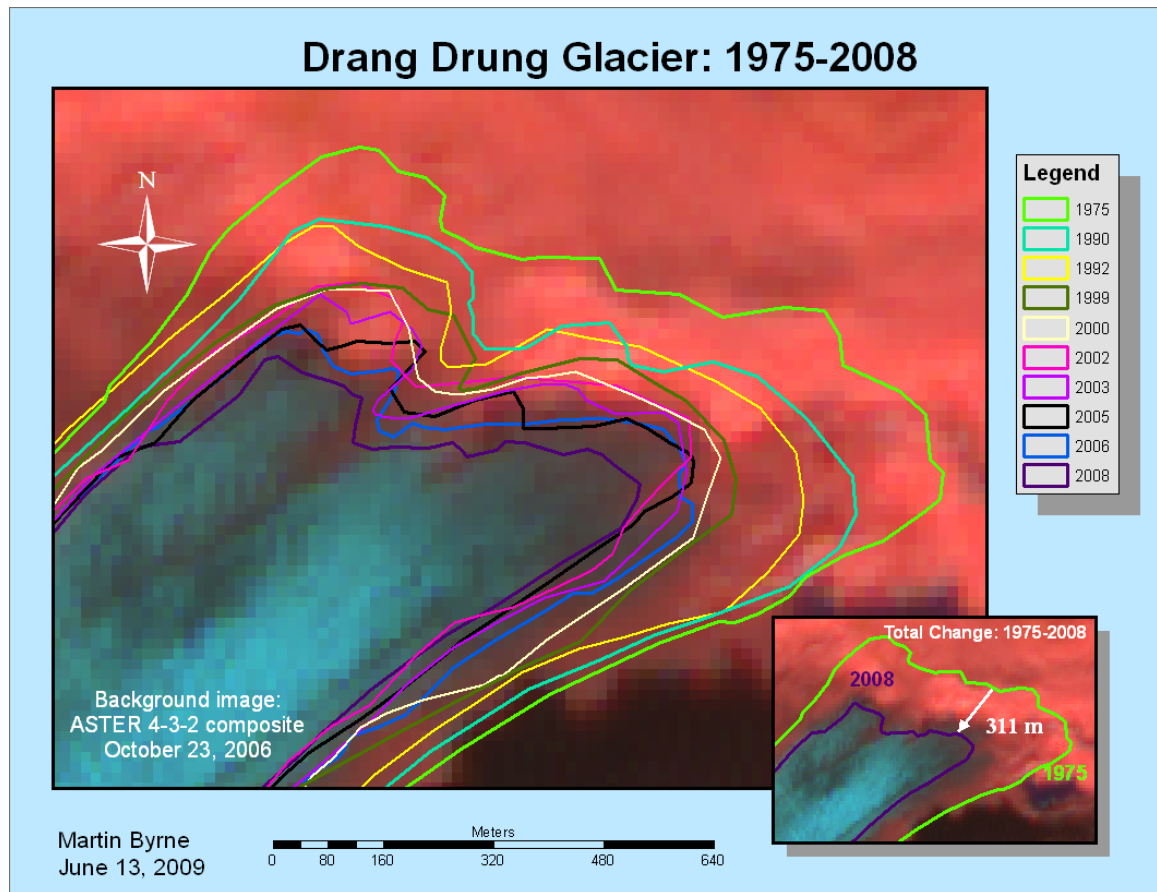


**Figure 44. Change in the Drang Drung Glacier terminus from 1975-2008 in Study Area 4.**

In addition to the retreat seen at Drang Drung's terminus, its tongue also experienced an increase of > 10% in debris cover from 1990 to 2006 (Table 4). From

1990 to 1999, the debris-covered ice area increased by > 6%, or 0.7% per year. Over the following seven years, from 1999 to 2006, the debris-covered area changed by 4%, a rate of change of 0.6% per year.

**Table 4. Debris-cover on Drang Drung Glacier between 1990 and 2006.**

| <i>Year</i> | <i>Percent debris-cover</i> |
|-------------|-----------------------------|
| 1990        | 70.6                        |
| 1992        | 73.0                        |
| 1999        | 76.9                        |
| 2000        | 74.9                        |
| 2002        | 80.8                        |
| 2003        | 76.6                        |
| 2005        | 80.9                        |
| 2006        | 81.0                        |
| 1990-2006   | +10.4                       |

### 5.3.3 Parkachik

During the period from 1979-1990, Parkachik Glacier retreated ~ 141 m—an average of ~ 13 m of loss per year. However, during the following decade, from 1990 to 1999, it readvanced 157 m—more than 17 m per year—so that in the summer of 1999 its terminus was farther down-valley than it had been in 1979. This trend continued for the following five years; from 1999 to 2004, Parkachik Glacier experienced an average advance rate of ~ 15 m per year (Table 5; Figure 45).

**Table 5: Terminal change of Parkachik Glacier between 1979 and 2008.**

| <i>Time Span</i> | <i>Number of years</i> | <i>Total change<br/>(in meters)</i> | <i>Avg. change per year<br/>(in meters)</i> |
|------------------|------------------------|-------------------------------------|---|
| 1979-1990        | 11                     | -141                                | -12.82                                      |
| 1990-1999        | 9                      | +157                                | +17.44                                      |
| 1999-2002        | 3                      | -17                                 | -5.67                                       |
| 2002-2003        | 1                      | +6                                  | +6  |
| 2003-2004        | 1                      | +33                                 | +33   |
| 2004-2008        | 4                      | -7                                  | -1.75                                       |
| 1979-2008        | 29                     | +31 (net); 361 (gross)              | +1.07                                       |

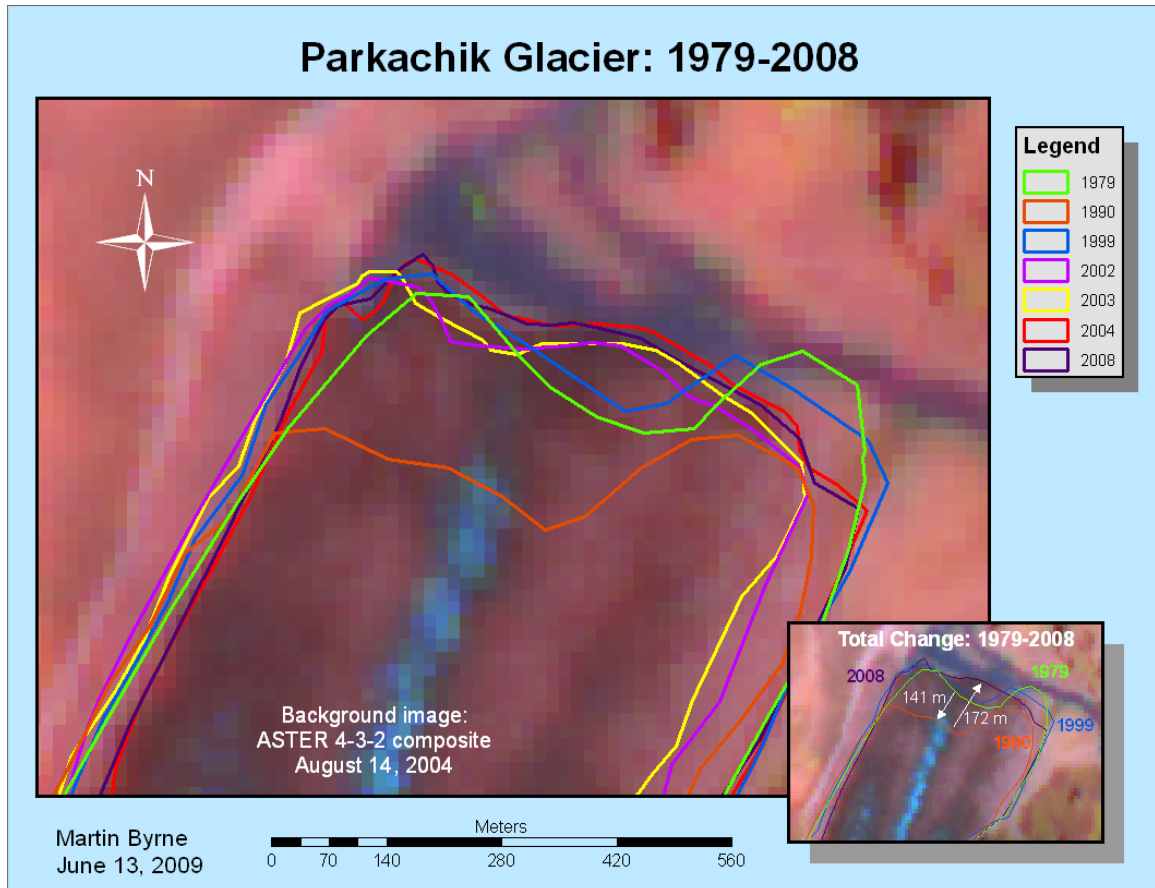


**Figure 45. Change in the Parkachik Glacier terminus from 1979 to 2008 in Study Area 3.**

The trend of advancement seems to have been temporary for Parkachik Glacier, however, as it experienced negligible retreat from 2004 to 2008. The retreat of 7 m was ever so slight—an average loss of 1.75 m per year—suggesting the glacier is neither advancing nor receding at the moment. This could be indicative of one of three things: a) the glacier has temporarily reached a state of equilibrium; b) the glacier's advance has begun to slow, and it will in future years begin to retreat once again; or c) the glacier is still in a state of advance, but its terminus is constantly being washed away as it encroaches into the Suru River. Without further evidence, it is difficult to say which of these situations best describes the conditions Parkachik Glacier is currently experiencing.

Contrary to the apparent advance experienced by Parkachik Glacier from 1990 to 2004, it did not experience a corresponding decrease in debris-cover. Indeed, debris-cover on Parkachik Glacier increased by  $< 8\%$  during that span, a rate of increase of  $\sim 0.6\%$  per year (Table 6).

**Table 6: Debris-cover on Parkachik Glacier between 1990 and 2004.**

| <i>Year</i> | <i>Percent debris-cover</i> |
|-------------|-----------------------------|
| 1990        | 87.2                        |
| 1999        | 91.7                        |
| 2002        | 93.8                        |
| 2003        | 93.1                        |
| 2004        | 95.1                        |
| 1990-2004   | +7.9                        |

## 6. Discussion

### 6.1 Mapping Small Glaciers

The ability of band ratios to map clean ice is not surprising, as its effectiveness has been demonstrated numerous times on glaciers throughout the world (e.g., Sadjak and Wheate 1999; Paul 2000a, 2000b; Gao and Liu 2001; Paul *et al.* 2002; Kääb *et al.* 2003; Ranzi *et al.* 2004; Bolch and Kamp 2006; Narama *et al.* 2006; Rees 2006; Racoviteanu *et al.* 2008). Additionally, as expected, Feature Analyst proved quite capable of distinguishing snow and ice from surrounding terrain, and extracting it.

One possible method of improving the mapping of small ( $< 2 \text{ km}^2$ ) glaciers with band ratios may be to combine them with a supervised classifier in a two-tiered approach. However, this method would rely entirely on multispectral data, and as such would still ignore the problem posed by a thick layer of debris, which has a similar spectral signature as its surrounding terrain. Thus, this method, too, would be limited primarily to clean glaciers.

The morphometric glacier mapping (MGM) approach's ineffectiveness for mapping small glaciers was also not surprising; it had previously been stated that it is only effective on lightly debris-covered glaciers and larger glaciers (Bolch and Kamp 2006). The glaciers of Igu and Himis-Shukpachan were lightly debris-covered or clean, but they certainly were not large. The purpose of MGM is to eliminate the deficiencies of multi-spectral imagery by relying on DEM-derived topographic parameters. While debris-covered glaciers' tongues may have a similar spectral signature to their

surrounding terrain, they have other characteristics—such as slope and curvature—which distinguish them from their forefields and ablation valleys.

Additionally, while the  $15 \times 15$  m spatial resolution of ASTER-derived DEMs may be sufficient for mapping large glaciers, it does not provide the necessary precision for mapping small glaciers. The glaciers that were analyzed in Igu and Himis-Shukpachan study areas were all smaller than  $1 \text{ km}^2$ —some of them substantially so. This is too small for  $15 \times 15$  m resolution imagery to be effective.

Bolch *et al.* (2007) concluded that, while MGM is effective for mapping large glaciers, it will be substantially more effective when better-resolution imagery and, particularly, better resolution DEMs, become available. Even if sub-meter resolution DEMs were to become available for Ladakh, it is still questionable whether the MGM would be effective—or appropriate—for mapping small glaciers. The paucity of unique characteristics that can be used to distinguish the glaciers from their surrounding topography will continue to limit the effectiveness of MGM on small glaciers.

## **6.2 Mapping Debris-covered Glaciers**

Much like with mapping small glaciers, the results of MGM on debris-covered glaciers offered little surprise. Morphometric mapping techniques had already been proven to be effective in the Khumbu Himal (Buchroithner and Bolch 2007; Bolch *et al.* 2007) and the northern Tien Shan (Bolch and Kamp 2006), both of which are characterized by glaciers having similar features to those in Ladakh. Thus, it is unsurprising that the same method could be successfully transferred to Ladakh, and it can be assumed that it will be



similarly effective in other regions with characteristics comparable to those in Ladakh, the Khumbu Himal, and the Tien Shan.

The MGM in Ladakh had more difficulties distinguishing glacier termini than one would hope. Bolch and Kamp (2006), Buchroithner and Bolch (2007), and Bolch *et al.* (2007) all experienced the aforementioned problem, concluding that MGM is often hindered by glaciers with a smooth transition from ice to forefield—that is, glaciers with little or no terminal moraine. One noticeable characteristic of the glaciers in Study Areas 3-5 was that they tended to lack large, discernable terminal moraines. As a result, many MGM-derived outlines were unreliable, and had to be manually mapped as a post-processing step.

Additionally, Bolch *et al.* (2007) found that delineation of glacier margins is further hindered by the presence of stagnant ice in the distal areas of the glacier's tongue. In many cases, they noted, it is not possible to tell where active ice ends as it transitions to stagnant ice, even when one is standing atop the glacier. This was often the case in Ladakh, and the MGM was confounded accordingly.

As Paul *et al.* (2004a) noted, morphometric mapping is infinitely faster than manual delineation when mapping large numbers of glaciers, and it provides an excellent starting place when mapping smaller numbers, even if the procedure is still less-than-perfect. Despite the issues discussed in the two previous paragraphs, MGM is a promising method for mapping glaciers in Ladakh. The outputs are adequate, although manual editing is required on a disappointingly high number of glaciers. Ultimately, just as Bolch *et al.* (2007) concluded, MGM will be substantially more effective when DEMs and images of higher spatial resolution become available. When that happens, it seems

likely that the creation of an automated glacier inventory will be viable for Ladakh, and automated glacier monitoring for all but the smallest glaciers will be possible there. Until then, MGM remains a useful and efficient method of mapping glaciers in Ladakh, but manual editing is still necessary.

## **6.3 Glacier Monitoring**

### ***6.3.1 Himis-Shukpachan and Drang Drung***

The findings on the glaciers of Himis-Shukpachan and Drang Drung are consistent with others (e.g., Kadota *et al.* 2000; Ageta *et al.* 2001; Khromova *et al.* 2003; Kulkarni *et al.* 2005, 2007; WWF 2005; Ren *et al.* 2006; Bolch 2007; IPCC 2007; UNEP 2008) who have found glaciers in the Himalaya and its surrounding mountain ranges to be receding. As Ren *et al.* (2006) explained, these changes are most likely caused by the combined effect of reduced precipitation and warmer temperatures due to global warming. As the climate continues to change, these effects will also continue and it seems likely that the glaciers' retreat will become even more dramatic.

On Drang Drung Glacier, the terminus appeared to retreat at a faster rate after 1999. While this apparent change could very well have occurred, it is nevertheless important to note that imagery was much more readily available for the period from 1999 to present, as opposed to the period prior to 1999, for which a total of three usable images were available. The increased availability of imagery after 1999, coupled with the enhanced spatial resolution of the images, means the precision with which the glaciers can be monitored is much greater for the latter period than for the former.

Nevertheless, although ASTER DEMs, with a spatial resolution of 15 m, are generally adequate for most functions (Bolch *et al.* 2005), the small increments of change experienced by glaciers such as Drang Drung and Parkachik may often occur within the space of a single pixel. Thus, it is very possible—and not at all unlikely—for manually delineated margins to be erroneous by several dozen meters (just two or three ASTER pixels). Therefore, a margin of error of up to several dozen meters must be taken into account when monitoring glacier change with ASTER imagery or Landsat ETM+ data. When using earlier imagery, the margin must be even larger.

The glacier retreat on Drang Drung Glacier from 1990 to 2006 was corresponded to by an increase in the area of debris-cover by > 10%. Bolch *et al.* (2008a) explained that the increase in debris-covered areas on a glacier such as Drang Drung is mainly due to the decrease of clean-ice areas in the transition zone between clean and debris-covered ice. This is to be expected, and is indicative of a receding glacier (Tobias Bolch, pers. comm.).

### **6.3.2 Parkachik Glacier**

It is likely the findings on Parkachik Glacier are consistent with those of Hewitt (2005) and Bishop and Shroder (2009), all of whom found anomalously advancing glaciers in the Karakoram. These glaciers tended to advance sporadically, particularly during the 1990s and early 2000s. Parkachik Glacier acted much the same way, following a large retreat during the 1980s with an even larger advance the following decade.

Additionally, Hewitt (2005) noted that the anomalous behavior of glaciers in the Karakoram was constrained to those glaciers with the highest levels of relief, and which

cover extreme altitudinal ranges. Parkachik Glacier, which flows from its catchment basin at ~ 6000 m asl to its terminus in the Suru River at 3560 m asl, and contains a steep icefall along its tongue, fits these criteria perfectly. Parkachik's accumulation zone, on the slopes of Nun Kun, is one of the highest in Ladakh, and it is a relatively short glacier, two factors that could account for its sudden and aberrant behavior, which seems to be unique among glaciers in Ladakh. This suggests some sort of temperature or precipitation differential that affects short steep glaciers with high accumulation zones, allowing them to collect snow which passes glaciers on lesser peaks; the results of this increased level of precipitation can also be seen sooner due to the shorter lag time of a short steep glacier.

Hewitt (2005) and Bishop and Shroder (2009) postulated that the factor behind these anomalous advances was an increased amount of precipitation at high elevations, as well as an increase in summer storm activity and a corresponding general decrease in summer mean and minimum temperatures—all due to global warming. This hypothesis would hold equally true in Ladakh, which is influenced by similar weather patterns as the Karakoram. Thus, it seems likely that the rapid advance of Parkachik Glacier in the 1990s and early 2000s was related to global warming.

A paucity of imagery of Parkachik Glacier from the 1980s and 1990s hampers the ability to truly understand what it has done the past few decades. It is important to be cautious before making any hasty conclusions about Parkachik Glacier, because the scene from 1990 is merely a snapshot in time, and could easily be an anomaly. The glacier ends in the Suru River, which also hinders our understanding of its actions. It is possible that there was a large flooding event in 1990, which washed away the terminus, giving

the appearance of retreat during that time. Additionally, the Suru River washes away any evidence around the glacier terminus that would decisively signify an advancing glacier. Without the availability of additional data from the 1980s and 1990s, it is impossible to conclude exactly what Parkachik Glacier was doing during those decades.

At any rate, a multi-temporal analysis of Parkachik Glacier suggested that it experienced rapid retreat during the 1980s, followed by an even more rapid advance in the 1990s. That advance seemed to continue for the first half of the 2000s, but has slowed down and possibly begun to reverse again since 2004. Right now it is difficult to determine exactly what the glacier is doing, and it will therefore be essential to continue to monitor it in the coming years, in order to more fully understand how it is behaving.

## 7. Conclusion

This thesis attempted to answer three separate questions regarding glacier mapping and monitoring in Ladakh, northwestern India. The first question concerned the ability of the morphometric glacier mapping (MGM) procedure (Bolch *et al.* 2007) to map small glaciers. The second question asked whether the aforementioned procedure was an effective method of mapping large debris-covered glaciers in Ladakh. The final question wondered whether glaciers in Ladakh have changed since the mid- to late-1970s.

The morphometric approach (*ibid.*) was found to be inadequate for mapping small glaciers; however, band ratios proved to be quite effective for this purpose, as long as the glacier had little or no debris on its surface. Band ratios have previously been shown to be effective for mapping clean ice. The inability of MGM to map small glaciers was also unsurprising, as these glaciers tend to conform to their surrounding terrain, and lack the unique topography necessary for them to be distinguished from nonglacial features. Thus, surface analyses are useless, rendering MGM ineffective for small glaciers.

MGM may be ineffective for small glaciers, but it shows great promise for large glaciers in Ladakh. Morphometric approaches have previously been shown to be effective in other areas of the Himalaya and its neighboring regions, so it is not surprising that it was generally effective in Ladakh. While it is quite a promising method, MGM still must be used with reservations in Ladakh, because it contains a number of faults. Glaciers which have a smooth transition from ice to forefield or ablation valley (i.e., glaciers that lack distinct terminal or lateral moraines) confound the process; stagnant ice in the distal areas of glaciers often causes problems with glacier mapping; and glacial

topography is sometimes too varied to fit within a set of morphometric parameters, forcing the mapmaker to choose between expanding the parameters to better include the glacier, or keeping them narrow in order to avoid erroneously mapping nonglacial features and valley walls.

All of these problems were present when mapping glaciers in Ladakh. Therefore a great deal of manual editing was necessary in post-processing. So long as this is kept in mind while performing the MGM process, it is not an issue of great concern. Therefore, it was concluded that glaciers of Ladakh can be mapped effectively with MGM, but caution must be taken to check results and verify their accuracy. Until this method is improved—most likely through the eventual availability of higher-resolution imagery and DEMs—it cannot yet be an automated process; human subjectivity is still required during several steps of the process, including post-processing. Morphometric mapping is nonetheless a promising method for mapping glaciers in Ladakh.

A variety of sources were used to measure glacial change in Ladakh over the last four decades. A multi-temporal analysis of three glaciers in Ladakh found that two have apparently receded—one since at least the mid-1970s, the other since at least 2000—and it seems likely that this change has been caused by a combination of reduced precipitation and a trend of generally increasing temperatures.

One exception in Ladakh to the apparent trend of glacier retreat across the Himalaya was Parkachik Glacier, which, after a period of retreat in the 1980s, experienced a readvance in the 1990s and early 2000s. This is consistent with the findings of Hewitt (2005) and Bishop and Shroder (2009), who found a number of glaciers in the nearby Karakoram to be anomalously advancing. The advances were



incongruous and sporadic, just like Parkachik's apparent advance. They were limited to glaciers with high levels of relief and which covered large altitudinal ranges, both of which are traits possessed by Parkachik Glacier. It was hypothesized that these glaciers were being fed by increased precipitation at the highest elevations due to climate change. Parkachik, having its accumulation zone below the peaks of Nun Kun, possesses the highest elevation of any glacier in the region, possibly explaining, at least partially, the increased precipitation; and it is relatively short and very steep, which explains the quick changes from retreat to advance experienced over the past few decades.

Parkachik Glacier offers an important clue regarding the climate forcings of glaciers in Ladakh. Thus, it is important to continue to monitor it in coming years, in order to gain insight into global warming's effects on glaciers in the region. It is similarly paramount to continue to monitor other glaciers, such as Drang Drung and Himis-Shukpachan, as these glaciers provide a standard by which the effects of climate change can be measured and monitored.

The effects of global climate change are wide ranging, from sea level change to changing precipitation patterns, to changing faunal zones of habitation (Kolbert 2006; IPCC 2007), and glaciers are some of the foremost indicators of those changes (Maisch 2000; Hinkel *et al.* 2003; Hewitt 2005; Quincy *et al.* 2005; Barry 2006; Kolbert 2006; Zemp *et al.* 2006; Racoviteanu *et al.* 2008; UNEP 2008), as well as harbingers of possible heretofore unforeseen future scenarios caused by such changes (Oerlemans 1994; Hinkel *et al.* 2003). Thus, it is imperative that we continue to map the world's glaciers, before it's too late. However, just mapping glaciers is not enough. In order to understand how they are reacting to climate change, they must be monitored continually.

Recent advances in technology and remote sensing capabilities have allowed the mapping of glaciers on a scale never before seen. Automated and semi-automated glacier monitoring is now possible, even in extremely remote areas and areas of extreme topography and difficult terrain; with remote sensing, it is now possible to monitor glaciers without ever even setting foot on them.

Many Himalayan glaciers are characterized by a thick layer of debris however, and this confounds the process of glacier mapping with satellite imagery. A number of methods have been developed to overcome this problem, but it is still a work in progress. ASTER imagery allows for the creation of DEMs, which have been used for topographically oriented approaches, such as MGM (Bolch *et al.* 2007); however, the spatial resolution of  $15 \times 15$  m is not always sufficient to delineate glacier margins with a high enough precision to be used for glacier monitoring. For many debris-covered glaciers, higher-resolution imagery must become readily available before they can viably be monitored on a continuing basis.

Thus, just as it is important to continue to map and monitor the world's glaciers, it is also essential to continuously test the limits of the currently available technology. By developing new methods, and testing new approaches with existing methods, the ability to map debris-covered glaciers will gradually improve, just as it has in the past decade.

By testing the morphometric process's capabilities on small glaciers and on large glaciers in Ladakh, this thesis has expanded our knowledge of the limits of technology. And, by monitoring glaciers in Ladakh, it has provided a glimpse of global warming's influence, as well as creating a base on which future monitoring projects can expand. This thesis was the first monitoring program of Ladakh's glaciers, and it is hoped that it

will inspire others to conduct studies there, adding to the literature of the currently underrepresented region.

## 8. References

- Ageta, Y., N. Naito, M. Nakawo, K. Fujita, K. Shankar, A.P. Pokhrel, and D. Wangda. 2001. Study project on the recent rapid shrinkage of summer-accumulation type glaciers in the Himalayas, 1997-1999.
- Altmaier, A., and C. Kany. 2002. Digital surface model generation from CORONA satellite images. *ISPRS Journal of Photogrammetry and Remote Sensing*, 56, 221-235.
- Andreassen, L.M., F. Paul, A. Kääb, and J.E. Hausberg. 2008. Landsat-derived glacier inventory of Jotunheimen, Norway, and deduced glacier changes since the 1930s. *The Cryosphere*, 2, 131-145.
- Aniya, M. 1988. Glacier inventory for the northern Patagonia Icefield, Chile, and variations 1944/45 to 1985/86. *Arctic and Alpine Research*, 20, 179-187.
- Aniya, M., H. Sato, R. Naruse, P. Skvarca, and G. Casassa. 1996. The use of satellite and airborne imagery to inventory outlet glaciers of the Southern Patagonia Icefield, South America. *Photogrammetric Engineering and Remote Sensing*, 62, 1361-1369.
- Arrhenius, S. 1896. On the influence of carbonic acid in the air upon the temperature of the ground. *Philosophical Magazine*, 41, 237-276.
- Auden, J.B. 1935. Traverses in the Himalaya. *Records of the Geological Survey of India*, 69, 123-167.
- \_\_\_\_\_. 1937. The structure of the Himalayas in Garhwal. *Records of the Geological Survey of India*, 71, 407-433.
- Barnard, P.L., L.A. Owen, and R.C. Finkel. 2004a. Style and timing of glacial and paraglacial sedimentation in a monsoonal influenced high Himalayan environment, the upper Bhagirathi Valley, Garhwal Himalaya. *Sedimentary Geology*, 165, 199-221.
- Barnard, P.L., L.A. Owen, M.C. Sharma, and R.C. Finkel. 2004b. Late Quaternary (Holocene) landscape evolution of a monsoon-influenced high Himalayan valley, Gori Ganga, Nanda Devi, NE Garhwal. *Geomorphology*, 61, 91-110.
- Barry, R. 2006. The status of research on glaciers and global glacier recession: a review. *Progress in Physical Geography*, 30, 285-306.
- Bassoulet, J.P., M. Conchan, M. Guex, J. Lys, J. Marcoux, and G. Mascle. 1978. Permien terminal méritique, Scythien pélagique et volcanisme sous-marin, indices de processus tectono- sédimentaires distensits á la limite Permien-Trias dans un bloc

- exotique de la suture de l'Indus (Himalaya du Ladakh). *Comptes rendus de l'Académie des Sciences, Paris, Series D*, 287, 675-678.
- Bassoulet, J.P., M. Conchan, T. Juteau, J. Marcoux, and G. Mascle. 1980. L'edifice de nappes du Zaskar (Ladakh Himalaya). *Comptes rendus de l'Académie des Sciences, Paris, Series D*, 290, 389-392.
- Benn, D.I. 2006. Glaciers. *Progress in Physical Geography*, 30, 432-442.
- Benn, D.I., and D.J.A. Evans. 1998. *Glaciers and Glaciation*. London: Arnold.
- Benn, D.I., and L.A. Owen. 1998. The role of the Indian summer monsoon and the mid-latitude westerlies in Himalayan glaciation: review and speculative discussion. *Journal of the Geological Society London*, 155, 353-363.
- \_\_\_\_\_. 2002. Himalayan glacial sedimentary environments: a framework for reconstructing and dating the former extent of glaciers in high mountains. *Quaternary International*, 97-98, 3-25.
- Berthelsen, A. 1953. On the geology of the Rupshu District, N.W. Himalaya: A contribution to the problem of the Central Gneisses. *Meddelelser fra Dansk Geologisk Forening*, 12, 350-414.
- Berthier, E., Y. Arnaud, R. Kumar, S. Ahmad, P. Wagnon, and P. Chevallier. 2007. Remote sensing estimates of glacier mass balances in the Himachal Pradesh (Western Himalaya, India). *Remote Sensing of Environment*, 108, 327-338.
- Berthier, E., and T. Toutin. 2008. SPOT5-HRS digital elevation models and the monitoring of glacier elevation changes in North-West Canada and South-East Alaska. *Remote Sensing of Environment*, 112, 2443-2454.
- Bhutani, R., K. Pande, and T.R. Venkatesan. 2004. Tectono-thermal evolution of the India-Asia collision zone based on  $^{40}\text{Ar}$ - $^{39}\text{Ar}$  thermochronology in Ladakh, India. *Proceedings Indian Academy of Science. (Earth Planet Science)*, 113, 737-754.
- Bishop, M.P., R. Bonk, U. Kamp, and J.F. Shroder Jr. 2001. Terrain analysis and data modeling for alpine glacier mapping. *Polar Geography*, 25, 182-201.
- Bishop, M.P., J.A. Olsenholler, J.F. Shroder, R.G. Barry, B.H. Raup, A.B.G. Bush, L. Copland, J.L. Dwyer, A.G. Fountain, W. Haeberli, A. Kääb, F. Paul, D.K. Hall, J.S. Kargel, B.F. Molnia, D.C. Trabant, and R. Wessels. 2004. Global Land Ice Measurements from Space (GLIMS): Remote sensing and GIS investigations of the Earth's Cryosphere. *Geocarto International*, 19, 57-84.
- Bishop, M.P., and J.F. Shroder, Jr. 2009. Glacier response to climate forcing in the Karakoram Himalaya, Pakistan. *Oral Presentation Association of American Geographers Annual Meeting, Las Vegas, NV, March 25*.

- Bishop, M.P., J.F. Shroder, Jr., and B.L. Hickman. 1999. Information extraction in a complex mountain environment. *Geocarto International*, 14, 17-26.
- Bishop, M.P., J.F. Shroder Jr., V.F. Sloan, L. Copland, and J.D. Colby. 1998. Remote sensing and GIS technology for studying Lithospheric processes in a mountain environment. *Geocarto International*, 13, 75-87.
- Bishop, M.P., J.F. Shroder, and J.L. Ward. 1995. SPOT multispectral analysis for producing supraglacial debris-load estimates for Batura Glacier, Pakistan. *Geocarto International*, 10, 81-90.
- Bolch, T. 2007. Climate change and glacier retreat in northern Tien Shan (Kazakhstan/Kyrgyzstan) using remote sensing data. *Global and Planetary Change*, 56, 1-12.
- Bolch, T., M.F. Buchroithner, A. Kunert, and U. Kamp. 2007. Automated delineation of debris-covered glaciers based on ASTER data. In: M.A. Gomasca (ed.), *GeoInformation in Europe*, Netherlands: Millpress.
- Bolch, T., M.F. Buchroithner, T. Pieczonka, and A. Kunert. 2008a. Planimetric and volumetric glacier changes in the Khumbu Himal, Nepal, since 1962 using Corona, Landsat TM and ASTER data. *Journal of Glaciology*, 54, 592-600.
- Bolch, T., and U. Kamp. 2006. Glacier mapping in high mountains using DEMs, Landsat and ASTER data. *Grazer Schriften der Geographie und Raumforschung*, 41, 13-24.
- Bolch, T., U. Kamp, and M.F. Buchroithner. 2006. Glaciers from Space: new methods for mapping debris-covered glaciers at Mr. Everest, Nepal from Space. *Geoconnexion International*, July/August, 58-59.
- Bolch, T., U. Kamp, and J. Olsenholler. 2005. Using ASTER and SRTM DEMs for studying geomorphology and glaciation in high mountain areas. In Oluić (ed.), *New Strategies for European Remote Sensing*, Rotterdam: Millpress, 119-127.
- Bolch, T., B. Menounos, and R. Wheate. 2008b. Remotely-sensed Western Canadian Glacier Inventory 1985-2005 and regional Glacier Recession Rates. *Geophysical Research Abstracts*, 10, EGU2008-A-10403.
- Bonk, R. 2002. Scale-dependent geomorphometric analysis for glacier mapping at Nanga Parbat: GRASS GIS approach. *Proceedings of the Open Source GIS – GRASS Users Conference*, Trento, Italy, September 11-13, 2002.
- Bray, J. 2005. Introduction: Locating Ladakhi History. In: Bray, J. (ed.), *Ladakhi Histories: Local and Regional Perspectives*. Leiden, The Netherlands: Koninklijke Brill NV, 1-30.

- Broecker, W.S. 1975. Climatic change: are we on the brink of a pronounced global warming? *Science*, 189, 460-463.
- Brookfield, M.E., and C.P. Andrews-Speed. 1984. Sedimentology, petrography and tectonic significance of the shelf, flysch and molasse clastic deposits across the Indus Suture Zone, Ladakh, NW India. *Sedimentary Geology*, 40, 249-286.
- Brookfield, M.E., and P.H. Reynolds. 1981. Late Cretaceous emplacement of the Indus Suture Zone ophiolitic mélanges and an Eocene Oligocene magmatic arc on the northern edge of the Indian Plate. *Earth and Planetary Science Letters*, 55, 157-162.
- Brown, D.G., D.P. Lusch, and K.A. Duda. 1998. Supervised classification of types of glaciated landscapes using digital elevation data. *Geomorphology*, 21, 233-250.
- Buchroithner, M.F., and T. Bolch. 2007. An automated method to delineate the ice extension of the debris-covered glaciers at Mt. Everest based on ASTER imagery. *Grazer Schriften der Geographie und Raumforschung*, 43, 71-78.
- Burbank, D.W., and M.B. Fort. 1985. Bedrock control on glacial limits: Examples from the Ladakh and Zaskar Ranges, north-western Himalaya, India. *Journal of Glaciology*, 31, 143-149.
- Burbank, D.W. 2002. Rates of erosion and their implications for exhumation. *Mineralogical Magazine*, 66, 25-52.
- Casassa, G. 1995. Glacier inventory in Chile: Current status and recent glacier variations. *Annals of Glaciology*, 21, 317-322.
- Casassa, G, K. Smith, A. Rivera, J. Araos, M. Schnirch, and C. Schneider. 2002. Inventory of glaciers in isla Riesco, Patagonia, Chile, based on aerial photography and satellite imagery. *Annals of Glaciology*, 34, 373-378.
- Chamberlin, T.C. 1897. A group of hypothesis bearing on climatic changes. *Journal of Geology*, 5, 653-683.
- \_\_\_\_\_. 1898. The influence of great epochs of limestone formation upon the constitution of the atmosphere. *Journal of Geology*, 6, 609-621.
- \_\_\_\_\_. 1899. An attempt to frame a working hypothesis of the cause of glacial periods on an atmospheric basis. *Journal of Geology*, 7, 454-584, 667-685, 751-787.
- Chinn, T.J. 1999. New Zealand glacier response to climate change of the past 2 decades. *Global and Planetary Change*, 22, 155-168.



- Chinn, T., S. Winkler, M.J. Salinger, and N. Haakensen. 2005. Recent glacier advances in Norway and New Zealand: a comparison of their glaciological and meteorological causes. *Geografiska Annaler*, 87A, 141-157.
- Chung, S.L., C.H. Lo, T.Y. Lee, Y. Zhang, Y. Xie, X. Li, K.L. Wang, and P.L. Wang. 1998. Diachronous uplift of the Tibetan plateau starting 40 Myr ago. *Nature*, 394, 769-773.
- Clift, P.D. 2002. A brief history of the Indus River. In Clift, P.D., d. Kroon, C. Gaedicke, and J. Craig (eds.): *The Tectonic and Climatic Evolution of the Arabian Sea Region*. London, Geological Society, Special Publications, 195, 237-258.
- Cotten, G., and J. Brown. 1907. Note on certain glaciers in Kumaon. *Records of the Geological Survey of India*, 35, 148-157.
- Coxall, M., and P. Greenway. 1996. *Indian Himalaya: a Lonely Planet travel survival kit*. Hawthorn, Australia: Lonely Planet.
- Cunningham, A. 1854. *Ladak: Physical, Statistical and Historical*. London.
- Dainelli, G. 1922. Studi sul Glaciale. In: *Risultati Geologici e Geografici, Ser. II, vol. 3. Relazioni scientifiche della Spedizione Italiana De Fillippi nell' Himalaya, Caracorum e Turchestan Cinese (1913-1914)*. Bologna.
- Dainelli, G. 1934. Spedizione italiana de Filippi nell' Himalaya, caracorum e Turchestan Cinese (1913-1914). Ser. 2: Risultati geologici e geografici, 12, Indici analitici Zanichelli, Bologna.
- Damm, B. 2006. Late Quaternary glacier advances in the upper catchment area of the Indus River (Ladakh and Western Tibet). *Quaternary International*, 154-155, 87-99.
- DeMets, C., Gordon, R.G., Argus, D.F., and Stein, S. 1994. Effect of recent revisions to the geomagnetic reversal time scale on estimates of current plate motion. *Geophysical Research Letters*, 21, 2191-2194.
- de Sigoyer, J., V. Chavagnac, J. Blichert-Toft, I. Villa, B. Luais, S. Guillot, G. Mascle, and M. Cosca. 2000. Dating continental subduction and collisional thickening in NW Himalaya: multichronometry of the Tso Morari eclogites. *Geology*, 28, 487-490.
- de Terra, H. 1934. Physiographic results of a recent survey in Little Tibet. *Geographical Review*, 24, 12-41.
- \_\_\_\_\_. 1935. Geological studies in the northwestern Himalaya between the Kashmir and Indus valleys. *Memoirs of the Connecticut Academy of Arts and Science*, 8, 18-76. New Haven: Yale north India expedition.

- de Terra, H., and T.T. Paterson. 1932. *Studies on the Ice Age in India and Associated Human Culture*. Washington: Carnegie Institute of Washington.
- Dewey, J.F. and J.M. Bird. 1970. Mountain belts and its new global tectonics. *Journal of Geophysical Research*, 75, 2625-2647.
- Dewey, J.F. and K. Burke. 1973. Tibetan, Variscan and Precambrian basement reactivation: products of continental collision. *Journal of Geology*, 81, 683-692.
- Dèzes, P. 1999. *Tectonic and Metamorphic Evolution of the Central Himalayan Domain in Southeast Zaskar (Kashmir, India)*. Ph.D. diss., Université de Lausanne.
- Dhanju, M.S. 1990. *Study of Himalayan Glaciers Using Remote Sensing Techniques*. Technical Report (unpub.), 70p.
- Dietrich, V.J., W. Frank, and K. Honnegggar. 1983. A Jurassic-Cretaceous island arc in the Ladakh Himalaya. *Journal of Volcanology and Geothermal Research*, 18, 405-433.
- Dikau, R. 1992. Aspects of constructing a digital geomorphological base map. *Geologisches Jahrbuch*, A122, 357-370.
- Dobhal, D.P., and S. Kumar. 1996. Inventory of glacier basins in Himachal Himalaya. *Journal of The Geological Society of India*, 48, 671-681.
- Dowdeswell, J.A., J.O. Hagen, H. Björnsson, A.F. Glazovsky, W.D. Harrison, P. Holmlund, J. Jania, R.M. Koerner, B. Lefauconnier, C.S.L. Ommanney, and R.H. Thomas. 1997. The mass balance of Circum-Arctic glaciers and recent climate change. *Quaternary Research*, 48, 1-14.
- Drew, F. 1875. *Jummoo and Kashmir Territories*. Stanford, E. (ed.), London.
- Duncan, C.C., A.J. Klein, J.G. Masek, and B.L. Isacks. 1998. Comparison of Late Pleistocene and modern glacier extents in Central Nepal based on digital elevation data and satellite imagery. *Quaternary Research*, 49, 241-254.
- Dyurgerov, M.B., and M.F. Meier. 2000. Twentieth century climate change: Evidence from small glaciers. *Proceedings of the National Academy of Sciences of the United States of America*, 97, 1406-1411.
- Eckert, S., T. Kellenberger, and K. Itten. 2005. Accuracy assessment of automatically derived digital elevation models from aster data in mountainous terrain. *International Journal of Remote Sensing*, 26, 1943-1957.
- Fagan, B. 2000. *The Little Ice Age: How Climate Made History, 1300-1850*. New York: Basic Books.

- Finkel, R.C., L.A. Owen, P.L. Barnard, and M.W. Caffee. 2003. Beryllium-10 dating of Mount Everest moraines indicates a strong monsoon influence and glacial synchronicity throughout the Himalaya. *Geology*, 31, 561-564.
- Flint, F.R. 1971. *Glacial and Quaternary Geology*. New York: John Wiley and Sons.
- Fort, M. 1978. Observations sur la géomorphologie du Ladakh. *Bulletin de l'Association de Géographes Français, Paris*, 472, 169-175.
- \_\_\_\_\_. 1983. Geomorphological observations in the Ladakh area (Himalayas): Quaternary evolution and present dynamics. *Stratigraphy and Structure of Kashmir and Ladakh Himalaya*, 39-58.
- Frank, W., A. Gansser, and V. Trommsdorff. 1977. Geological observations in the Ladakh area (Himalayas): a preliminary report. *Schweizerische Mineralogische und Petrographische Mitteilungen*, 57, 89-113.
- Frenzel, B. 1960. Die Vegetations- und Landschaftszonen Nordeurasiens während der letzten Eiszeit und während der postglazialen Warmzeit. *Abhandlungen der mathematisch-naturwissenschaftlichen Klasse der Akademie der Wissenschaften und der Literatur*, 13, 937-1099.
- Fuchs, G. 1986. The geology of the Markha-Khurnak Region in Ladakh (India). *Geologisches Jahrbuch*, 128, 403-437.
- Gansser, A., 1964. *Geology of the Himalayas*. Wiley-Interscience, London, 289p.
- \_\_\_\_\_. 1974. The ophiolitic mélange, a world-wide problem on Tethyan examples. *Eclogae Geologicae Helvetiae*, 57, 479-507.
- Gao, J., and Y. Liu. 2001. Applications of remote sensing, GIS and GPS in glaciology: a review. *Progress in Physical Geography*, 25, 520-540.
- Global Climate Observing System (GCOS). 2003. *The Second Report on the Adequacy of the Global Observing System for Climate in support of the UNFCCC*. GCOS 82 (WMO/TD no. 1143): Geneva.
- GLIMS: Global Land Ice Measurements from Space. <http://www.glims.org>. (Accessed March 12, 2009).
- Gratton, D.J., P.J. Howarth, and D.J. Marceau. 1990. Combining DEM parameters with Landsat MSS and TM imagery in a GIS for mountain glacier characterization. *IEEE Transactions on Geoscience and Remote Sensing*, GE-28, 766-769.
- Guillot, S., E. Garzanti, D. Baratoux, D. Marquer, G. Maheo, and J. de Sigoyer. 2003. Reconstructing the total shortening history of the NW Himalaya. *Geochemistry, Geophysics and Geosystems*, 4, 1-22.

- Hall, D.K., and J. Martinec. 1985. *Remote Sensing of Snow and Ice*. London: Chapman and Hall.
- Harris, N. 2007. Channel flow and the Himalayan-Tibetan orogen: a critical review. *Journal of the Geological Society London*, 164, 511-523.
- Heim, A. and A. Gansser. 1939. The Central Himalayas: geological observations of the Swiss Expedition of 1936. *Memoires de la Societe Helvetique des Sciences Naturelles*, 73, 1-245.
- Herzfeld, U.C., and O. Zahner. 2001. A connectionist-geostatistical approach to automated image classification, applied to the analysis of crevasse patterns in surging ice. *Computers and Geosciences*, 27, 499-512.
- Hewitt, K. 2005. The Karakoram anomaly? Glacier expansion and the 'elevation effect,' Karakoram Himalaya. *Mountain Research and Development*, 25, 332-340.
- Hinkel, K.M., A.W. Ellis, and E. Mosley-Thompson. 2003. "Cryosphere". In G.L. Gaile and C.J. Willmott (eds.), *Geography in America at the Dawn of the 21<sup>st</sup> Century*, 47-55. Oxford: Oxford University Press.
- Hodges, K.V. 2000. Tectonics of the Himalaya and southern Tibet from two perspectives. *GSA Bulletin*, 112, 324-350.
- Honegger, K., V. Dietrich, W. Frank, A. Gansser, M. Thöni, and V. Trommsdorff. 1982. Magmatism and metamorphism in the Ladakh Himalayas (the Indus-Tsangpo suture zone). *Earth and Planetary Science Letters*, 60, 253-292.
- Honegger, K., P. LeFort, G. Mascle, and J.L. Zimmermann. 1989. The blueschists along the Indus Suture Zone in Ladakh, NW Himalaya. *Journal of Metamorphological Geology*, 7, 57-72.
- Hubbard, B., and N. Glasser. 2005. *Field Techniques in Glaciology and Glacial Geomorphology*. Chichester, England: John Wiley & Sons.
- Inoue, J. 1977. Mass budget of Khumbu Glacier. *Seppyo*, 39, Special Issue, 15-19.
- IPCC. 2007. Summary for Policy Makers. In M.L. Parry, O.F. Canziani, J.P. Palutikof, P.J. van der Linden, and C.E. Hanson (eds.), *Climate Change 2007: Impacts, Adaptation and Vulnerability. Contribution of Working Group II to the Fourth Assessment Report of the Intergovernmental Panel on Climate Change*. Cambridge, UK: Cambridge University Press, 7-22.
- Jain, A.K., S. Singh, and R.M. Manickavasagam. 2002. *Himalayan Collision Tectonics*. Gondwana Research Group Memoir 7, 114 pp.
- Jain, A.K., S. Singh, R.M. Manickavasagam, M. Joshi, and P.K. Verma. 2003. HIMPROBE Programme: integrated studies on geology, petrology, geochronology and geophysics of the Trans-Himalaya and Karakoram. In:

- Mahadevan, T.M., B.R. Arora, K.R. Gupta (Eds.), *Indian Continental Lithosphere: Emerging Research Trends, Memoir Geological Society of India*, 53, 1-56.
- Jamieson, S.S.R., H.D. Sinclair, L.A. Kirstein, and R.S. Purves. 2004. Tectonic forcing of longitudinal valleys in the Himalaya: morphological analysis of the Ladakh Batholith, North India. *Geomorphology*, 58, 49-65.
- Jones, M.D.H., and A. Henderson-Sellers. 1990. History of the greenhouse effect. *Progress in Physical Geography*, 14, 1-18.
- Kääb, A. 2005. Combination of SRTM3 and repeat ASTER data for deriving alpine glacier flow velocities in the Bhutan Himalaya. *Remote Sensing of Environment*, 94, 463-474.
- Kääb, A., C. Huggel, F. Paul, R. Wessels, B. Raup, H. Kieffer, and J. Kargel. 2003. Glacier monitoring from ASTER imagery: accuracy and applications. *EARSeL eProceedings*, 2, 43-53.
- Kääb, A., F. Paul, M. Maisch, M. Hoelzle, and W. Haeberli. 2002. The new remote-sensing-derived Swiss glacier inventory: II. First results. *Annals of Glaciology*, 34, 362-366.
- Kadota, T., K. Seko, T. Aoki, S. Iwata, and S. Yamaguchi. 2000. Shrinkage of Khumbu Glacier, east Nepal from 1978 to 1995. *IAHS Publication*, 264, 235-243.
- Kahn, Y. 2007. *The Great Partition: The Making of India and Pakistan*. New Haven, CT: Yale University Press.
- Kamp, U., T. Bolch, and J. Olsenholler. 2003. DEM generation from ASTER satellite data for geomorphometric analysis of Cerro Sillajhuay, Chile/Bolivia. *ASPRS Annual Conference Proceedings*, May 5-9, Anchorage, 9 pp.
- \_\_\_\_\_. 2005. Geomorphometry of Cerro Sillajhuay (Andes, Chile/Bolivia): Comparison of Digital Elevation Models (DEMs) from ASTER remote sensing data and contour maps. *Geocarto International*, 20, 23-33.
- Kamp, U., B.J. Growley, G.A. Khattak, and L.A. Owen. 2008. GIS-based landslide susceptibility mapping for the 2005 Kashmir earthquake region. *Geomorphology*, 101, 631-642.
- Karma, Y. Ageta, N. Naito, S. Iwata, and H. Yabuki. 2003. Glacier distribution in the Himalayas and glacier shrinkage from 1963 to 1993 in the Bhutan Himalayas. *Bulletin of Glaciological Research*, 20, 29-40.
- Kaser, G., J.G. Cogley, M.B. Dyurgerov, M.F. Meier, and A. Ohmura. 2006. Mass balance of glaciers and ice caps: Consensus estimates for 1961-2004. *Geophysical Research Letters*, 33, L19501.

- Kaul, S., and H.N. Kaul. 1992. *Ladakh through the Ages: Towards a New Identity*. Springfield, VA: Nataraj.
- Kazami, T. 1979. *The Himalayas*. Tokyo: Kodansha.
- Khalsa, S.J.S., M.B. Dyurgerov, T. Khromova, B.H. Raup, and R.G. Barry. 2004. Space-based mapping of glacier changes using ASTER and GIS tools. *IEEE Transactions of Geoscience and Remote Sensing*, 42, 2177-2183.
- Khromova, T.E., M.B. Dyurgerov, and R.G. Barry. 2003. Late-twentieth century changes in glacier extent in the Ak-shirak Range, Central Asia, determined from historical data and ASTER imagery. *Geophysical Research Letters*, 30, 1863.
- Klein, A.G., and B.L. Isacks. 1998. Alpine glacial geomorphological studies in the central Andes using Landsat Thematic Mapper images. *Glacial Geology and Geomorphology*, rp01/1998.
- Klute, F. 1930. Verschiebung der Klimagebiete der letzten Eiszeit. *Petermanns Geographische Mitteilungen, Ergänzungsheft*, 209, 166-182.
- Kolbert, E. 2006. *Field Notes from a Catastrophe: Man, Nature, and Climate Change*. New York: Bloomsbury.
- Krajik, K. 2002. Ice man: Lonnie Thompson scales the peaks for science. *Science*, 298, 518-522.
- Krishna, A.P. 1996. Satellite remote sensing applications for snow cover characterization in the morphogenetic regions of upper Tista river basin, Sikkim Himalaya. *International Journal of Remote Sensing*, 17, 651-656.
- Kulkarni, A.V. 1991. Glacier inventory of Himachal Pradesh using satellite imagery. *Journal of Indian Remote Sensing*, 19, 195-203.
- Kulkarni, A.V., I.M. Bahuguna, B.P. Rathore, S.K. Singh, S.S. Randhawa, R.K. Sood, and S. Dhar. 2007. Glacial retreat in Himalaya using Indian Remote Sensing satellite data. *Current Science*, 92 (1), 69-74.
- Kulkarni, A.V., B.P. Rathore, S. Mahajan, and P. Mathur. 2005. Alarming retreat of Parbati glacier, Beas basin, Himachal Pradesh. *Current Science*, 88, 1844-1850.
- Lall, J. 1989. *Aksaichin and Sino-Indian Conflict*. New Delhi: Allied Publishers.
- Lamb, A. 1966. *The Kashmir Problem: A Historical Survey*. New York: Frederick A. Praeger.
- Lambert, C. 1877. *A Trip to Cashmere and Ladâk*. London: Henry S. King & Co.

- Langley, S.P. 1884. Researches on solar heat. *Professional Papers of the Signal Service*, 15, 123.
- \_\_\_\_\_. 1886. Observations on invisible heat-spectra and the recognition of hitherto unmeasured wave-lengths, made at the Allegheny Observatory. *Philosophical Magazine*, 31, 394-409.
- Le Fort, P. 1975. Himalayas: the collided range, present knowledge of the continental arc. *American Journal of Science*, 275, 1-44.
- \_\_\_\_\_. 1986. Metamorphism and magmatism during the Himalayan collision, in: Cowards, M.P. and Ries, A.C. (Eds.), *Collision Tectonics*. Geological Society of London, Special Publication, 19, 159-172.
- Lehmkuhl, F., and L.A. Owen. 2005. Late Quaternary glaciation of Tibet and the bordering mountains: a review. *Boreas*, 34, 87-100.
- Lillesand, T.M., R.W. Kiefer, and J.W. Chipman. 2004. *Remote Sensing and Image Interpretation*. New York: John Wiley & Sons.
- Loram, C. 1996. *Leh & Trekking in Ladakh*. Surrey, UK: Trailblazer.
- Lydekker, R. 1876. Notes on the geology of the Pir Panjal and neighbouring districts. *Records of the Geological Survey of India*, 9, 155-183.
- \_\_\_\_\_. 1880. Geology of Ladak and neighbouring districts. *Records of the Geological Survey of India*, 13, 26-59.
- \_\_\_\_\_. 1883. The geology of the Kashmir and Chamba territories and the British district of Khagan. *Memoirs of the Geological Survey of India*, 22, 1-344.
- Maisch, M. 2000. The longterm signal of climate change in the Swiss Alps: glacier retreat since the end of the Little Ice Age and future ice decay scenarios. *Geografia Fisica e Dinamica Quaternaria*, 23, 139-152.
- Malanson, G.P., and R. Honey. 2009. Water towers, the metaphor. *Oral Presentation Association of American Geographers Annual Meeting, Las Vegas, NV, March 25*.
- Marston, R.A. 2008. Land, life, and environmental change in mountains. *Annals of the Association of American Geographers*, 98, 507-520.
- Mason, K. 1930. The glaciers of Karakoram and neighbourhood. *Records of the Geological Survey of India*, 633, 214-228.
- Meier, M.F., M.B. Dyurgerov, and G.J. McCabe. 2003. The health of glaciers: recent changes in glacier regime. *Climatic Change*, 59, 123-135.



- Messerli, B., D. Viviroli, and R. Weingartner. 2004. Mountains of the world: vulnerable water towers for the 21<sup>st</sup> Century. *Ambio*, Special Report, 13, 29-34.
- Molnar, P. and Tapponnier, P. 1978. Active tectonics in Tibet. *Journal of Geophysical Research*, 85, 5361-5375.
- Molnia, B.F. 2007. Late Nineteenth to early twenty-first century behavior of Alaskan glaciers as indicators of changing regional climate. *Global and Planetary Change*, 56, 23-56.
- Mool, P.K., S.R. Bajracharya, and S.P. Joshi. 2001a. *Inventory of Glaciers, Glacial Lakes and Glacial Lake Outburst Floods: Monitoring and Early Warning Systems in the Hindu Kush-Himalaya Region; Nepal*. Kathmandu: International Centre for Integrated Mountain Development.
- Mool, P.K., D. Wangda, S.R. Bajracharya, K. Kunzang, D.R. Gurung, and S.P. Joshi. 2001b. *Inventory of Glaciers, Glacial Lakes and Glacial Lake Outburst Floods: Monitoring and Early Warning Systems in the Hindu Kush-Himalaya Region; Bhutan*. Kathmandu: International Centre for Integrated Mountain Development.
- Mountain Agenda. 2002. *Mountains of the World: Sustainable Development in Mountain Areas. The Need for Adequate Policies and Instruments*. Berne, Switzerland: Mountain Agenda.
- Nakawo, M., and B. Rana. 1999. Estimate of ablation rate of glacier ice under a supraglacial debris layer. *Geografiska Annaler*, 81A, 695-701.
- Narama, C., Y. Shimamura, D. Nakayama, and K. Abdrakhmatov. 2006. Recent changes of glacier coverage in the western Terskey-Alatoo range, Kyrgyz Republic, using Corona and Landsat. *Annals of Glaciology*, 43, 223-229.
- National Snow and Ice Data Center. World Glacier Inventory. <http://nsidc.org/data/g01130.html> [accessed on April 6, 2009].
- National Aeronautics and Space Administration. The Landsat Program. <http://landsat.gsfc.nasa.gov/> [accessed on June 10, 2009].
- Negi, S.S. 2002. *Cold Deserts of India*. 2<sup>nd</sup> Ed. Indus Publishing Company, New Delhi.
- Norberg-Hodge, Helena. 1991. *Ancient Futures: Learning from Ladakh*. San Francisco: Sierra Club.
- \_\_\_\_\_. 1995. Ladakh: development without destruction. In: J.S. Lall (ed.), *The Himalaya: Aspects of change*, Delhi: Oxford University, 142-148.
- Norin, E. 1946. Geological explorations in Western Tibet. *Reports of the Sino-Swedish Expedition*, 29. Stockholm: Aktiebolaget Thule.

- Oerlemans, J. 1994. Quantifying global warming from the retreat of glaciers. *Science*, 264, 243-245.
- Osmaston, H. 1994. The geology, geomorphology and Quaternary history of Zaskar. In: Crook, J., and H. Osmaston (eds.), *Buddhist Himalayan Villages in Ladakh*. Bristol, 1-35.
- Owen, L. 2004 Cenozoic evolution of global mountain systems. In: P.N. Owens and O. Slaymaker (Eds.), *Mountain Geomorphology*, Oxford University Press, New York.
- Owen, L.A., R.M. Bailey, E.J. Rhodes, W.A. Mitchell, and P. Coxon. 1997. Style and timing of glaciation in the Lahul Himalaya, northern India: a framework for reconstructing late Quaternary palaeoclimatic change in the western Himalayas. *Journal of Quaternary Science*, 12, 83-109.
- Owen, L.A., M.W. Caffee, K.R. Bovard, R.C. Finkel, and M.C. Sharma. 2006. Terrestrial cosmogenic nuclide surface exposure dating of the oldest glacial successions in the Himalayan orogen: Ladakh Range, northern India. *GSA Bulletin*, 118, 383-392.
- Owen, L.A., E. Derbyshire, and M. Fort. 1998. The Quaternary glacial history of the Himalaya. *Quaternary Proceedings*, 6, 91-120.
- Owen, L.A., R.C. Finkel, M.W. Caffee, and L. Gualtieri. 2002. Timing of multiple glaciations during the late Quaternary in the Hunza Valley, Karakoram Mountains, northern Pakistan: Defined by cosmogenic radionuclide dating of moraines. *Geological Society of America Bulletin*, 114, 593-604.
- Owen, L.A., L. Gualtieri, R.C. Finkel, M.W. Caffee, D.I. Benn, and M.C. Sharma. 2001. Cosmogenic radionuclide dating of glacial landforms in the Lahul Himalaya, northern India: defining the timing of late Quaternary glaciation. *Journal of Quaternary Science*, 16, 555-563.
- Owen, L.A., U. Kamp, J.Q. Spencer, and K. Haserodt. 2002. Timing and style of Late Quaternary glaciation in the eastern Hindu Kush, Chitral, northern Pakistan: a review and revision of the glacial chronology based on new optically stimulated luminescence dating. *Quaternary International*, 97-98, 41-55.
- Pal, D., R.A.K. Srivastava, and N.S. Mathur. 1978. Tectonic framework of the miogeosynclinal sedimentation in Ladakh Himalaya: a critical analysis. *Himalayan Geology*, 8, 500-523.
- Pant, R.K., N.R. Phadtare, L.S. Chamyal, and N. Juyal. 2005. Quaternary deposits in Ladakh and Karakoram Himalaya: a treasure trove of palaeoclimate records. *Current Science*, 88, 11.

- Patriat, P., and J. Achache. 1984. India-Eurasia collision chronology has implications for crustal shortening and driving mechanism of plates. *Nature*, 311, 615-621.
- Paul, F. 2000a. Evaluation of different methods for glacier mapping using Landsat TM. *Proceedings of EARSeL-SIG-Workshop Land Ice and Snow*, Dresden/FRG, June 16-17.
- \_\_\_\_\_. 2000b. The new Swiss glacier inventory 2000: application of remote sensing and GIS. Ph.D. dissertation, University of Zurich.
- \_\_\_\_\_. 2002. Changes in glacier area in Tyrol, Austria, between 1969 and 1992 derived from Landsat 5 Thematic Mapper and Austrian Glacier Inventory data. *International Journal of Remote Sensing*, 23, 787-799.
- Paul, F., C. Huggel, and A. Kääb. 2004a. Combining satellite multispectral image data and a digital elevation models for mapping debris-covered glaciers. *Remote Sensing of Environment*, 89, 510-518.
- Paul, F., and A. Kääb. 2005. Perspectives on the production of a glacier inventory from multispectral satellite data in Arctic Canada: Cumberland Peninsula, Baffin Island. *Annals of Glaciology*, 42, 59-66.
- Paul, F., A. Kääb, and W. Haeberli. 2007. Recent glacier changes in the Alps observed by satellite: consequences for future monitoring strategies. *Global and Planetary Change*, 56, 111-122.
- Paul, F., A. Kääb, M. Maisch, T. Kellenberger, and W. Haeberli. 2002. The new remote-sensing-derived Swiss glacier inventory: I. Methods. *Annals of Glaciology*, 34, 355-361.
- Paul, F., A. Kääb, M. Maisch, T. Kellenberger, and W. Haeberli. 2004b. Rapid disintegration of Alpine glaciers observed with satellite data. *Geophysical Research Letters*, 31, L21402.
- Paul, T.V. 2005. Causes of the India-Pakistan enduring rivalry. In: Paul, T.V. (ed.), *The India-Pakistan Conflict: An Enduring Rivalry*. Cambridge: Cambridge University Press.
- Pelto, M. 2008. Glacier programme shows the value of 'ground truth'. *Nature*, 451, 244.
- Phartiyal, B., A. Sharma, R. Upadhyay, Ram-Awatar, and A.K. Sinha. 2005. Quaternary geology, tectonics and distribution of palaeo- and present fluvio/glacio lacustrine deposits in Ladakh, NW Indian Himalaya – a study based on field observations. *Geomorphology*, 65, 241-256.
- Phillips, W.M., V.F. Sloan, J.F. Shroder, Jr., P. Sharma, M.L. Clarke, and H.M. Rendell. 2000. Asynchronous glaciation at Nanga Parbat, northwestern Himalaya Mountains, Pakistan. *Geology*, 28, 431-434.

- Pope, A., T. Murray, and A. Luckman. 2007. DEM quality assessment for quantification of glacier surface change. *Annals of Glaciology*, 46, 189-194.
- Quattrochi, D.A., S.J. Walsh, J.R. Jensen, and M.K. Ridd. 2003. Remote sensing. In: Gaile, G.L., and C.J. Willmott (eds.), *Geography in America at the Dawn of the 21<sup>st</sup> Century*, 376-416. Oxford: Oxford University Press.
- Quincey, D.J., R.M. Lucas, S.D. Richardson, N.F. Glasser, M.J. Hambrey, and J.M. Reynolds. 2005. Optical remote sensing techniques in high-mountain environments: application to glacial hazards. *Progress in Physical Geography*, 29, 475-505.
- Racoviteanu, A.E., M.W. Williams, and R.G. Barry. 2008. Optical remote sensing of glacier characteristics: a review with focus on the Himalaya. *Sensors*, 8, 3355-3383.
- Rahman, M. 1996. *Divided Kashmir: Old Problems, New Opportunities for India, Pakistan, and the Kashmiri People*. Boulder, CO: Lynne Rienner Publishers.
- Rai, H. 1983. Geology of the Nubra Valley and its significance on the evolution of Ladakh Himalaya. In: Thakur, V.C., K.K. Sharma (Eds.), *Geology of Indus Suture Zone of Ladakh*. Dehradun: Wadia Institute of Himalayan Geology, 79-97.
- Rana, B., M. Nakawo, Y. Fukushima, and Y. Ageta. 1997. Application of a conceptual precipitation-runoff model (HYCYMODEL) in a debris-covered glacierized basin in the Langtang Valley, Nepal Himalaya. *Annals of Glaciology*, 25, 226-231.
- Ranzi, R., G. Grossi, L. Iacovelli, and S. Taschner. 2004. Use of multispectral ASTER images for mapping debris-covered glaciers within the GLIMS Project. *IEEE International Geoscience and Remote Sensing Symposium*, 2, 1144-1147.
- Raup, B., A. Kääb, J.S. Kargel, M.P. Bishop, G. Hamilton, E. Lee, F. Paul, F. Rau, D. Soltesz, S.J.S. Khalsa, M. Beedle, and C. Helm. 2007a. Remote sensing and GIS technology in the Global Land Ice Measurements from Space (GLIMS) Project. *Computers and Geosciences*, 33, 104-125.
- Raup, B., A. Racoviteanu, S.J.S. Khalsa, C. Helm, R. Armstrong, and Y. Arnaud. 2007b. The GLIMS geospatial glacier database: a new tool for studying glacier change. *Global and Planetary Change*, 56, 101-110.
- Rees, W.G. 2006. *Remote Sensing of Snow and Ice*. Boca Raton, FL: Taylor and Francis.
- Ren, J., Z. Jing, J. Pu, and X. Qin. 2006. Glacier variations and climate change in the central Himalaya over the past few decades. *Annals of Glaciology*, 43, 218-222.
- Reuber, I. 1989. The Dras Arc: two successive volcanic events on eroded oceanic crust. *Tectonophysics*, 161, 93-106.

- Reuber, I., R. Montigny, R. Thuizat, and Heitz. 1990. K/Ar ages of ophiolites and arc volcanics of the Indus Suture Zone (Ladakh): comparison with other Himalaya-Karakorum data. *Journal of Himalayan Geology*, 1, 115-125.
- Rignot, E., A. Rivera, and G. Casassa. 2003. Contribution of the Patagonia Icefields of South America to Sea Level Rise. *Science*, 302, 434-437.
- Rizvi, J. 1998. *Ladakh: Crossroads of High Asia*. Oxford University Press, Delhi.
- Ruddiman, W.F. 2001. *Earth's Climate: Past and Future*. New York: W.H. Freeman and Company.
- Sachan, H.K., B.K. Mukherjee, Y. Ogasawara, S. Maruyama, H. Ishida, A. Muko, and N. Yoshioka. 2004. Discovery of coesite from Indus Suture Zone, (ISZ), Ladakh, India: evidence for deep subduction. *European Journal of Mineralogy*, 16, 235-240.
- Scharer, U., J. Hamet, and C.J. Allegre. 1984. The Transhimalaya (Gangdese) plutonism in the Ladakh region: a U-Pb and Rb-Sr study. *Earth and Planetary Science Letters*, 67, 327-339.
- Schicker, I. 2005. Changes in Area of Stubai Glaciers analysed by means of Satellite Data for the GLIMS Project. Master's thesis, Leopold-Franzens University, Innsbruck.
- Schmidt, J., and R. Dikau. 1999. Extracting geomorphometric attributes and objects from digital elevation models: semantic, methods, and future needs. In: Dikau, R., and H. Saurer (eds.), *GIS for Earth Surface Systems*, 154-171. Berlin-Stuttgart: Gebrüder Borntraeger.
- Schofield, V. 2003. *Kashmir in Conflict: India, Pakistan and the Unending War*. London: I.B. Taurus.
- Searle, M.P., D.J.W. Cooper, and A.J. Rex. 1988. Collision tectonics of the Ladakh-Zaskar Himalaya. *Philosophical Transactions of Royal Society of London*, A-326, 117-150.
- Shah, S.K., M.L. Sharma, J.T. Gergan, and C.S. Tara. 1976. Stratigraphy and structure of the western part of the Indus Suture belt, Ladakh, Northwestern Himalaya. *Himalayan Geology*, 8, 288-295.
- Sharma, K.K., and S. Kumar. 1978. Contribution to the geology of Ladakh, north western Himalaya. *Himalayan Geology*, 8, 252-287.
- Sharma, K.K., A.K. Sinha, G.P. Bagdasarian, and R.C. Gukasian. 1978. Potassium-argon dating of Dras volcanics, Shyok volcanics and Ladakh granite, Ladakh, northwest Himalaya. *Himalayan Geology*, 8, 288-295.

- Shroder, J.F. Jr. 1993. Himalaya to the sea: geomorphology and the Quaternary of Pakistan in the regional context. In: J.F. Shroder, Jr. (Ed.), *Himalaya to the Sea: Geology, geomorphology and the Quaternary*. Routledge, London, 1-42.
- Shroder, J.F. Jr. 1998. Slope failure and denudation in the western Himalaya. *Geomorphology*, 26, 81-105.
- Shroder, J.F. Jr., and M.P. Bishop. 1998. Mass movement in the Himalaya: new insights and research directions. *Geomorphology*, 26, 13-35.
- Sidjak, R.W., and R.D. Wheate. 1999. Glacier mapping of the Illecillewaet icefield, British Columbia, Canada, using Landsat TM and digital elevation data. *International Journal of Remote Sensing*, 20, 273-284.
- Simpson, G.C. 1928. Some studies in terrestrial radiation. *Memoir of the Royal Meteorological Society*, 2, 69-95.
- Singh, S., R. Kumar, M.E. Barley, and A.K. Jain. 2007. SHRIMP U-Pb ages and depth of emplacement of Ladakh Batholith, Eastern Ladakh, India. *Journal of Asian Earth Sciences*, 30, 490-503.
- Singh, S. M.L. Leech, A.K. Jain, and R.M. Manickavasagam. 2003. U-Pb SHRIMP ages from the Ultrahigh-Pressure Tso Morari Crystallines, eastern Ladakh, India. *Himalayan Tectonics (HIMPROBE Results)*, 31-35.
- Solomina, O., R. Barry, and M. Bodnya. 2004. The retreat of Tien Shan glaciers (Kyrgyzstan) since the Little Ice Age estimated from aerial photographs, lichenometric and historical data. *Geografiska Annaler*, 86A, 205-215.
- Stampfli, G.M, and J. Mosar. 1998. The plate tectonics of the western Tethyan region. *Geological Dynamics of Alpine type Mountain belts: Ancient and Modern*, Bern, 74-75.
- Stokes, C.R., V. Popovnin, A. Aleynikov, S.D. Gurney, and M. Shahgedanova. 2007. Recent glacier retreat in the Caucasus Mountains, Russia, and associated increase in supraglacial debris cover and supra-/proglacial lake development. *Annals of Glaciology*, 46, 195-203.
- Stoliczka, F. 1865. Geological sections across the Himalayan mountains, from Wangtu Bridge on the River Sutlej to Sumdo on the Indus, with an account of the formations in Spiti, accompanied by a revision of all known fossils from that district. *Memoirs of the Geological Survey of India*, 5, 1-154.
- \_\_\_\_\_. 1866. Summary of geological observations during a visit to the provinces – Rupshu, Karnag, South Ladak, Zaskar, Suroo, and Dras of Western Tibet. *Memoirs of the Geological Survey of India*, 5, 337-354.

- Su, Z., and Y. Shi. 2002. Response of monsoonal temperate glaciers to global warming since the Little Ice Age. *Quaternary International*, 97-98, 123-131.
- Suzuki, R., K. Fujita, and Y. Ageta. 2007. Spatial distribution of thermal properties on debris-covered glaciers in the Himalayas derived from ASTER data. *Bulletin of Glacier Research*, 24, 13-22.
- Svoboda, F., and F. Paul. 2009. A new glacier inventory on southern Baffin Island, Canada, from ASTER data: I. Methods, challenges and solutions. *Geophysical Research Abstracts*, 11, EGU2009-11392.
- Tanner, H.C.B. 1891. Our present knowledge of the Himalayas. *Proceedings of the Royal Geographical Society and Monthly Record of Geography*, 13, 403-423.
- Taschner, S. and R. Ranzi. 2002. Comparing the opportunities of Landsat-TM and Aster data for monitoring a debris-covered glacier in the Italian Alps within the GLIMS project. *Proceedings of the IGARSS*, 2, 1044-1046.
- Taylor, P.J., and W.A. Mitchell. 2000. The Quaternary glacial history of the Zaskar Range, north-west Indian Himalaya. *Quaternary International*, 65/66, 81-99.
- Tewari, A.P. 1964. On the Upper Tertiary deposits of Ladakh Himalaya and correlation of various geotectonic units of Ladakh with those of the Kumaun-Tibet region. *Report of the 22<sup>nd</sup> Session of the International Geological Congress*, New Delhi, 11, 37-58.
- Thakur, V.C., and N.S. Viridi. 1979. Lithostratigraphy, structural framework, deformation and metamorphism of the southeastern region of Ladakh, Kashmir Himalaya, India. *Himalayan Geology*, 9, 63-78.
- Thakur, V.C. 1981. Regional framework and geodynamic evolution of the Indus Tsangpo suture zone in the Ladakh Himalaya. *Transactions of the Royal Society of Edinburgh: Earth Science*, 72, 89-97.
- Thakur, V.C., B.S. Rawat, and R. Islam. 1990. Zaskar Crystallines: some observations on its lithostratigraphy, deformation, metamorphism and regional framework. *Journal of Himalayan Geology*, 1, 11-25.
- Thakur, V.C. 1992. *Geology of the Western Himalaya*. Physics and Chemistry of the Earth 19. Oxford: Pergamon.
- Thompson, L.G., E. Mosley-Thompson, M.E. Davis, T.A. Mashiotta, K.A. Henderson, P.N. Lin, and Y. Tangdong. 2006. Ice core evidence for asynchronous glaciation on the Tibetan Plateau. *Quaternary International*, 154-155, 3-10.
- Toutin, T. 2008. ASTER DEMs for geomatic and geoscientific applications: a review. *International Journal of Remote Sensing*, 29, 1855-1875.



- Tyndall, J. 1861. On the absorption and radiation of heat by gases and vapours, and on the physical connexion of radiation, absorption, and conduction. *Philosophical Magazine*, 22, 169-194, 273-285.
- UNEP. 2008. *Global Glacier Changes: facts and figures*. WGMS.
- Vance, D., M. Bickle, S. Ivy Ochs, and P.W. Kubik. 2003. Erosion and exhumation in the Himalaya from cosmogenic isotope inventories and river sediments. *Earth and Planetary Science Letters*, 206, 273-288.
- Varma, S.P. 1971. *Struggle for the Himalayas. A Study in Sino-Indian Relations*. New Delhi: Sterling.
- Virdi, N.S., V.C. Thakur, and R.J. Azmi. 1978. Discovery and significance of Permian microfossils in the Tso Morari Crystallines of Ladakh, J & K, India. *Himalayan Geology*, 8, 993-1000.
- Vohra, C.P. 1978. Glacier resources of the Himalaya and their importance to environment studies. *Proceedings of the National Seminar on Resources Development and Environment in the Himalaya Region*, DST, 441-460.
- \_\_\_\_\_. 1980. Some problems of glacier inventory in the Himalayas. *IANS-AISH Publications*, 126, 67-74.
- Wadia, D.N. 1937. The Cretaceous volcanic series of Astor-Deosai, Kashmir and its intrusions. *Records of the Geological Survey of India*, 72, 151-161.
- \_\_\_\_\_. 1957. *Geology of India*. London: MacMillan and Co.
- Weare, G. 2002. *Trekking in the Indian Himalaya*. Melbourne: Lonely Planet.
- Weart, S.R. 2008. *The Discovery of Global Warming*. Cambridge: Harvard University Press.
- Weinberg, R.F., and W.J. Dunlap. 2000. Growth and deformation of the Ladakh Batholith, northwest Himalayas: implications for timing of continental collision and origin of calc-alkaline batholith. *Journal of Geology*, 108, 303-320.
- Williams, R.S., Jr., D.K. Hall, O. Sigurdsson, and J.Y.L. Chien. 1997. Comparison of satellite-derived with ground-based measurements of the fluctuations of the margins of Vatnajökull, Iceland, 1973-1992. *Annals of Glaciology*, 24, 72-80.
- Winkler, S., N. Haakensen, A. Nesje, and N. Rye. 1997. Glaziale Dynamik in Westnorwegen: Ablauf und Ursachen des aktuellen Gletschervorstoßes am Jostedalsbreen. *Petermanns Geographische Mitteilungen*, 141, 43-63.
- Wood, R.W. 1909. Note on the theory of the greenhouse. *Philosophical Magazine*, Series 6, 17, 319-320.

- WWF. 2005. An overview of glaciers, glacier retreat, and subsequent impacts in Nepal, India and China. *WWF Nepal Program*.
- Yablokov, A. 2006. Climate change impacts on the glaciation in Tajikistan. In: *Assessment Report for the Second National Communication of the Republic of Tajikistan on Climate Change*. Dushanbe: Tajik Meteorological Service. (In Russian).
- Yin, A., and T.M. Harrison. 2000. Geologic evolution of the Himalayan-Tibetan orogen. *Annual Review of Earth and Planetary Science*, 28, 211-280.
- Zemp, M., W. Haeberli, M. Hoelzle, and F. Paul. 2006. Alpine glaciers to disappear within decades? *Geophysical Research Letters*, 33, L13504.
- Zgorzelski, M. 2006. Ladakh and Zaskar. *Miscellanea Geographica*, 12, 13-24.
- Zollinger, S. 2003. Ableitung von Parametern für die Identifikation und Beobachtung gefährlicher Gletscherseen in Nepal aus ASTER Satellitendaten. Diploma Thesis, University of Zurich.
- Zurick, D., J. Pacheco, B. Shrestha, and B. Bajracharya. 2005. *Atlas of the Himalaya*. Kathmandu: International Centre for Integrated Mountain Development.